CHAPTER 3

CENTRALLY LOADED COLUMNS

3.1 INTRODUCTION

The cornerstone of column theory is the Euler column, a mathematically straight, prismatic, pin-ended, centrally loaded[1] strut that is slender enough to buckle without the stress at any point in the cross section exceeding the proportional limit of the material. The *buckling load* or *critical load* or *bifurcation load* (see Chapter 2 for a discussion of the significance of these terms) is defined as

$$P_E = \frac{\pi^2 EI}{L^2} \tag{3.1}$$

where E is the modulus of elasticity of the material, I is the second moment of area of the cross section about which buckling takes place, and L is the length of the column. The Euler load, P_E, is a reference value to which the strengths of actual columns are often compared.

If end conditions other than perfectly frictionless pins can be defined mathematically, the critical load can be expressed by

$$P_E = \frac{\pi^2 EI}{(KL)^2} \tag{3.2}$$

where KL is an *effective length* defining the portion of the deflected shape between points of zero curvature (inflection points). In other words, KL is the length of an equivalent pin-ended column buckling at the same load as the end-restrained

[1]Centrally loaded implies that the axial load is applied through the centroidal axis of the member, thus producing no bending or twisting.

column. For example, for columns in which one end of the member is prevented from translating with respect to the other end, K can take on values ranging from 0.5 to l.0, depending on the end restraint.

The isolated column can be considered a theoretical concept; it rarely exists in practice. Usually, a column forms part of a structural frame and its stability is interrelated with the stability, stiffness, and strength of the surrounding structure. The structure imposes not only axial forces on the column, but also flexural and torsional forces as well as end restraints. This interrelationship is treated elsewhere in many parts of this guide. This chapter considers only the isolated column because (1) many structural design situations are idealized such that elements can be thought of as centrally loaded columns (e.g., truss members) and (2) the centrally loaded column is a limiting point in the mathematical space defining the interaction between axial and flexural forces in a member of a structure. Thus, an understanding of the behavior of individual centrally loaded columns is essential to the development of design criteria for compression members in general.

Columns are made in a variety of cross sections and by several processes, depending on their size and shape. Most steel columns are prismatic (i.e., the cross section is the same from end to end), although tapered columns are also used in certain circumstances. Virtually all rolled shapes can be used as columns, but some are much more efficient than others because of such factors as the ratio of the governing second moment of area to the weight per unit length, the ratio of the radii of gyration about perpendicular axes, double or single symmetry or asymmetry of the cross section, and the propensity toward torsional or flexural–torsional buckling or local buckling of elements.

Section 3.2 discusses general concepts related to column stability and design, whereas Sections 3.3 and 3.4 focus on key properties that have specific influences on column capacity, namely, imperfections related to residual stresses and out-of-straightness (Section 3.3) and end restraint (Section 3.4). Section 3.5 discusses specific concepts related to the development of column design curves and design criteria.

Although the majority of this chapter deals with either general concepts or the specific behavior of steel columns, other metals are also used for columns in practice. Sections 3.6 and 3.7 cover aspects particular to aluminum and stainless steel columns, respectively.

Section 3.8 deals with tapered columns, generally fabricated by welding flange plates to a tapered web plate. These are common in rigid moment-resisting steel frames, where they act, of course, as beam-columns. For frames with hinged bases, the cross-section depth increases from the base to the knee, where the bending moments are large. A component of the understanding of the behavior of these beam-columns comes from an appreciation of their behavior under axial loads.

Section 3.9 covers issues related to built-up columns. These find use in bridges and mill buildings where either the loads are relatively large or particular circumstances suggest their use. Analysis or rehabilitation of historical structures may also require an understanding of these special structural elements. Section 3.10 provides a discussion pertaining to stepped columns, commonly used to support crane runway girders in industrial structures. Section 3.11 addresses the unique problem of guyed towers.

Although this chapter provides a broad overview of the behavior and design of centrally loaded columns, it is impossible to address all related aspects of such a diverse subject. A comprehensive list of additional reference material on topics related to centrally loaded columns can be found in the annotated bibliography by Driver et al. (2003).

3.2 COLUMN STRENGTH

3.2.1 Critical-Load Theory

The strength of a perfectly straight prismatic column with central loading and well-defined end restraints that buckles elastically in a flexural mode is the Euler load, P_E (Eq. 3.2). When the axial load attains the value P_E, a stable equilibrium configuration is possible even in the presence of lateral deflection (Fig. 3.1*a*), while the load remains essentially constant (Fig. 3.1*b*, lines *OAB*). Even if an initial deflection and/or an initial load eccentricity is present, the maximum load will approach the Euler load asymptotically as long as the material remains elastic (curve C in Fig. 3.1*b*).

Many practical columns are in a range of slenderness where at buckling portions of the columns are no longer linearly elastic, and thus one of the key assumptions underlying Euler column theory is violated due to a reduction in the stiffness of the column. This degradation of the stiffness may be the result of a nonlinearity

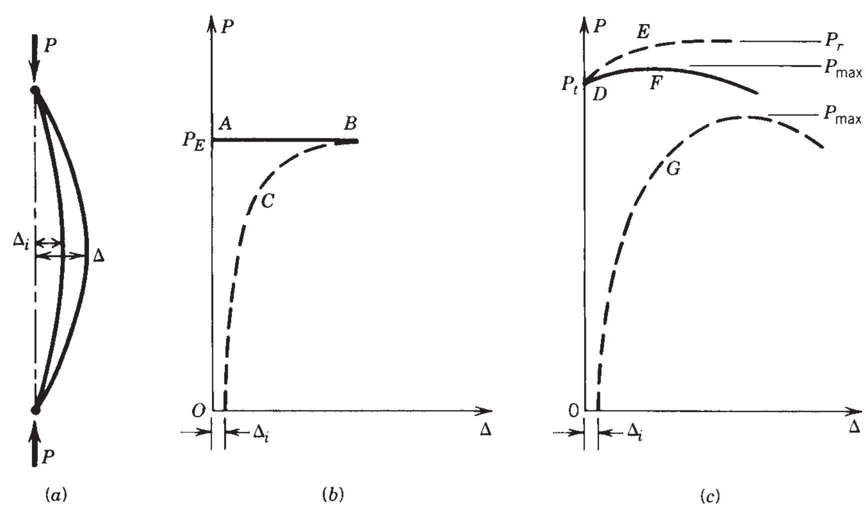

FIGURE 3.1 Behavior of perfect and imperfect columns.

in the material behavior itself (e.g., aluminum, which has a nonlinear stress–strain curve), or it may be due to partial yielding of the cross section at points of compressive residual stress (e.g., steel shapes). The postbuckling behavior of such a column is fundamentally different from the perfect elastic column: bifurcation buckling occurs for an initially straight column at the tangent-modulus load (point D in Fig. 3.1c) defined as

$$P_t = \frac{\pi^2 E_t I}{L^2} \tag{3.3}$$

but further lateral deflection is possible only if the load increases. If there were no further changes in stiffness due to yielding, the load would asymptotically approach the *reduced-modulus load* (point E in Fig. 3.1c)

$$P_r = \frac{\pi^2 E_r I}{L^2} \tag{3.4}$$

as the deflection tends to large values. The increase in load is due to the elastic unloading of some fibers in the cross section, which results in an increase in stiffness. The tangent modulus, E_t, is the slope of the stress–strain curve (Fig. 3.2) when the material is nonlinear, but E_r and E_t when residual stresses are present also depend on the shape of the cross section. Because increased loading beyond the tangent-modulus load results in further yielding, stiffness continues to be reduced and the load–deflection curve achieves a peak ($P_{\max}$, point F in Fig. 3.1c) beyond which it falls off.

The improved understanding of the post-buckling behavior of inelastic columns made possible by Shanley (1947) represented the single most significant step in understanding column behavior since Euler's original development of elastic buckling theory in 1744. Thus, a perfect inelastic column will begin to deflect laterally when $P = P_t$ and $P_t < P_{\max} < P_r$.

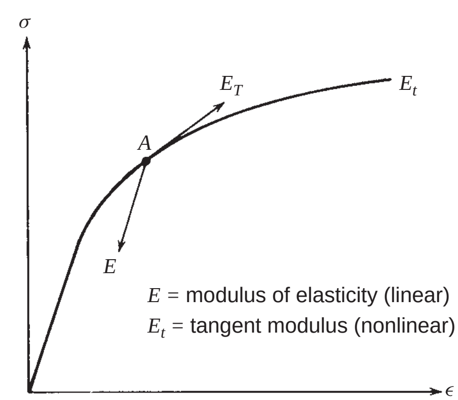

FIGURE 3.2 General stress–strain relationship.

The Euler buckling behavior described above pertains to the flexural (in-plane) mode, which is the dominant mode experienced by most standard hot-rolled shapes with doubly symmetric cross sections in typical applications. It must be recognized, however, that centrally loaded columns may potentially experience a torsional buckling mode or, in the case of singly symmetric or asymmetric sections, a combination mode, generally referred to as flexural–torsional buckling. Because these behaviors are more commonly associated with angle struts and thin-walled compression members, these concepts are covered in Chapters 11 and 13.

3.2.2 Imperfect Column Theory

Geometric imperfections, in the form of tolerable but unavoidable out-of-straightness of the column and/or eccentricity of the applied axial load, introduce bending from the onset of loading, and curve G in Fig. 3.1c characterizes the behavior of an out-of-straight column. Lateral deflection exists from the start of loading, and the maximum load is reached when the internal moment capacity (in the presence of axial load) at the critical section is equal to the external moment caused by the product of the load and the deflection. The maximum load is thus a function of the imperfection. For some types of columns, the nature of the problem is such that the maximum capacity of the imperfect column is closely approximated by the tangent-modulus load of the perfect column, but for many types of columns the imperfections must be included to give a realistic maximum load. In general, the strength of columns must be determined by including both the imperfections and material nonlinearity and/or the residual stress effects.

3.2.3 Approaches to the Design of Metal Columns

Accurate determination of the maximum strength of metal columns is a complicated process involving numerical integration that may use various solution procedures for nonlinear problems. The nonlinear approach is essential when initial imperfections, material nonlinearities, residual stresses, and other column strength parameters have to be considered.

Simplified column formulas are usually provided for design office practice. These formulas incorporate the major strength parameters, such as the yield stress, the column length, and the cross-section properties, and resistance factors are prescribed to arrive at acceptable levels of reliability. Many column formulas have been used throughout the history of structural engineering, and the reader can consult standard textbooks, including the previous editions of this Guide, to find the equations that have been used and the rationales behind the various models. A brief description of these models is provided below, strictly to offer the historical background of the most important approaches.

1. ***Empirical formulas based on the results of column tests***. Such formulas are applicable only to the material and geometry for which the tests were performed. The earliest column formulas (from the 1840s) are of this type.

Some contemporary studies (Hall, 1981; Fukumoto et al., 1983), however, have utilized the availability of computerized databases that contain a number of the column tests reported in the literature. The reader is referred to the paper by Hall (1981) for numerous plots that include accumulated test data from the literature for a variety of column types. Empirical factors can account approximately for initial imperfections of geometry and loading, but the formulas do not consider the inelastic basis of general column behavior, nor can they rationally account for end restraint.

2. ***Formulas based on the yield limit state***. These formulas define the strength of a column as the axial load that gives an elastic stress for an initially imperfect column equal to the yield stress. Such column formulas have a long history, also dating back to the middle of the nineteenth century, and they continue to enjoy popularity to the present, for example, the use of the Perry–Robertson (Robertson, 1925) formula (Trahair, 1988).
3. ***Formulas based on the tangent-modulus theory***. Such formulas can account rationally for the bifurcation load, but not the maximum strength, of perfectly straight columns. If the effects of imperfections are such that they just reduce the maximum strength to the tangent-modulus strength, these formulas have empirical justification. On the other hand, if the perfect column can be thought of as an anchor point in an interaction surface, initial imperfections of geometry and loading can be represented as flexural effects in the interaction equation.

   The "CRC Column Strength Curve," named after the acronym of the former name of the Structural Stability Research Council (i.e, Column Research Council), was recommended in the first edition of this guide (1960) and has been used for many steel design specifications in North America and elsewhere. It is based on the average critical stress for small- and medium-sized hot-rolled wide-flange shapes of mild structural steel, with a symmetrical residual stress distribution typical of such members. The column curves based on the tangent-modulus theory can also accurately account for end restraints (Yura, 1971).
4. ***Formulas based on maximum strength***. State-of-the-art column design formulas are based on extensive studies of the maximum strength of representative geometrically imperfect columns containing residual stresses. The analyses have incorporated comprehensive numerical data, as well as evaluations of test results and how well these compare. Reliability analyses have been performed, leading to the resistance factors that are given in state-of-the-art design standards. The third edition of this guide presented new column curves based on this principle (Bjorhovde, 1972). Subsequently, SSRC published Technical Memorandum No. 5, stating the principle that design of metal structures should be based on the maximum strength, including the effects of geometric imperfections.

It was also suggested that the strength of columns might be represented better by more than one column curve, thus introducing the concept of multiple column curves (Bjorhovde and Tall, 1971, Bjorhovde, 1972). SSRC curves 1, 2, and 3 and curves 1P, 2P, and 3P are two sets of such curves; another example is the set of five curves in Eurocode 3 [European Committee for Standardisation (CEN, 2005)]. The Canadian Standards Association (CSA, 2009) provides two column curves that are based on SSRC curves 1 and 2. The column curve of the American Institute of Steel Construction (AISC) specifications (AISC, 2005a) is the same as SSRC curve 2P, although the equation takes a different form. Finally, end-restraint effects are readily incorporated with the maximum-strength approach.

3.2.4 Local Buckling

When structural members composed of slender elements, such as the flanges and webs of many steel shapes, are loaded axially, the overall column capacity can be limited by the capacity of the individual cross-section elements. This phenomenon is known as local buckling and is closely related to classical plate-bucking theory. This topic is covered in Chapter 4.

3.2.5 Bracing

The strength of a compression member can be influenced greatly by the method with which it is braced. Although brace locations between the member ends influence the effective length of the member, as discussed in Section 3.4, the type, strength, and stiffness of the braces, as well as the means of connecting them to the column, can affect the behavior significantly. Torsional buckling modes can only be restrained using braces that restrain twisting deformations. Bracing of members is a complex topic that is largely beyond the scope of this chapter. Column bracing topics are covered in Section 3.4.2 and Chapter 12.

3.3 INFLUENCE OF IMPERFECTIONS

3.3.1 Residual Stresses

Structural steel shapes and plates contain residual stresses that result primarily from nonuniform cooling after rolling. Welded built-up members also exhibit tensile residual stresses in the vicinity of the welds due to the cooling of the weld metal. These are generally equal to the yield stress of the weld metal, which will normally be somewhat greater than the yield stress of the base metal (Tall, 1966; Alpsten and Tall, 1970; Bjorhovde et al., 1972). Flame cutting (also called oxygen cutting) introduces intense heat in a narrow region close to the flame-cut edge. As a result, the material in this region acquires properties that are significantly different from those of the base metal, and residual stresses develop that are often much higher than the yield stress of the parent material (McFalls and Tall, 1970; Alpsten and Tall, 1970; Bjorhovde et al., 1972). Finally, cold forming and cold straightening introduce residual stresses, especially in regions with the most severe bending effects, such as in corners of cold-formed shapes (Alpsten, 1972b; Sherman, 1976; Yu, 1992).

In 1908, in a discussion of the results of column tests at the Watertown Arsenal, residual stresses due to the cooling of hot-rolled steel shapes were cited as the probable cause of the reduced column strength in the intermediate slenderness range (Howard, 1908) The possible influence of residual stresses on the buckling strength of both rolled members and welded plates in girders was subsequently noted by others (Salmon, 1921; Madsen, 1941). Systematic research on the effect of residual stress on column strength was initiated in the late 1940s under the guidance of Research Committee A of the Column Research Council (Osgood, 1951; Yang et al., 1952; Beedle and Tall, 1960). This work continued through the early 1970s in extensive research projects, primarily at Lehigh University (Kishima et al., 1969; McFalls and Tall, 1970; Alpsten and Tall, 1970; Brozzetti et al., 1970a; Bjorhovde et al., 1972). Work in Europe and Canada on these effects must also be noted to appreciate fully the magnitude and complexity of the problem (Sfintesco, 1970; Beer and Schultz, 1970; Alpsten, 1972a; Chernenko and Kennedy, 1991).

At the time of the first edition of this guide (1960), the tangent-modulus curve appeared to be the proper basis for the determination of allowable column design stresses. This curve was based on the effect of typical residual stress distributions in hot-rolled steel shapes. The CRC column curve, based on computed column curves for hot-rolled wide-flange shapes and taken as an approximate average of the major and minor axis buckling curves, served as a basis for the column design provisions of the AISC and CSA specifications. The second edition of this guide (1966) mentioned the increasing use of columns made of (1) high-strength steels with yield stresses up to 70 ksi (480 Mpa) and (2) heat-treated steels with yield stresses up to 100 ksi (690 Mpa) or more. It noted the importance of initial imperfections as well as of residual stresses in determining the strengths of pin-ended columns made of higher strength steels.

One of the possible ways of differentiating between categories of column strength is by the use of the concept of multiple column curves, such as those that were developed through research at Lehigh University (Bjorhovde and Tall, 1971; Bjorhovde, 1972) and those that have been provided by the studies in Europe (Beer and Schultz, 1970). In addition, large numbers of column tests have also been performed, in some cases on a systematic basis, to provide further assurance of the theoretical results obtained by computer studies. The single largest group of such column tests is probably the more than 1000 tests that were conducted at a number of European universities and laboratories, as well as a number of tests on heavy shapes at Lehigh University, under the auspices of the European Convention for Constructional Steelwork (ECCS) (Sfintesco, 1970). Over the years, a great many other tests have also been performed, and these have been summarized by Fukumoto et al. (1983).

Residual Stresses in Hot-Rolled Shapes The magnitude and distribution of residual stresses in hot-rolled shapes depend on the type of cross section, rolling temperature, cooling conditions, straightening procedures, and the material properties of the steel (Beedle and Tall, 1960). Examples of residual stress distributions resulting from cooling without straightening of wide-flange shapes are shown in

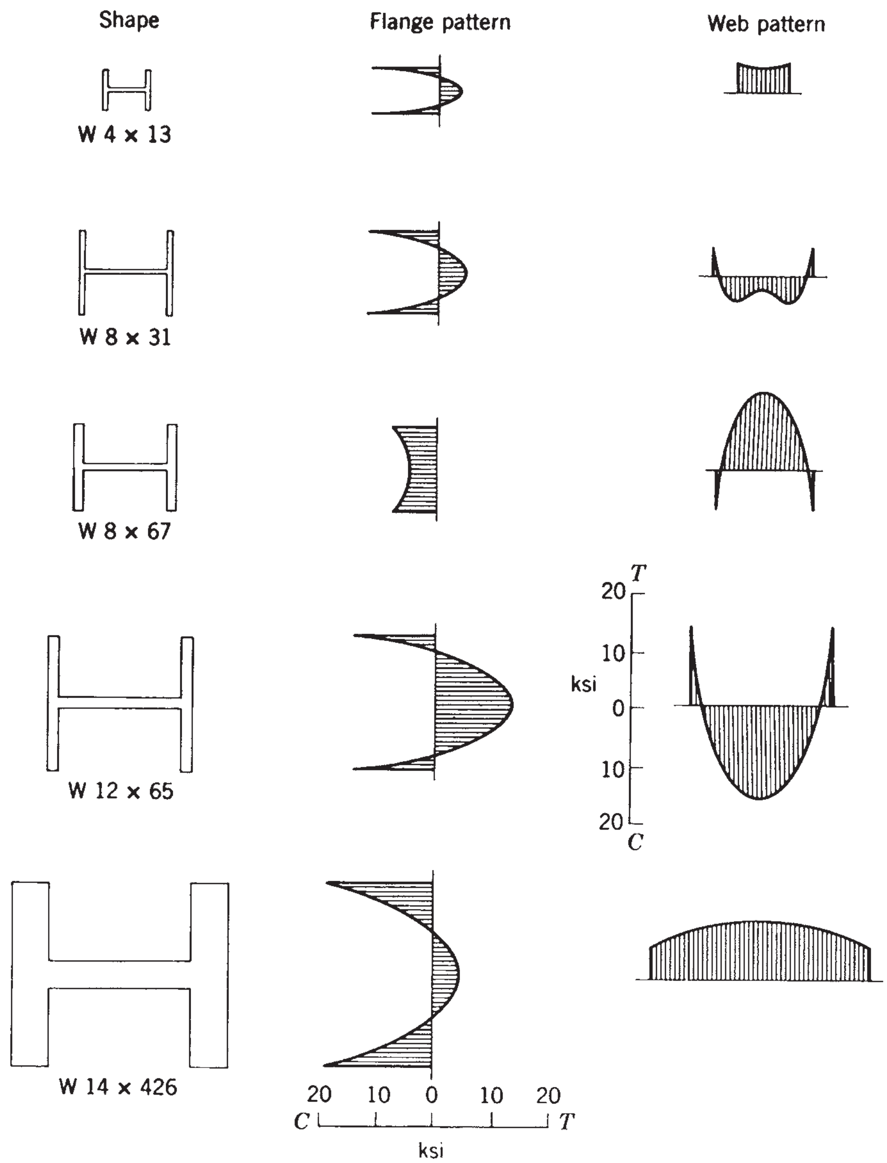

FIGURE 3.3 Residual-stress distribution in rolled wide-flange shapes.

Fig. 3.3 (Tall, 1964). For heavier shapes, residual stresses vary significantly through the thickness. Figure 3.4 shows the measured residual stresses in one of the heaviest rolled shapes that is currently produced (Brozzetti et al., 1970a).

The effect of the strength of the steel on the residual stress distribution is not as great as the effect of geometry (Tall, 1964). Residual stress measurements in the

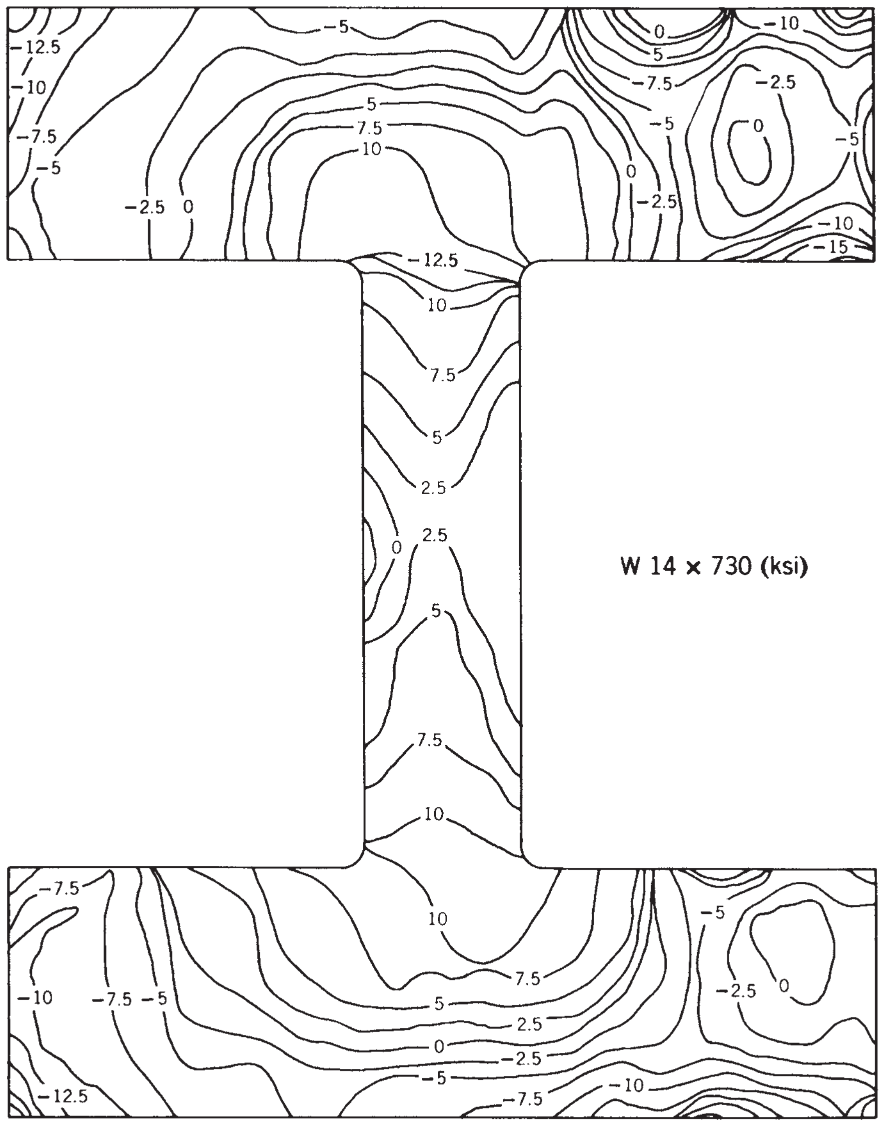

FIGURE 3.4 Residual-stress distribution in W14X730 shape.

flanges of similar shapes made of different steel grades show that the distributions and magnitudes of the residual stresses are very similar. For H-shaped columns, it is residual stresses in the flanges that have the most significant effect on the column strength.

Computed column curves based on the residual stresses in the five shapes of Fig. 3.3 are shown in Fig. 3.5 for buckling about the minor axis. The figure

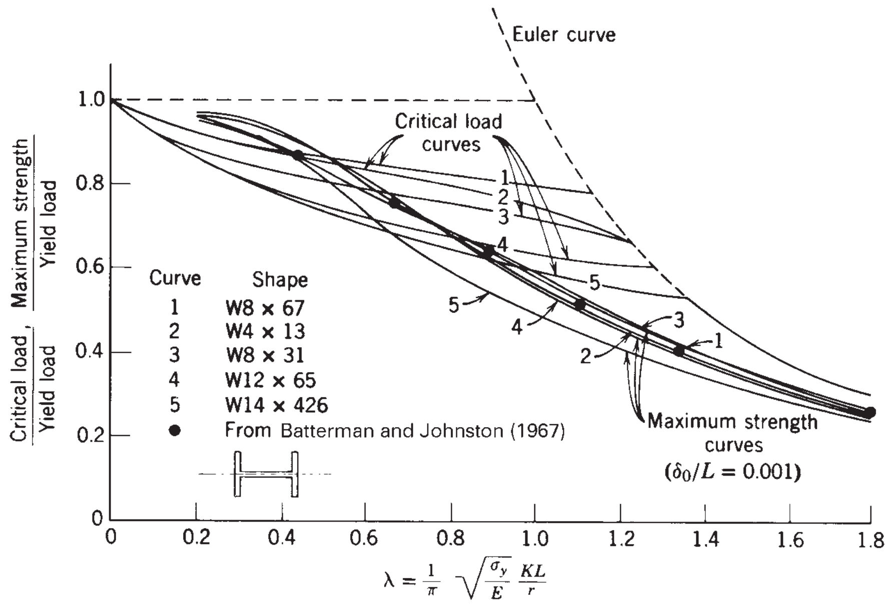

FIGURE 3.5 Critical-load curves for straight columns compared with maximum-strength curves for initially curved rolled steel W-shapes.

also shows the computed maximum strength curves for these shapes, using a combination of the measured residual stresses and an initial out-of-straightness equal to the approximate maximum of $L/1000$ that is permitted by the ASTM standard for delivery of structural shapes, ASTM A6 (the actual maximum is $L/960$, as defined by ASTM A6).

To provide a systematic examination of the separate and the combined effects of the residual stresses and the initial out-of-straightness, extensive column strength analyses were carried out at the University of Michigan (Batterman and Johnston, 1967). The studies included the following parameters:

1. Yield stresses of 36, 60, and 100 ksi (approximately 250, 415, and 700 Mpa)
2. Maximum compressive residual stresses of 0, 10, and 20 ksi (0, 70, and 140 Mpa)
3. Five initial out-of-straightnesses ranging from 0 to 0.004L
4. Slenderness ratios ranging from 20 to 240.

The mode of failure was flexural buckling about the minor axis. The results of this condition are presented graphically in the work by Batterman and Johnston (1967), and permit the maximum-strength evaluation within the range of the parameters cited. On the basis of a maximum residual stress of 13 ksi (90 Mpa), which is the scaled average maximum for the five sections shown in Fig. 3.3, together with a yield stress of 36 ksi (250 Mpa), the maximum column strength predicted by Batterman and Johnston is shown by the solid circles in Fig. 3.5. The solid curves are from an analysis neglecting the webs. Although the shapes and the residual stress distributions are different, there is good correlation between the two independently developed analysis procedures.

The findings of Batterman and Johnston are corroborated by those of a wide-ranging investigation of column strength, which examined the behavior and strength of a large and diverse number of structural shapes, grades of steel, and manufacturing methods (Bjorhovde, 1972). Bjorhovde's computational procedure is very accurate but requires knowledge of the residual stresses and the out-of-straightness. The work was performed at Lehigh University and included the full range of practical structural steel grades and shapes. A number of welded built-up box and H-shapes were also examined.

The results provided by the studies of Batterman and Johnston (1967) and Bjorhovde (1972) show clearly that:

1. The separate effects of residual stress and initial out-of-straightness cannot be added to give a good approximation of the combined effect on the maximum column strength. In some cases, and for some slenderness ratios, the combined effect is less than the sum of the parts (intermediate slenderness ratios, low residual stresses). In other cases the combined effect is more than the sum of the parts. The latter applies to the intermediate slenderness ratio range for heavy hot-rolled shapes in all steel grades and for welded built-up H-shapes. It is emphasized that the magnitudes of the maximum compressive residual stresses in a large number of these shapes were 50% or more of the yield stress of the steel.
2. As would be expected, residual stresses had little effect on the maximum strength of very slender columns, either straight or initially crooked. Such members have strengths approaching the Euler load. Very slender higher strength steel columns, however, can tolerate much greater lateral deflection before yielding or otherwise becoming unstable.
3. Strengths are slightly underestimated in a computer analysis that is based on the assumption that the initial out-of-straightness will remain in the shape of a half-sine wave during further loading.
4. Differences in column strength caused by variations in the shape of the residual stress pattern are smaller for initially crooked columns than for initially straight columns. This is a result of the early flexural behavior of the initially curved members.

Additional data on the residual stresses and column strengths of very heavy hot-rolled shapes confirmed the findings of Brozzetti et al. (1970a). The relative maximum column strength (i.e., computed maximum strength divided by the yield load) reaches a minimum for flange thicknesses around 3 to 4 in. (75 to 100 mm). The relative strength increases as the flange thickness exceeds this magnitude (Bjorhovde, 1988; 1991).

Residual Stresses in Welded Built-Up Shapes Residual stresses resulting either from welding or from the manufacturing of the component plates have a significant influence on the strength of welded H- and box-section columns. The maximum tensile residual stress at a weld or in a narrow zone adjacent to a flame-cut edge is generally equal to or greater than the yield stress of the plates (Alpsten and Tall, 1970; McFalls and Tall, 1970; Alpsten, 1972a; Brozzetti et al., 1970b; Bjorhovde et al., 1972). Welding modifies the prior residual stresses due either to flame cutting or cooling after rolling.

Figure 3.6 shows that the strengths of welded columns made of higher-strength steels appear to be influenced relatively less by residual stresses than are the strengths of similar columns made of lower-strength steels (Kishima et al., 1969; Bjorhovde, 1972). It is also evident that the differences in strengths of columns with the maximum permissible initial out-of-straightness are less than the differences in critical loads of initially straight columns (see Fig. 3.5).

As shown in Fig. 3.7, plates with mill-rolled edges (often referred to as universal mill plates) have compressive residual stresses at the plate edges, whereas flame-cut plates have tensile residual stresses at the edges. In built-up H-shapes made of universal mill plates, the welding increases the compressive stress at the flange tips, enlarging the region of compressive residual stress and adversely affecting the column strength. Conversely, as illustrated in Fig. 3.8, an H-shaped column made from flame-cut plates will have favorable tensile residual stresses at the flange tips and will therefore have greater strength than a column of the same section with flanges consisting of universal mill plates. It is also seen that for short welded

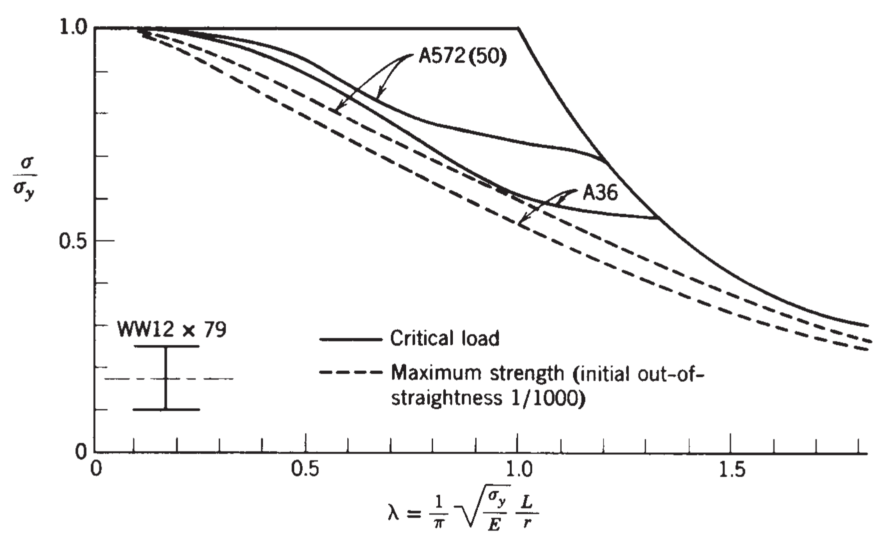

FIGURE 3.6 Critical-load curves for welded WW12X79 of flame-cut plates compared with maximum-strength curves for initially curved members (Kishima et al., 1969; Bjorhovde, 1972).

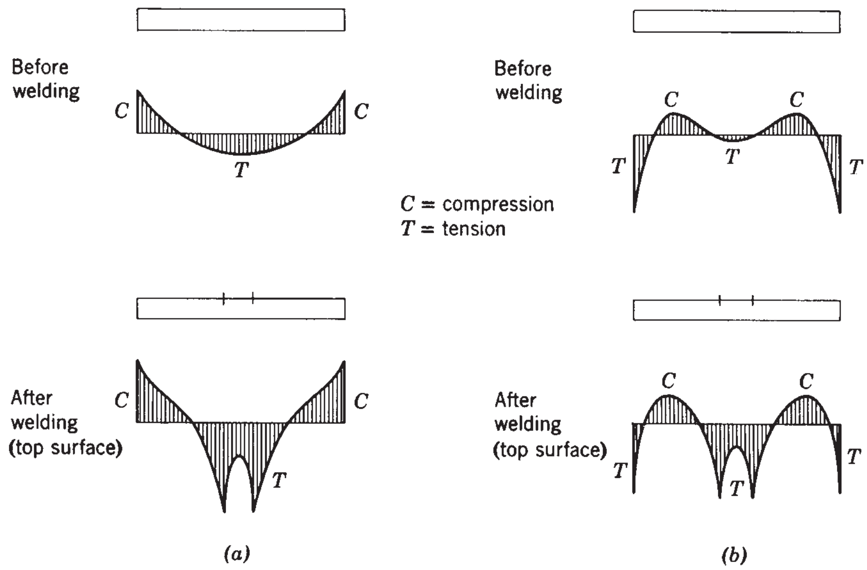

FIGURE 3.7 Qualitative comparison of residual stresses in as-received and center-welded (a) universal mill plate; (b) oxygen-cut plate.

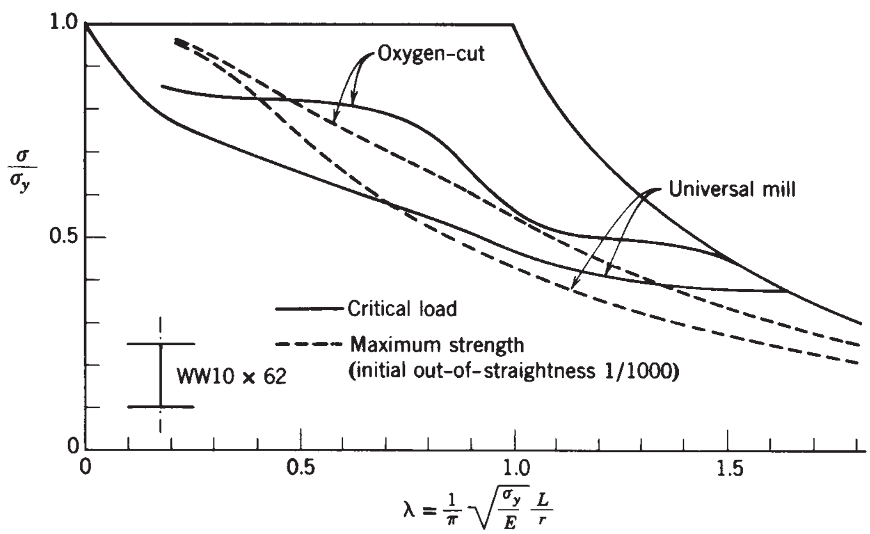

FIGURE 3.8 Comparison of column curves for WW10X62 (A7 steel) with universal mill versus oxygen-cut plates (Bjorhovde, 1972).

columns the maximum strength of an initially curved column may in some cases be greater than the critical load of a straight column. Obviously, the maximum strength of an initially straight column will always be greater than the critical load of the same column with an initial imperfection.

Strength differences between boxsection columns made of universal mill and flame-cut plates tend to be very small because the edge welds override the residual stresses in the component plates (Bjorhovde and Tall, 1971). The sequence of welding can be a significant factor for such columns, particularly for those with large welds (Beer and Tall, 1970).

Several investigations have considered the effects of column size. It has been shown conclusively that welding has a greater influence on the overall distribution of residual stress in small- and medium-sized shapes than in heavy shapes (Kishima et al., 1969; Alpsten and Tall, 1970; Brozzetti et al., 1970b; Bjorhovde et al., 1972).

The distribution of residual stress in heavy plates and shapes is not uniform through the thickness (Brozzetti et al., 1970a; Alpsten and Tall, 1970). As the thickness increases, the difference between surface and interior residual stresses may be as high as 10 ksi (70 Mpa). As an example, Fig. 3.9 shows an isostress diagram for a heavy welded shape made from flame-cut plates. It has been found, however, that calculated critical loads and maximum column strengths are only

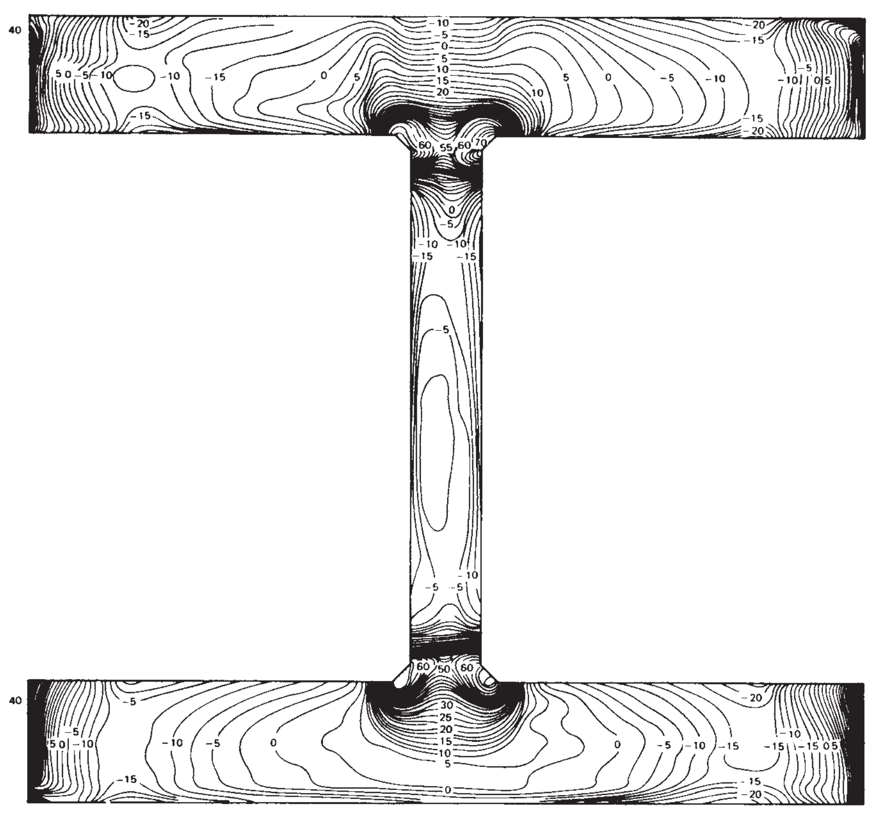

FIGURE 3.9 Isostress diagrams for WW23X681 welded built-up shape (stresses in kips per square inch) (Alpsten and Tall, 1970).

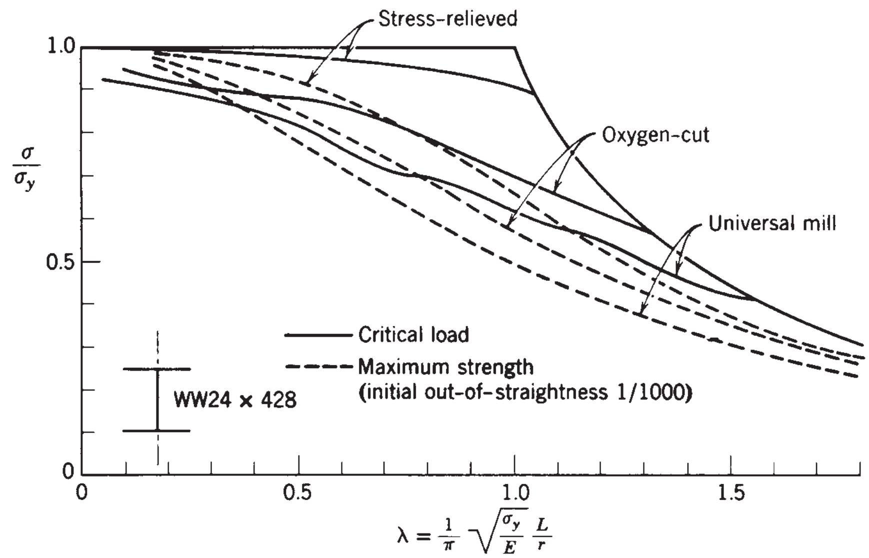

FIGURE 3.10 Column curves for heavy and light welded wide-flange shapes (Bjorhovde, 1972).

a few percent less when based on the complete residual stress distributions, as compared with analyses that assume the stress to be constant through the thickness and equal to the surface-measured residual stress.

In general, shapes made from flame-cut plates exhibit higher strength than shapes that are made from universal mill plates. This is demonstrated by the curves in Fig. 3.10. Similarly, flame-cut shapes tend to have strengths that are comparable with those of similar rolled shapes, whereas universal mill shapes tend to be comparatively weaker.

Figure 3.11 compares the strengths of two typical welded columns with flame-cut flange plates, and one being distinctly heavier than the other. It is seen that the heavier shape tends to be relatively stronger than the lighter one. This is even more accentuated for shapes that are welded from universal mill plates, for which the strength of the lighter shape will be significantly lower than the heavy one (Bjorhovde and Tall, 1971; Bjorhovde, 1972).

In a major study, Chernenko and Kennedy (1991) examined an extensive range of welded built-up H-shapes. In addition to performing maximum-strength computations for columns with a variety of residual stress distributions and out-of-straightnesses, the work also examined statistical data on material and other properties. Resistance factors for use with limit states criteria for welded columns were developed. It is shown that current approaches are conservative. As a consequence, since 1994 these shapes (made from plates with flame-cut edges) have been assigned to the higher of the two column curves of the CSA steel design standard (CSA, 2009).

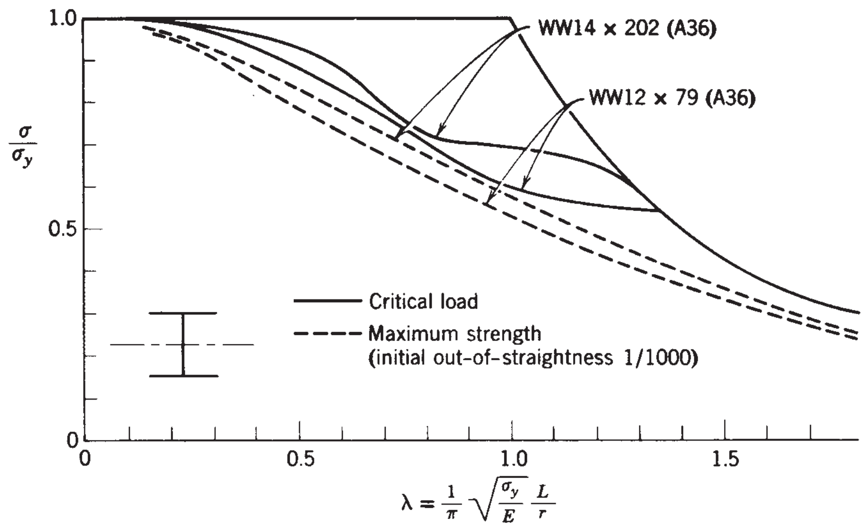

FIGURE 3.11 Comparison of column curves for WW24X428 (A36 steel) with stress-relieved, oxygen-cut, and universal mill plates (Bjorhovde, 1972).

The sequence of welding and the number of welding passes are factors that influence the distribution of residual stresses. Other welding parameters, such as voltage, speed of welding, and temperature and areas of preheating, have less influence (Brozzetti et al., 1970b). Stress-relief annealing of the component plates prior to welding of the shape raises column strength very significantly by reducing the magnitude of the residual stresses, even though it lowers the yield stress of the steel. Figure 3.10 compares the column curves for shapes made from flame-cut and universal mill plates, along with curves for the same shapes made from stress-relieved plates.

Residual Stresses in Cold-Straightened Columns Cold straightening of structural sections to meet tolerances for camber and sweep induces a redistribution and reduction of the residual stresses that were caused by earlier rolling and cooling. In current practice for all steel mills around the world, shapes are cold straightened as a matter of course, either by rotary or gag straightening (Brockenbrough, 1992; Bjorhovde, 2006). In rotary straightening the shape is passed through a series of rolls that bend the member back and forth with progressively diminishing deformation. In gag straightening, concentrated forces are applied locally along the length of the member to bend it to the required straightness. Rotary straightening is applied for small- and medium-size shapes; gag straightening is typically used for heavy shapes.

The rotary straightening process redistributes and reduces the initial residual stresses in the flanges, as shown in Fig. 3.12. In gag straightening, moments that approximate the full plastic value, M_p, are produced at the points where the forces

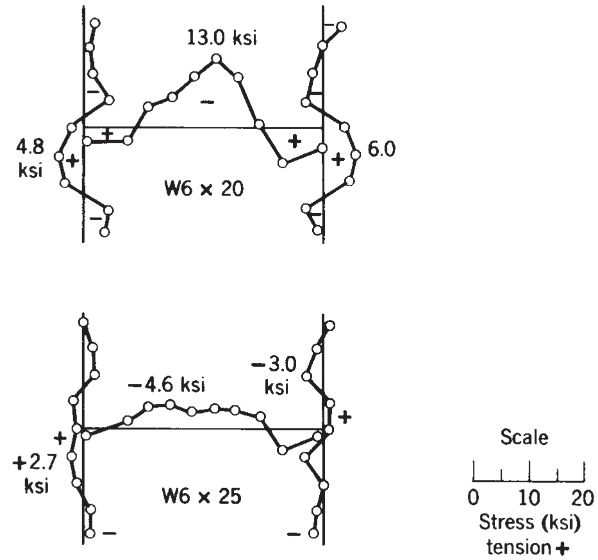

• Q1

FIGURE 3.12 Residual stresses in roller-straightened shapes,

are applied, and the cooling residual stresses are therefore redistributed only at or near the points of gag pressing. In the usual case of gag straightening, to remove sweep (curvature about the minor axis of a wide-flange shape), the change in residual stress from compression to tension takes place locally at the edges on the side of the flanges where the load is applied. Figure 3.13 shows the residual stresses measured in a W8X31 shape after gag straightening about the minor axis (Huber, 1956). It should be noted that a W8X31 would most likely not be gag straightened today, and instead it would be run through the rotary procedure.

The strength of a cold-straightened column is generally greater than that of the corresponding as-rolled member because of the improved straightness and the redistribution of residual stress (Frey, 1969; Alpsten, 1970). Rotary straightening produces a greater improvement than gag straightening, and according to theoretical analyses and experimental results the column strength may be increased by as much as 20% when compared at the same slenderness ratio and initial out-of-straightness (Alpsten, 1970, 1972b).

The strength and behavior of cold-straightened columns still have not been documented satisfactorily, and research should be undertaken to detail all of the individual influences and effects. This is particularly important in view of the fact that almost all hot-rolled wide-flange shapes are straightened in the mill to meet straightness requirements.

For tubular shapes the situation is somewhat different. The final mill process in most cases is cold forming or rolling, producing a very small initial out-of-straightness, which is then followed in some mills by partial stress relieving (Birkemoe, 1977a; Bjorhovde and Birkemoe, 1979). This is also the case for welded built-up wide-flange columns (Chernenko and Kennedy, 1991).

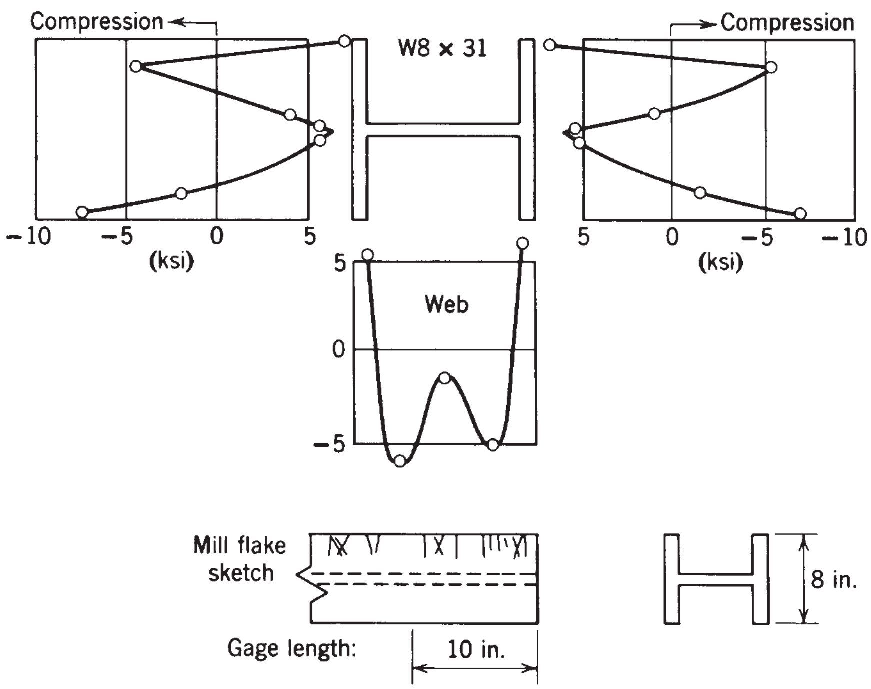

FIGURE 3.13 Residual stresses in a gag-straightened shape, bent about the weak axis to remove sweep (Huber, 1956).

3.3.2 Out-of-Straightness

Another major factor influencing the behavior of columns is the initial out-of-straightness (also referred to as initial crookedness or initial curvature). Some of the characteristics of the behavior and strength of inelastic, initially curved columns have been discussed in the previous evaluation of residual stress influences, and the two parameters interact in many ways. The explanation of the ranges of slenderness ratios and column types, for which the combined effect of residual stress and initial crookedness is more than the sum of the parts, emphasizes the complexity of the phenomenon.

The analyses that have been made of the strength of inelastic, initially curved columns either have made use of assumed values and shapes of the initial out-of-straightness, or have used measured data. The former is by far the most common, mostly because the measurements that are available for columns are scarce. This applies in particular to the magnitude of the maximum out-of-straightness, normally assumed to occur at midlength of the member, as well as the shape of the bent member. The latter is usually thought to be that of a half sine wave (Batterman and Johnston, 1967; Bjorhovde, 1972). The real configuration of the initial out-of-straightness of a column may be very complicated, often expressed as a simultaneous crookedness about both principal axes of the cross section. Systematic measurements have been made in some laboratories in conjunction with testing programs (Beer and Schultz, 1970; Bjorhovde, 1972, 1977; Bjorhovde and Birkemoe, 1979; Fukumoto et al., 1983, Essa and Kennedy, 1993), but very few data are available for columns in actual structures (Tomonaga, 1971; Lindner and Gietzelt, 1984; Beaulieu and Adams, 1980). Chernenko and Kennedy (1991) measured the out-of-straightness of welded wide-flange shapes at the steel mill.

Magnitudes and Limitations The magnitude of the maximum initial out-of-straightness is limited by the structural steel delivery specifications (e.g., ASTM A6 in the United States; CSA G40.20 in Canada) and is normally expressed as a fraction of the length of the member. Hot-rolled wide-flange shapes are required to have a maximum initial crookedness of $L/960$ [measured as 1/8 in. (3 mm) in 10 ft (3 m) of length], which is usually given as $L/l000$ for convenience. Tubular shapes are required to meet a straightness tolerance of $L/480$, commonly given as $L/500$.

The measurements that are available show that most hot-rolled W-shapes tend to have values toward the maximum permissible, with an average of $L/1470$ (Bjorhovde, 1972), although Dux and Kitipornchai (1981) and Essa and Kennedy (1993) give a mean value for the maximum initial imperfection of $L/3300$ and $L/2000$, respectively, for wide-flange shapes of lengths of 20 to 33 feet (6 to 10 m). Tubular members typically exhibit values significantly smaller than the specification limitations, with out-of-straightnesses on the order of $L/3000$ to $L/8000$, with an average of $L/6300$ (Bjorhovde, 1977; Bjorhovde and Birkemoe, 1979). The data for welded wide-flange shapes indicate a relatively small initial crookedness, with a mean of approximately $L/3300$ (Chernenko and Kennedy, 1991). With this in mind, it is rare to encounter columns with out-of-straightnesses larger than the maximum permitted.

In the development of column strength criteria such as the SSRC curves (Bjorhovde, 1972) and the ECCS curves (Beer and Schultz, 1970), the maximum permissible values of the initial out-of-straightness were utilized. This was done for several reasons, the primary one being that $L/1000$ constituted the upper limit of what is acceptable for actually delivered members and therefore could be regarded as a conservative measure. On the other hand, because mean characteristics were used for the other strength parameters, it can be rationally argued that the mean values for out-of-straightness also should be utilized. This was done by Bjorhovde (1972) in parallel with his development of the original SSRC curves, using the mean of $L/1470$ that was determined through statistical evaluations. The resulting multiple column curves are shown in Fig. 3.14, where the curves labeled as 1P, 2P, and 3P have used $L/1470$. For comparison, the SSRC curves have been included in the figure; these have used an initial out-of-straightness of $L/1000$. The mathematical equations for both sets of curves are given in Section 3.5.

Variations in the magnitude of the initial crookedness were considered in the study by Bjorhovde (1972). The strengths of the 112 columns that were included in the investigation were examined using maximum initial out-of-straightnesses of

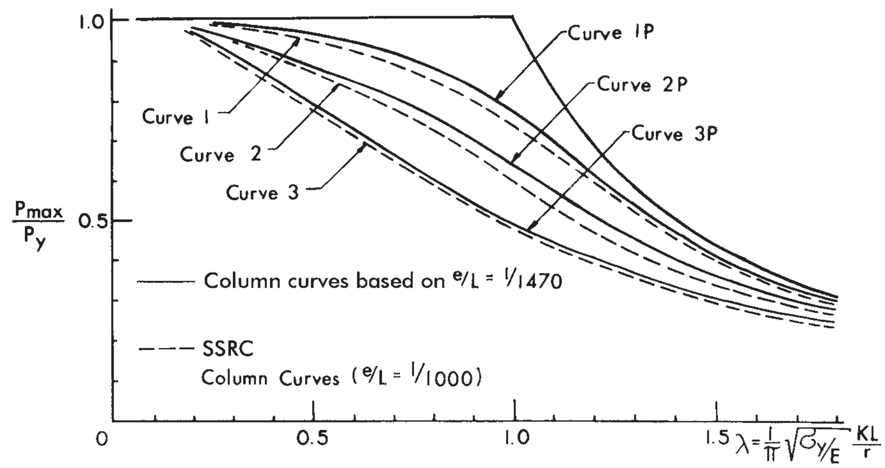

FIGURE 3.14 Comparison of multiple column curves developed on the basis of mean out-of-straightness ($L/1470$) and maximum permissible out-of-straightness ($L/1000$) (Bjorhovde, 1972).

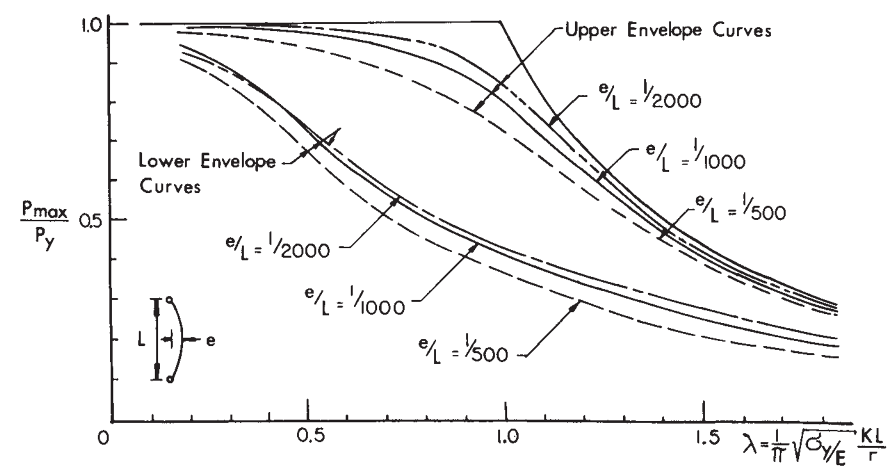

FIGURE 3.15 Column curve bands for 112 columns, based on initial out-of-straightnesses of $L/500$, $L/1000$, and $L/2000$ (Bjorhovde, 1972).

$L/500$, $L/2000$, and $L/10{,}000$. The results for the band of column strength curves are given in Fig. 3.15 (curves that are shown include only the data for $L/500$ to $L/2000$). The results of the studies on the maximum strength of columns emphasize the need for incorporation of the initial out-of-straightness into column strength models that form the basis for design criteria.

3.4 INFLUENCE OF END RESTRAINT

Extensive studies on the influence of end restraint on the strength and behavior of columns have been conducted by Chen (1980), Jones et al. (1980, 1982), Razzaq and Chang (1981), Chapuis and Galambos (1982), Vinnakota (1982, 1983, 1984), and Shen and Lu (1983), among others. In addition, the analysis of frames with semi-rigid connections has been dealt with in several studies (DeFalco and Marino, 1966; Romstad and Subramanian, 1970; Frye and Morris, 1975; Ackroyd, 1979; Lui and Chen, 1988; Nethercot and Chen, 1988; Goto et al, 1993; King and Chen, 1993, 1994; Kishi et al., 1993a,b).

A series of important international workshops on connections in steel structures has provided a large number of references related to the behavior and strength of connections, the influence of connections on column and frame stability, detailed evaluations of methods of frame analysis, and the development of design criteria that take these effects into account. Called semi-rigid or partially restrained (PR) connections, the state-of-the-art of their impact on column stability is very advanced, although design criteria offer only limited practical suggestions. Eurocode 3 (CEN, 2005) provides the most specific criteria, including a classification system for connections. Such a system has also been developed by Bjorhovde et al. (1990). Finally, the Commentary to the AISC specification (AISC, 2005a) offers an extensive assessment of column and frame stability as influenced by connection behavior and strength.

The publications of the international connections workshops are given in the following books, which are listed here because of the large number of papers that are provided by these works:

1. Bjorhovde, Reidar; Brozzetti, Jacques; and Colson, Andre (1988), *Connections in Steel Structure—Behaviour, Strength and Design*, Elsevier Applied Science, London, England.
2. Bjorhovde, Reidar; Colson, Andre; Haaijer, Geerhard; and Stark, Jan W. B. (1992), *Connections in Steel Structures II—Behavior, Strength and Design*, AISC, Chicago, Illinois.
3. Bjorhovde, Reidar; Colson, Andre; and Zandonini, Riccardo (1996), *Connections in Steel Structures III—Behaviour, Strength and Design*, Pergamon/ Elsevier Science, London, England.
4. Leon, Roberto; and Easterling, W. Samuel (2002), *Connections in Steel Structures I—Behavior, Strength and Design*, AISC, Chicago, Illinois.
5. Bijlaard, F. S. K.; Gresnigt, A. M.; and van der Vegte, G. J. (2005), *Connections in Steel Structures V—Behaviour, Strength and Design*, Bouwen met Staal, The Netherlands.
6. Bjorhovde, Reidar; Bijlaard, F. S. K; and Geschwindner, L. F. (2008), *Connections in Steel Structures VI—Behavior, Stremgth amf Design*, AISC, Chicago, Illinois.

3.4.1 Column Stability as Influenced by End Restraint

Column investigations have examined different aspects of restrained-member behavior, specifically determining the influence of:

1. Type of beam-to-column connection
2. Length of column
3. Magnitude and distribution of residual stress
4. Initial out-of-straightness

The frame analysis studies have focused on evaluations of the drift characteristics of frames with less than fully rigid connections, in part prompted by a study by Disque (1975). Frame-related subjects of this kind, however, are beyond the scope of this chapter. In fact, connection flexibility and member instability are closely related, and their interaction effects can have a significant influence on the overall performance of the frame.

As would be expected, the stiffness of the restraining connection is a major factor. One illustration of the influence is given by the moment–rotation curves in Fig. 3.16 and another by the load–deflection curves for columns with different end restraint that are shown in Fig. 3.17. A British wide-flange shape was used for the data generated for Fig. 3.17, incorporating an initial out-of-straightness of $L/1000$. The curves that are shown apply for a slenderness ratio of $L/r = 120$ ($\lambda = 1.31$), but similar data were developed for longer as well as shorter columns. Other investigators have provided additional load–deflection curves and the primary differences between the individual studies are the methods of column analysis and end-restraint modeling. The resulting load–deflection curves are very

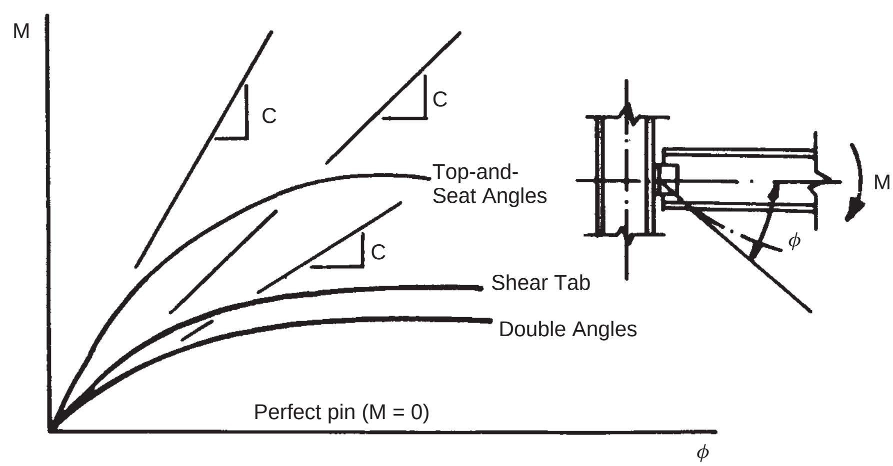

FIGURE 3.16 Moment–rotation curves for some typical simple connections (schematic).

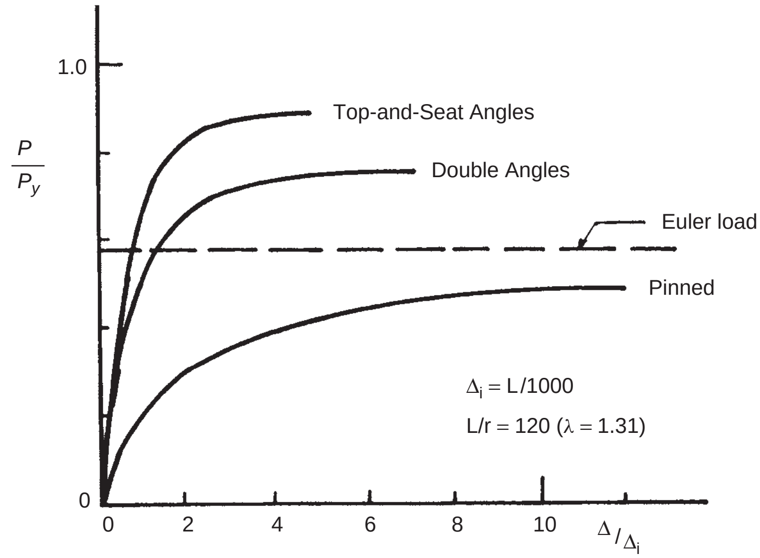

FIGURE 3.17 Typical load–deflection curves for columns (Jones et al., 1982).

similar (Jones et al., 1980, 1982; Razzaq and Chang, 1981; Sugimoto and Chen, 1982).

Figure 3.17 also includes the load–deflection curve for a pin-ended column. As is evident from the figure, the greater the connection restraint, the stiffer will be the initial response of the column, and the greater the maximum load that can be carried as compared to a pin-ended column. The same relative picture emerges for all slenderness ratios, although the magnitude of the increase becomes small for values of L/r less than 50.

A further illustration of the influence of end restraint is given by the data in Fig. 3.18, which shows column strength curves for members with a variety of end conditions (Jones et al., 1982; Lui and Chen, 1983a). The effect of the connection type is again evident, as is the fact that the influence diminishes for shorter columns. Also included in the figure is the Euler curve as well as SSRC curve 2.

It is emphasized that the connections that were used to develop the column curves in Fig. 3.18 are all of the "simple" or partially restrained type. The potential for the structural economies that may be gained by incorporating the end restraint into the column design procedure is clear, although the realistic ranges for the values of λ must be borne in mind and the possible use of bracing to reduce frame drift in designing semirigid frames with flexible base joints must be considered. The ranges for λ have been delineated in Fig. 3.18 for steels with yield stresses of 36 and 50 ksi (250 and 345 Mpa). Consequently, the very large column strength increases that have been reported by several researchers are real (Chen, 1980; Jones et al., 1980, 1982; Razzaq and Chang, 1981; Sugimoto and Chen, 1982; Lui and Chen, 1983b), but they occur for slenderness ratios that are in excess of practical

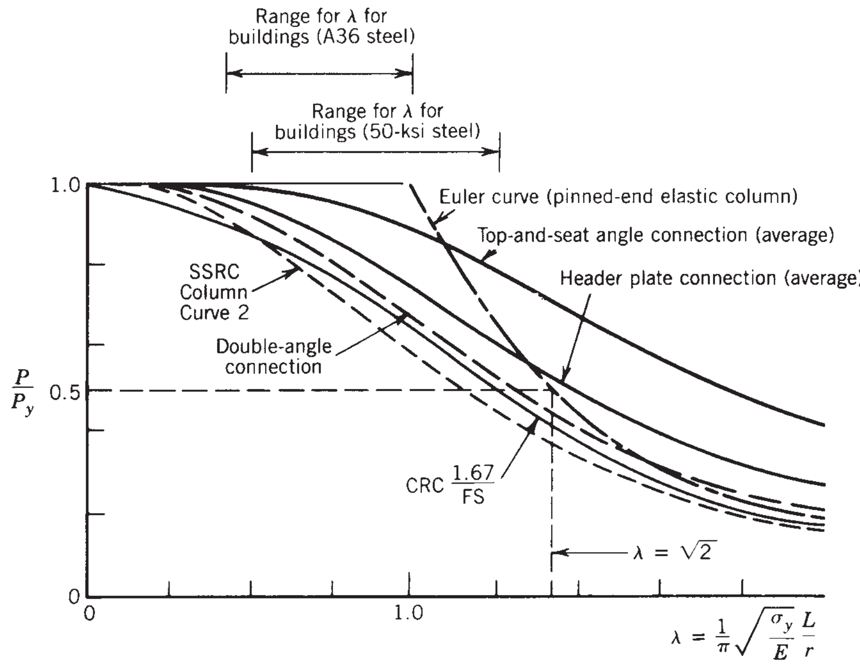

FIGURE 3.18 Column curves for members with different types of end restraint.

values (Bjorhovde, 1981; Ackroyd and Bjorhovde, 1981). In general, end restraint clearly increases strength.

Using the individual column strength studies as the basis, much research has demonstrated the application of end restraint to the design of columns in frames (Bjorhovde, 1984; Chen and Lui, 1991; Chen and Sohal, 1995; Chen et al., 1996). Taking into account actual connection stiffness and the influence of beams, effective-length factors for columns in frames have been developed. The method incorporates the use of alignment charts for the effective length of framed columns and recognizes that buckling of a column in a frame is influenced by the end-restraint relative stiffness distribution factor, G_r, given as

$$G_r = \frac{\sum (EI/L)_{columns}}{C^*} \tag{3.5}$$

where C^* is the effective end restraint that is afforded to a column in a beam and column subassemblage, using connections whose initial stiffness is C, the initial slope of the moment–rotation curve. Barakat and Chen (1990) state that the initial connection stiffness should be used for the design of columns in braced frames, but a secant connection stiffness based on the beam-line concept should be used for columns in unbraced frames. The key findings of this study have been corroborated by major projects aimed at developing practical design methods for semirigid frames (Christopher and Bjorhovde, 1999; Surovek et al., 2005). In particular, the studies of Surovek et al. (2005) provide significant advances in practical applications, and include close correlation with the direct analysis approach of the AISC specification (AISC, 2005a).

The G_r procedure can incorporate design recommendations as well as applications of inelastic K-factor principles, as developed by Yura (1971), expanded by Disque (1973), refined by Barakat and Chen (1990), and implemented in Chen and Lui (1991) and Chen et al. (1996). Practical design examples illustrate the potential for significant structural economies. It is emphasized, however, that in all these methods of analysis the data for the actual end-restraint characteristics of the connection are required. Specifically, the C value must be known. This is a significant drawback, but connection classification schemes similar to those provided by Bjorhovde et al. (1990) and the approaches of Eurocode 3 (CEN, 2005) are useful.

Numerous studies have been aimed at developing methods of accounting for the connection flexibility in providing effective end restraint to framed columns. An extensive review of research on the behavior and modeling of connections is provided in Chen (1987, 1988), Chen and Lui (1991), Beedle (1993), and Chen et al. (1996). Based on the evaluation of different connection models available in the literature, a three-parameter connection power model proposed by Kishi and Chen (1990), together with its large database (Kishi and Chen, 1986; Chen and Kishi, 1989) and design aids (Kishi et al., 1993a), can be recommended for general use.

3.4.2 Effective-Length Factors

The effective-length factor, K, was discussed briefly when introduced in Eq. 3.2. This concept has seen extremely wide acceptance and use for stability assessments of columns in various types of structures since its introduction in the AISC specification in 1961. Despite its wide acceptance, however, it is recognized that the K-factor approach involves a number of major assumptions. Refinements for effective-length computations continue to be made by researchers (e.g., Hellesland and Bjorhovde, 1996a,b), but at the same time it is also recognized that the analytical and computational tools that are available to engineers today clearly necessitate more comprehensive procedures. The direct analysis method (Surovek et al., 2005) that is presented in the most recent AISC specification (AISC, 2005a) is clearly the preferred approach. Detailed examination of this and other procedures is presented in Chapter 16.

The coverage of effective column length in this chapter is limited to certain idealized cases and to certain special situations that occur in compression members of trusses. The effective-length concept has also been applied to members of nonprismatic cross section, whereby they are converted to an equivalent pin-ended member with an effective second moment of area that refers to a particular location of the member (Jimenez and Galambos, 2001).

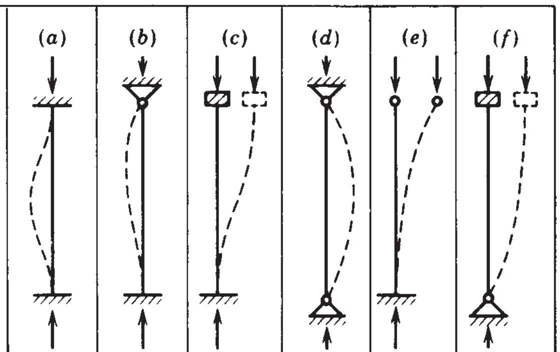

	(a)	(b)	(c)	(d)	(e)	(f)
Buckled shape of column is shown by dashed line						
Theoretical K value	0.5	0.7	1.0	1.0	2.0	2.0
Recommended K value when ideal conditions are approximated	0.65	0.80	1.2	1.0	2.10	2.0

End condition code	
	Rotation fixed, Translation fixed
	Rotation free, Translation fixed
	Rotation fixed, Translation free
	Rotation free, Translation free

FIGURE 3.19 Effective-length factors K for centrally loaded columns with various end condition.

Figure 3.19 gives theoretical K values for idealized conditions in which the rotational and/or translational restraints at the ends of the column are either full or nonexistent. At the base, shown fixed for conditions a, b, c, and e in Fig. 3.19, the condition of full fixity is approached only when the column is anchored securely to a footing for which the rotation is negligible. Restraint conditions a, c, and f at the top are approached when the top of the column is framed integrally to a girder many times more rigid than itself. Column condition c is the same as a except that translational restraint is either absent or minimal at the top. Condition f is the same as c except that there is no rotational restraint at the bottom. The recommended design values of K (see Fig. 3.19) are modifications of the ideal values that reflect the fact that neither perfect fixity nor perfect flexibility is attained in practice. The notion of the perfect pin, however, is retained simply for conservatism (e.g., condition d).

The more general determination of K for a compression member as part of any framework requires the application of methods of indeterminate structural analysis, modified to take into account the effects of axial load and inelastic behavior on the rigidity of the members. Gusset plate effects can be included, and for this case extensive charts for modified slope–deflection equations and for moment–distribution stiffness and carryover factors, respectively, have been developed (Goldberg, 1954; Michalos and Louw, 1957). These procedures are not suitable for routine design, but they can be used to determine end restraints and result in modified effective lengths of the component members of a framework.

3.4.3 Effective-Length Factors in Trusses

In triangulated frameworks (trusses), the loads are usually applied at the joints. Thus, if the joints are truly pinned, the members are axially loaded. Deflections of the joints and the truss as a whole are caused by the axial deformations of the members. The angles between members meeting at a joint also change because of these deformations. If the members are connected together at the joints by welds or bolts, the angle changes produce secondary bending stresses. These have little effect on the buckling strength (and tensile strength) of the truss members. Because of local yielding of extreme fibers of the members near the joints, the secondary moments gradually dissipate as the truss is loaded to its ultimate strength. They can therefore be neglected in the buckling analysis (Korol et al., 1986).

When a truss is designed and loaded such that all members reach their factored resistances simultaneously, no member restrains any other. Therefore, the effective-length factors for compression chord members and compression diagonals would be 1.0 for in-plane buckling. In a roof truss of constant or nearly constant depth, and where the compression chord has the same cross section for the full length of the truss, this does not occur, and K may be taken as 0.9. In a continuous truss, K may be taken as 0.85 for the compression chord connected to the joint where the force in the chord changes to compression.

When the magnitude of the force in the compression chord changes at a subpanel point that is not braced normal to the plane on the main truss (Fig. 3.20a), the effective-length factor for chord buckling normal to the plane of the main truss can be approximated from the two compressive forces P_2 and P_1, as follows:

$$K = 0.75 + 0.25\left(\frac{P_1}{P_2}\right) \qquad (3.6)$$

where $P_2 < P_1$.

Web members in trusses designed for moving live loads may be designed with $K = 0.85$. This is because the position of the live load that produces maximum force in the web member being designed will result in less than the maximum forces in members framing into it, so that rotational restraints are developed.

The design of vertical web members, U_iL_i, of a K-braced truss (Fig. 3.20b) should be based on the effective length KL. Web-member buckling occurs normal to the plane of the truss, and Eq. 3.6 again applies. Also, P_2 is negative in Eq. 3.6 because it is a tensile force. When P_1 and P_2 are equal but opposite in sign, Eq. 3.6 yields a value of $K = 0.5$.

For buckling normal to the plane of a main truss, the web compression members should be designed for $K = 1$ unless detailed knowledge of the makeup of the cross frames (perpendicular to the truss) is available.

In the case of redundant trusses, there is reserve strength above the load at initial buckling of any compression member. Masur (1954) has reviewed developments

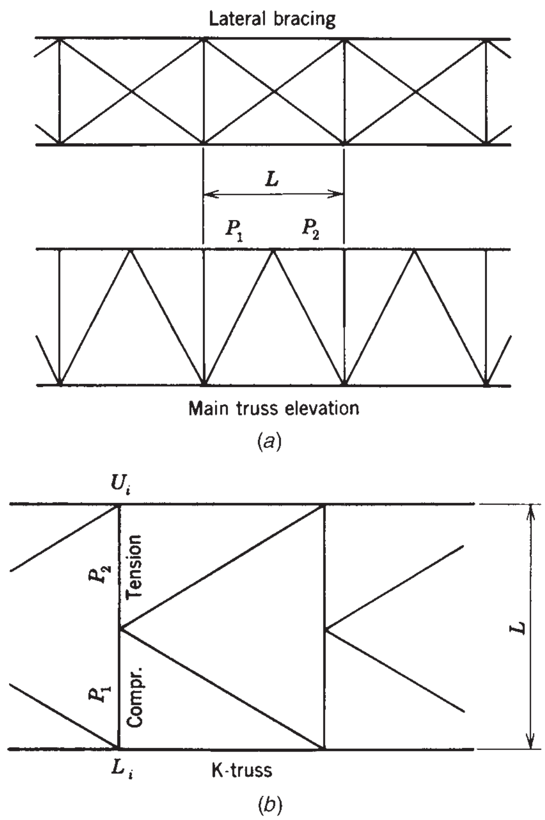

FIGURE 3.20 Effective-length factors in trusses: (*a*) compression chords; (*b*) compression verticals.

on this subject and established upper and lower bounds for the ultimate load of the buckled members of elastic redundant trusses.

3.4.4 Faulty Column Bracing Detail

Numerous structural failures have occurred because of a misunderstanding of the end restraint provided by the structural arrangement shown in Fig. 3.21. The beam (or truss) is continuous over the top of the column. The critical components are the column in compression, compression in the bottom flange of the beam or chord of the truss, and no bottom-flange bracing at point a and possibly other points, b. The sway at the top of the column shown in section B-B can result in a K factor much greater than 2.0. The bottom flange of the beam can possibly provide bracing to the top of the column if there are braces at points b and consideration is given to the compression in the flange when evaluating its stiffness. In general, a brace, such as a bottom chord extension from the joist, should be used at point a. Beam

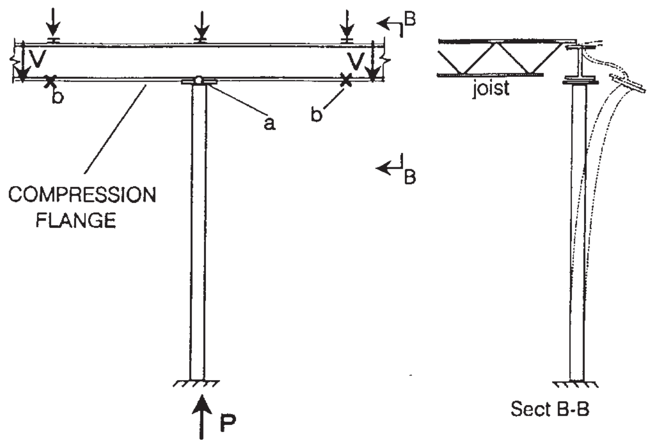

FIGURE 3.21 Structural detail with probable instability.

web stiffeners at the column location will also be effective unless bottom flange lateral buckling is critical.

3.5 STRENGTH CRITERIA FOR STEEL COLUMNS

The position of the SSRC on the basis for the design of columns is stated in Technical Memorandum[2] No. 5 and can be summarized with the following quote:

> Maximum strength, determined by the evaluation of those effects that influence significantly the maximum load-resisting capacity of a frame, member, or element, is the proper basis for the establishment of strength design criteria.

The proper column strength model is therefore one that incorporates both residual stresses and initial out-of-straightness.

3.5.1 Column Design Curves

Multiple Column Curves In a wide-ranging, landmark study, Bjorhovde (1972) examined the deterministic and probabilistic characteristics of column strength in general and developed an extensive database for the maximum strengths of centrally loaded compression members. Covering the full practical range of shapes, steel grades, and manufacturing methods, the study demonstrated the wide variability of column strength. Figure 3.22 illustrates this variability through a collection of 112 maximum-strength column curves. Subsequent and parallel investigations

[2]All SSRC technical memorandums are provided in Appendix B.

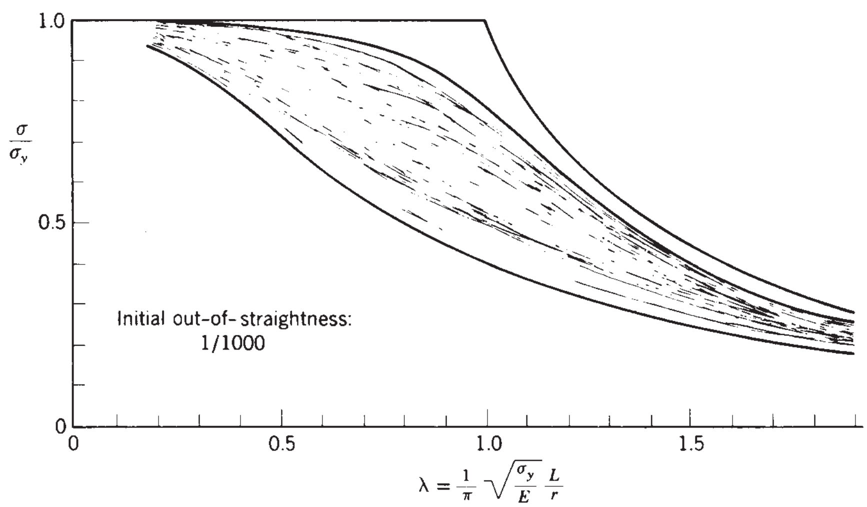

FIGURE 3.22 Maximum-strength column curves for a number of different column types (Bjorhovde, 1972).

of other researchers have added to and confirmed this relatively wide band of column strength (Birkemoe, 1977a; Bjorhovde, 1988, 1991; Bjorhovde and Birkemoe, 1979; Fukumoto et al., 1983; Jacquet, 1970; Kato, 1977; Sherman, 1976).

The key problem in developing a rational, representative, and sufficiently reliable column strength criterion is how to take this large variability into account. This may be achieved by using a mean or other central curve of the band of strength variation of Fig. 3.22, or it may be done by subdividing the band into groups of curves with a mean or similar curve for each group. The latter defines the *multiple column curve concept* (Bjorhovde and Tall, 1971; Bjorhovde, 1972).

Research and development leading to the use of multiple column curves were actively pursued from the late 1950s to the early 1980s. In 1959, the German standard DIN 4114 introduced a special curve for tubes and another curve for all other shapes. Subsequently, the work under the auspices of the ECCS (Beer and Schultz, 1970; Jacquet, 1970; Sfintesco, 1970) resulted in recommended design application and code adoption in several countries (Sfintesco, 1976). The ECCS curves in somewhat modified form are now part of the column design criteria of Eurocode 3 (CEN, 2005). In 1984, the CSA adopted SSRC curve 1 for use with heat-treated tubes; CSA had earlier (1974) adopted SSRC curve 2 as the basic column strength criterion and in 1994 assigned welded wide-flange columns made from a flame-cut plate to SSRC column curve 1 (Chernenko and Kennedy,1991).

Research basic to the development of multiple column curves in North America was conducted at Lehigh University starting in the 1960s (Bjorhovde and Tall, 1971; Bjorhovde, 1972, 1988), and elsewhere (Birkemoe, 1977a,b; Bjorhovde, 1977; Bjorhovde and Birkemoe 1979; Kato, 1977; Sherman, 1976). In addition to length, cross-section dimensions, and the material properties, the maximum strength of steel columns depends on (1) the residual stress magnitude and distribution, (2) the shape and magnitude of the initial out-of-straightness, and (3) the end restraint. The effects of these three variables were discussed in Sections 3.3 and 3.4. Unless special procedures are utilized in the manufacture of steel columns, such as stress relieving or providing actual pins at each end, all three of these effects are present and should be accounted for. The state-of-the-art is such that if the following information is known, accurate calculation of the maximum strength is possible (Bjorhovde, 1972, 1978, 1988; Chen and Lui, 1985):

1. *Material properties* (i.e., the yield stress, σ_y, and the modulus of elasticity, E). In some cases it is necessary to know the variation of the yield stress across the cross section (e.g., welded built-up shapes) or the entire stress–strain curve (e.g., cold-formed shapes).
2. *Cross-section dimensions*. For nonprismatic columns the dimensions along the column length must be known.
3. *Distribution of the residual stresses* in the cross section, including variations through the plate thickness if the shape is tubular or if the plate elements are thick.
4. *Shape and magnitude of the initial out-of-straightness.*
5. *Moment–rotation relationship of the end restraint.*

Maximum strength may be calculated by postulating suitable but realistic idealizations so that closed-form algebraic expressions may be derived or one of many available numerical techniques may be used. In numerical calculations it is usually assumed that deformations are small and that plane sections remain plane. The literature on determining the maximum strength of columns is rich and diverse, but the major methods are described in various textbooks (e.g., Chen and Atsuta, 1976; Chen and Han, 1985).

Residual stresses, initial out-of-straightness, and end restraint vary randomly, and complete statistical information is lacking for most shapes and design situations. In particular, data on end restraint in terms of beam-to-column moment–rotation curves are limited; this is a result of the great variety of connections that are used in steel construction practice. Techniques for evaluating end-restraint effects have been discussed in Section 3.4, and much research has been conducted over the past 25 years (Ackroyd, 1979; Chen, 1980; Jones et al., 1980; 1982; Ackroyd and Bjorhovde, 1981; Bjorhovde, 1981, 1984, 1988; Bjorhovde et al., 1990; Chapuis and Galambos, 1982; Christopher and Bjorhovde, 1999; Lui and Chen, 1983a,b; Sugimoto and Chen, 1982; Shen and Lu, 1983; Surovek et al., 2005). The five books that were published after the international workshops on connections in steel structures provide a large database for analytical and design approaches. The publication data for these books are given in Section 3.4; they are also listed among the references for this chapter. Although the procedures that have been developed are applicable to a range of problems, additional work needs to be done to make such concepts suitable for design specifications.

The reference compression element continues to be the pin-ended, centrally loaded column. The key research work that focused on this issue and the studies that were done for multiple column curves used this basic column concept. An answer to the problem of a suitable specification format was provided by Bjorhovde (1972), who proceeded as detailed in the following.

A computerized maximum-strength analysis was performed first on basic data available from column tests performed at Lehigh University, and it was demonstrated that the method of numerical analysis gave accurate predictions of the test strengths. Next, a set of 112 column curves was generated for members for which measured residual stress distributions were available, assuming that the initial out-of-straightness was of a sinusoidal shape having a maximum amplitude of 1/l000 of the column length and that the end restraint was zero. These shapes encompassed the major shapes used for columns, including rolled and welded shapes from light to heavy dimensions. The column curves thus obtained represent essentially the complete spectrum of steel column behavior. The resulting curves are shown in Fig. 3.22.

Bjorhovde then observed that there were definite groupings among the curves, and from these, three subgroups were identified, each giving a single "average" curve for the subgroup (Bjorhovde and Tall, 1971; Bjorhovde, 1972). The resulting three curves are known as *SSRC column strength curves* 1, 2, *and* 3, and they are reproduced in Figs. 3.23 through 3.25. These figures contain:

1. The number of column curves used as a basis for the statistical analysis and the width of their scatter band
2. The calculated 2.5 and 97.5 percentile lower and upper probability limits for the particular set of curves
3. The column types to which each of the three curves is related

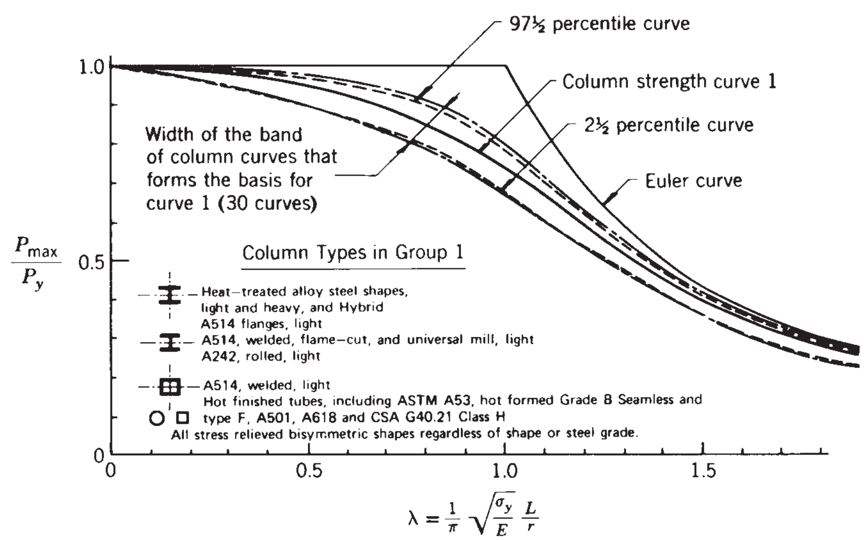

FIGURE 3.23 SSRC Column strength curve 1 for structural steel (Bjorhovde, 1972) (based on maximum strength and initial out-of-straightness of $\delta_0 = 0.001L$).

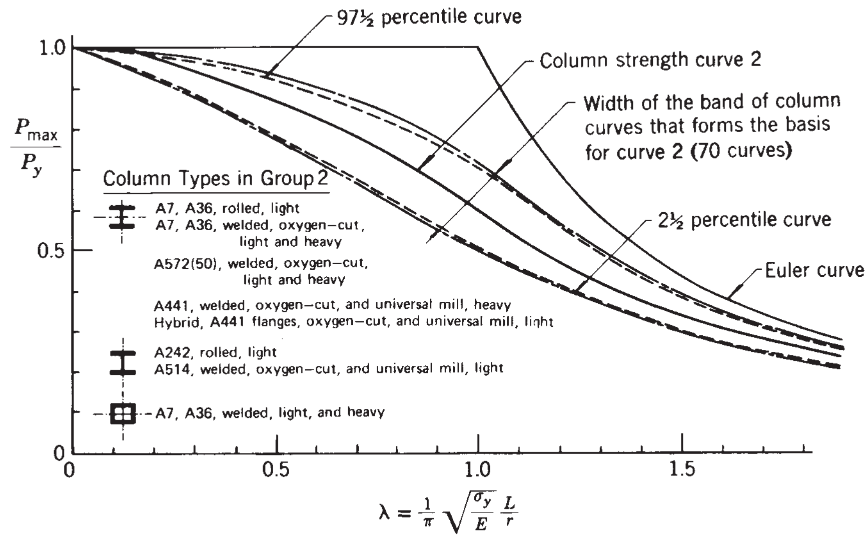

FIGURE 3.24 SSRC column strength curve 2 for structural steel (Bjorhovde, 1972) (based on maximum strength and initial out-of-straightness of straightness of $\delta_0 = 0.001L$).

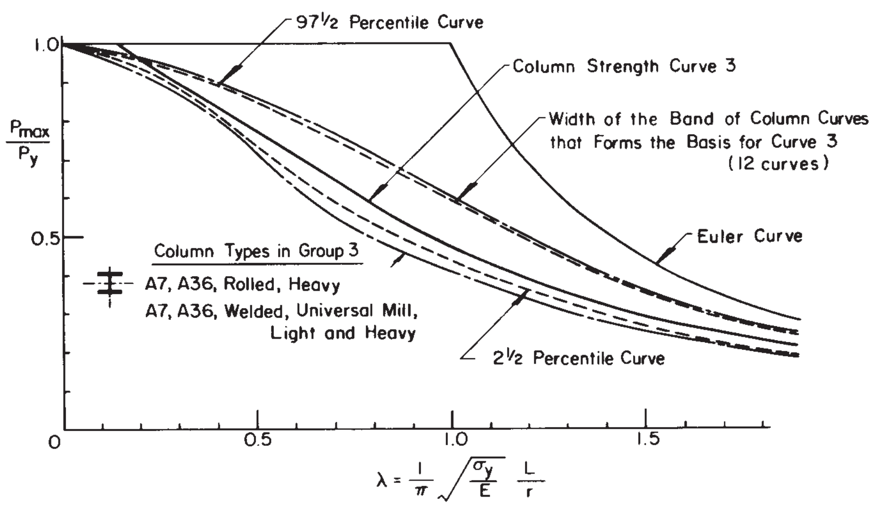

FIGURE 3.25 SSRC column strength curve 2 for structural steel (Bjorhovde, 1972) (based on maximum strength and initial out-of-straightness of straightness of $\delta_0 = 0.001L$).

Algebraic representations of the three column strength curves were obtained by curve fitting, and the resulting equations are as follows:

SSRC curve 1:

$$
\begin{array}{lll}
1. & 0 \le \lambda \le 0.15 & \sigma_u = \sigma_y \\
2. & 0.15 \le \lambda \le 1.2 & \sigma_u = \sigma_y (0.990 + 0.112\lambda - 0.367\lambda^2) \\
3. & 1.2 \le \lambda \le 1.8 & \sigma_u = \sigma_y (0.051 + 0.801\lambda^{-2}) \\
4. & 1.8 \le \lambda \le 2.8 & \sigma_u = \sigma_y (0.008 + 0.942\lambda^{-2}) \\
5. & \lambda \ge 2.8 & \sigma_u = \sigma_y \lambda^{-2} (\text{Euler curve})
\end{array}
\tag{3.7}
$$

SSRC curve 2:

$$
\begin{array}{lll}
1. & 0 \le \lambda \le 0.15 & \sigma_u = \sigma_y \\
2. & 0.15 \le \lambda \le 1.0 & \sigma_u = \sigma_y (1.035 - 0.202\lambda - 0.222\lambda^2) \\
3. & 1.0 \le \lambda \le 2.0 & \sigma_u = \sigma_y (-0.111 + 0.636\lambda^{-1} + 0.087\lambda^{-2}) \\
4. & 2.0 \le \lambda \le 3.6 & \sigma_u = \sigma_y (0.009 + 0.877\lambda^{-2}) \\
5. & \lambda \ge 3.6 & \sigma_u = \sigma_y \lambda^{-2} (\text{Euler curve})
\end{array}
\tag{3.8}
$$

SSRC curve 3:

$$
\begin{array}{lll}
1. & 0 \le \lambda \le 0.15 & \sigma_u = \sigma_y \\
2. & 0.15 \le \lambda \le 0.8 & \sigma_u = \sigma_y (1.093 - 0.622\lambda) \\
3. & 0.8 \le \lambda \le 2.2 & \sigma_u = \sigma_y (-0.128 + 0.707\lambda^{-1} - 0.102\lambda^{-2}) \\
4. & 2.2 \le \lambda \le 5.0 & \sigma_u = \sigma_y (0.008 + 0.792\lambda^{-2}) \\
5. & \lambda \ge 5.0 & \sigma_u = \sigma_y \lambda^{-2} (\text{Euler curve})
\end{array}
\tag{3.9}
$$

These expressions can also be represented accurately by a single equation (Rondal and Maquoi, 1979; Lui and Chen, 1984), as shown below. The maximum deviations from the SSRC curves are −2.1 to +3.6%.

$$\sigma_u = \frac{\sigma_y}{2\lambda^2}\left(Q - \sqrt{Q^2 - 4\lambda^2}\right) \le \sigma_y \tag{3.10}$$

where

$$Q = 1 + \alpha\,(\lambda - 0.15) + \lambda^2 \tag{3.11}$$

and

$$\alpha = \begin{cases} 0.103 & \text{for curve 1} \\ 0.293 & \text{for curve 2} \\ 0.622 & \text{for curve 3} \end{cases}$$

Another expression with a single parameter n in a double exponential representation is used in the Canadian steel design standard CSA S16–09 (CSA, 2009; Loov, 1996)

$$\sigma_u = F_y \left(1 + \lambda^{2n}\right)^{-1/n} \tag{3.12}$$

where n equals 2.24 for curve 1 and 1.34 for curve 2. Loov (1996) also provided the value 0.96 for curve 3, although this curve was not adopted by the CSA standard, primarily because welded built-up shapes using universal mill plates are not representative of Canadian practice. These expressions give strengths generally within 1% of the polynomials of Eqs. 3.7 through 3.9 and are never more than 3% unconservative.

Bjorhovde (1972) also developed multiple column curves where the initial out-of-straightness was equal to its mean value of 1/1470 of the column length (Fig. 3.14). The mathematical equations describing these curves are as follows:

SSRC curve 1P:

$$\begin{array}{lll} 1. & 0 \le \lambda \le 0.15 & \sigma_u = \sigma_y \\ 2. & 0.15 \le \lambda \le 1.2 & \sigma_u = \sigma_y(0.979 + 0.205\lambda - 0.423\lambda^2) \\ 3. & 1.2 \le \lambda \le 1.8 & \sigma_u = \sigma_y(0.030 + 0.842\lambda^{-2}) \\ 4. & 1.8 \le \lambda \le 2.6 & \sigma_u = \sigma_y(0.018 + 0.881\lambda^{-2}) \\ 5. & \lambda \ge 2.6 & \sigma_u = \sigma_y\lambda^{-2}(\text{Euler curve}) \end{array} \tag{3.13}$$

SSRC curve 2P:

$$\begin{array}{lll} 1. & 0 \le \lambda \le 0.15 & \sigma_u = \sigma_y \\ 2. & 0.15 \le \lambda \le 1.0 & \sigma_u = \sigma_y(1.030 - 0.158\lambda - 0.206\lambda^2) \\ 3. & 1.0 \le \lambda \le 1.8 & \sigma_u = \sigma_y(-0.193 + 0.803\lambda^{-1} + 0.056\lambda^{-2}) \\ 4. & 1.8 \le \lambda \le 3.2 & \sigma_u = \sigma_y(0.018 + 0.815\lambda^{-2}) \\ 5. & \lambda \ge 3.2 & \sigma_u = \sigma_y\lambda^{-2}(\text{Euler curve}) \end{array} \tag{3.14}$$

SSRC curve 3P:

$$\begin{array}{lll} 1. & 0 \le \lambda \le 0.15 & \sigma_u = \sigma_y \\ 2. & 0.15 \le \lambda \le 0.8 & \sigma_u = \sigma_y(1.091 - 0.608\lambda) \\ 3. & 0.8 \le \lambda \le 2.0 & \sigma_u = \sigma_y(0.021 + 0.385\lambda^{-1} - 0.066\lambda^{-2}) \\ 4. & 2.2 \le \lambda \le 4.5 & \sigma_u = \sigma_y(0.005 + 0.900\lambda^{-2}) \\ 5. & \lambda \ge 4.5 & \sigma_u = \sigma_y\lambda^{-2}(\text{Euler curve}) \end{array} \tag{3.15}$$

A single expression for all of the SSRC-P curves has not been developed; however, this can be achieved relatively easily using the approaches of Ronda1 and Maquoi (1979), Loov (1996), or Rotter (1982). The single curve that is used in

Chapter E of the previous AISC (1999) Load and Resistance Factor Design (LRFD) specification and the unified AISC (2005a) specification is identical to SSRC 2P. Two equations are used to describe this curve for two regions of slenderness, λ_c (employed in the 1999 specification), or stress ratio F_y/F_e (employed in the 2005 specification). The equations give the same results. For the 1999 specification:

$$F_{cr} = \begin{cases} (0.658^{\lambda_c^2})F_y & \text{for } \lambda_c \leq 1.5 \\ \left(\dfrac{0.877}{\lambda_c^2}\right)F_y & \text{for } \lambda_c > 1.5 \end{cases} \tag{3.16a}$$

where the first equation applies for inelastic buckling and the second equation applies for elastic buckling. For the 2005 specification:

$$F_{cr} = \begin{cases} [0.658^{F_y/F_e}]F_y & \text{for } \dfrac{KL}{r} \leq 4.71\sqrt{\dfrac{E}{F_y}} \quad (\text{or } F_e \geq 0.44F_y) \\ 0.877F_e & \text{for } \dfrac{KL}{r} > 4.71\sqrt{\dfrac{E}{F_y}} \quad (\text{or } F_e < 0.44F_y) \end{cases} \tag{3.16b}$$

where F_e is the Euler flexural buckling stress for the slenderness ratio *KL/r* and F_y $(= \sigma_y)$ is the specified minimum yield stress.

Design Procedure Alternatives It was demonstrated in the preceding section that it is possible to develop multiple column curves into which column types can be grouped for convenience. In developing column design criteria, the following questions should be considered:

1. *What should be the shape and the amplitude of the initial out-of-straightness?* As to the shape, there is general agreement that a sinusoidal shape with the maximum amplitude at midlength is a conservative and reasonable assumption. The maximum amplitude is a crucial quantity, because changes affect the strength, especially in the intermediate slenderness range. Knowledge about initial out-of-straightness is available from measurements of laboratory specimens used for column tests, but there is a lack of field data. Initial out-of-straightness is a function of the manufacturing process, and some column types, such as manufactured tubes, tend to be very straight. In the development of the SSRC and ECCS multiple column curves the position was taken that an initial amplitude of 1/1000 of the length, essentially the mill tolerance, is a reasonable and conservative value for the basis of developing column curves.

In opposition, it can be argued that all geometric imperfections are small enough so that their effect can be relegated to be accounted for by the resistance factor. This was the underlying philosophy of the use of the CRC column curve, which has its basis in tangent-modulus theory, with a factor of safety that depends on the column slenderness ratio. This design approach was entirely sensible when it was initially formulated in the 1950s, but a large body of research work has since shown that the maximum strength can be determined from a knowledge of initial imperfections and the proper design and use of steel columns must take the out-of-straightness explicitly into account.

A task force of SSRC (1985) took an intermediate position, recommending that the basis for the development of design curves for steel columns should be an initial out-of-straightness of 1/1500 of the length. This is close to the average measured in laboratory columns (Bjorhovde, 1972; Fukumoto et al., 1983) and reflects the position of the SSRC in this matter. For all practical purposes, Eqs. 3.13 through 3.15 represent this condition. By its adoption of Eqs. 3.16a and 3.16b, AISC is effectively using $L/1500$ as the governing out-of-straightness criterion.

2. *Should design be based on the concept of multiple column curves or should one composite column curve be used for the design of all steel columns?* The European answer to this question has been to recommend multiple column curves, as shown in Fig. 3.26. As a first step in North America, in 1974 the CSA in 1974 adopted the use of SSRC curve 2 as the basic design curve. In 1984, the CSA also adopted SSRC curve 1 for hollow structural sections, either hot formed or cold formed to final shape and then heat treated. This recommendation was based in part on research on such columns (Bjorhovde, 1977; Birkemoe, 1977b; Bjorhovde and Birkemoe, 1979; Kennedy and Gad Aly, 1980). The original reluctance to adopt multiple column curves for the American structural steel design specification was founded on the belief that the design criteria would become too complicated. Another reason was that it was felt necessary to complete certain additional studies, to ensure that all conceivable column types and materials would be properly assigned to one of the three strength categories (Bjorhovde, 1980). The results of

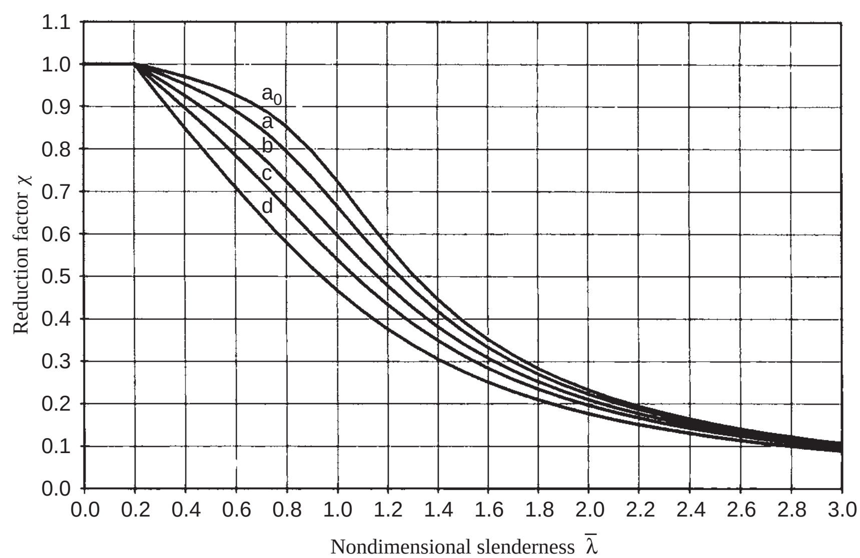

FIGURE 3.26 Eurocode 3 multiple column curves (CEN, 2005).

Fabrication Details		Axis	Specified Minimum Yield Stress of Steel (ksi) ≤ 36	37 to 49	50 to 59	60 to 89	≥ 90
Hot-rolled W-shapes	Light and medium W-shapes	Major	2	2	1	1	1
		Minor	2	2	2	1	1
	Heavy W-shapes (flange over 2 in.)	Major	3	2	2	2	2
		Minor	3	3	2	2	2
Welded Built-up H-shapes	Flame-cut plates	Major	2	2	2	1	1
		Minor	2	2	2	2	1
	Universal mill plates	Major	3	3	2	2	2
		Minor	3	3	3	2	2
Welded Box Shapes	Flame-cut and universal mill plates	Major	2	2	2	1	1
		Minor	2	2	2	1	1
Square and Rectangular Tubes	Cold-formed	Major	N/A	2	2	2	2
		Minor	N/A	2	2	2	2
	Hot-formed and cold-formed heat-treated	Major	1	1	1	1	1
		Minor	1	1	1	1	1
Circular Tubes	Cold-formed	N/A	2	2	2	2	2
	Hot-formed	N/A	1	1	1	1	1
All stress-relieved Shapes		Major and Minor	1	1	1	1	1

FIGURE 3.27 Column curve selection table (Bjorhovde, 1972, 1988).

this study are summarized in the column curve selection table (CCS table) shown in Fig. 3.27 (Bjorhovde, 1972, 1988). The CCS table will facilitate the column curve selection process and is also suited for a decision-table format for use with computer-based design.

3. *What end restraint should be assumed for nominally pin-ended columns?* As indicated in Section 3.4, any practical framing scheme or column base condition will increase the column strength. There are really no truly pin-ended columns in existence. Methods have been developed to use this end restraint in determining the maximum strength of columns, but the question of how to use the available information in design is still unresolved. Should explicit restraint factors for different kinds of end conditions be tabulated for use with effective-length-factor alignment charts, or should the design curves implicitly contain minimal end restraints? The latter approach was used in the development of the AISC column curve, which is based on an implicit end restraint producing an elastic effective-length factor of 0.96 ($G = 10$), as well as an initial out-of-straightness of 1/1500 of the length.

Summary In the previous discussion on the strength of steel columns, a number of alternatives were presented. Specification-writing groups need to make decisions to select the column curve or curves satisfying their needs. The necessary theory is available to do so, and much information is on hand. It is the SSRC's opinion that design criteria for steel columns should be based on a column with an initial out-of-straightness column and residual stresses. With this concept as a basis, intelligent choices for column design can be made, resulting in a rational method of design.

3.5.2 Development of Strength Design Criteria

The following gives a description of data and computational techniques that are needed for the development of maximum-strength column curves and other results for pin-ended, centrally loaded columns. Further details can be found in the references of Batterman and Johnston (1967), Bjorhovde (1972, 1988, 1992), Chen and Atsuta (1976), Chen and Han (1985), Chernenko and Kennedy (1991), Kennedy and Gad Aly (1980), and Albert et al. (1995).

When detailed strength and performance data are not available for a specific column shape, it is possible to develop column curves of types that are similar to those that have been presented in this guide. The following gives a brief outline of the assumptions that should be used, the types of data that are required, and the computational technique that is suitable for these types of problems.

Required Data The following data are needed for the computation of the maximum strength of columns:

1. Type of material and its material properties (i.e., yield stress, yield strain, modulus of elasticity).
2. Distribution of the residual stresses in the cross section, including variation through the thickness, if the shape is large or it is tubular.
3. Variation of the yield stress throughout the cross section. This is in most cases needed only for welded built-up shapes and cold-formed shapes, where the yield stress at a weld or a cold-formed corner, for example, may differ significantly from the nominal properties.
4. When the material is of a type or grade that exhibits nonlinear stress–strain characteristics (e.g., stainless steel), a complete, typical stress–strain curve is required.
5. Maximum value of the initial out-of-straightness.

Assumptions for the Analysis The following assumptions are normally conservative in nature, with the result that computed column strengths are usually somewhat less than those obtained in actual tests:

1. Material is linearly elastic, perfectly plastic.
2. The initial and all subsequent deflection shapes of the column can be described by a half sine wave.
3. The residual stresses are constant in an element of the cross section along the full length of the column.

4. Sections that are originally plane remain so for the range of deflections that is suitable for column studies.
5. Yielded fibers in the cross section will unload elastically.
6. The yield stress may vary across the width and through the thickness of the component plates of the cross section but does not vary along the length of the column.
7. In line with assumption 2, only stresses and strains at midlength of the column are considered in the analysis.

It should be pointed out that if detailed yield-stress and other material data are not available for the elements in the cross section, the results of a stub-column test (see Technical Memorandum No. 3 in Appendix B) can be used. If this is not available, tension test results for various parts of the shape can be used; the properties to utilize in the computations should then be based on a weighted average.

Computational Technique Maximum column strength requires the solution of a nonlinear problem. It is best achieved through an incremental, iterative computation algorithm. Internal force and moment equilibrium are established for every load and deflection level, requiring iteration over the cross section to determine when individual fibers yield, unload, or continue to load. The computations are carried to a level where the column cannot take any additional load when an additional amount of deflection is imposed; this constitutes the maximum strength level. It is recommended that deflection increments be used rather than load increments, as convergence problems may be encountered as the maximum load is approached when load increments are used. The procedure above leads to the development of a load–deflection curve for a column of given slenderness ratio or length. To obtain the complete column curve, the process must be repeated for a range of lengths. As an illustration of the basic steps in the column strength computations, Fig. 3.28 gives a flowchart that indicates the necessary major parts of the solution.

3.6 ALUMINUM COLUMNS

3.6.1 Material Properties

The stress–strain curves of aluminum alloys are rounded, or nonlinear, as distinct from the bilinear elastic–perfectly plastic curve used for some structural steels. In the absence of a yield plateau it is standard practice to define the yield stress as the 0.2% offset stress, $\sigma_{0.2}$. Alloying elements, heat treatment, and cold working influence the stress–strain curve but have little effect on the elastic modulus, which for tension falls within the range of 9900 to 10,200 ksi (68 to 70 Gpa) for other than aircraft alloys. A value of 10,000 ksi (68.3 Gpa) is often used.

Yield strength is more strongly influenced by heat treatment and cold working than is the ultimate strength. For precipitation heat-treated alloys there is also an

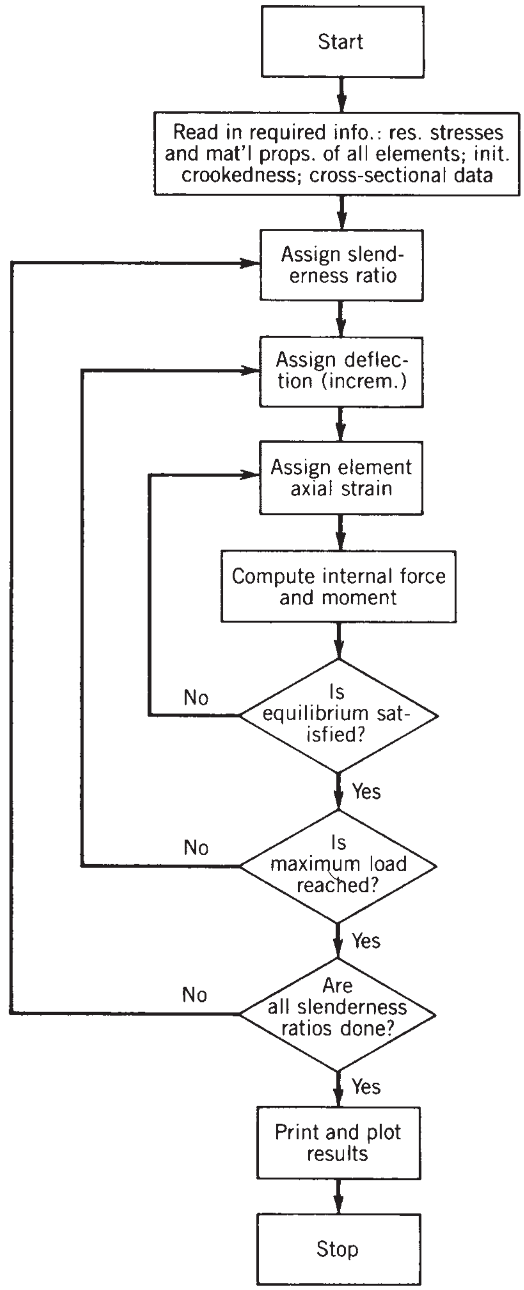

FIGURE 3.28 Flowchart for preparation of column strength curve.

increased sharpness of the "knee" between the elastic and plastic ranges, which is significant for columns in the lower range of slenderness ratios. For this reason, column formulas for aluminum alloys are divided into two groups, precipitation heat-treated tempers and all other tempers, which reflect the differing ratio $\sigma_{0.2}/\sigma_{0.1}$. Guaranteed values for the yield strength, defined by the 0.2% offset, and the ultimate strength are established at levels at which 99% of the material is expected to conform at a 0.95 confidence level. In practice, typical values are about 15% above the guaranteed value; thus, the use of the guaranteed value in a design formula which has been formulated on the basis of measured values provides an additional factor to be considered when selecting resistance factors for columns with short and medium slenderness ratios..

3.6.2 Imperfections

Deviations of real columns from the perfect geometric and material idealizations are of two essential forms: geometric imperfections such as eccentricity and initial out-of-straightness and built-in residual stresses such as those arising from welding. Residual stresses in aluminum extruded members are small because of the method of production and the straightening of the finished member by stretching. The fact that residual stress effects on column strength of aluminum extruded members are insignificant has been confirmed in European studies (Mazzolani and Frey, 1977). The value of the yield strength does not vary significantly across a profile (Bernard et al., 1973).

Welding introduces residual tensile stresses in the weld bead on the order of the yield strength for the annealed material and compressive stresses elsewhere. There is also a local reduction in mechanical properties affected by welding that is significant in precipitation heat-treated or cold-worked material. Residual stresses created by cold forming are related to the yield strength in the same manner as in steel; longitudinal bends, however, are considered to have little influence on column strength, as a result of either the residual stresses or any strain hardening. Geometric imperfections fall into two groups: those that are length dependent, such as initial out-of-straightness, and those independent of length, such as imperfections introduced by tolerances on cross-section dimensions.

Commercial tolerances on initial out-of-straightness are $L/960$ for most extruded structural members. If a member with such an initial out-of-straightness forms two or more bays of the chord of a truss, the final out-of-straightness will be negligible in comparison to the inaccuracies in the assembly. Even in laboratory tests, the initial out-of-straightness of the member as supplied has usually been less than the error in centering the specimen. End moments, due to frame action or eccentricities in joints, will in most cases dominate any moments due to initial crookedness. For large assembled columns, such as latticed masts, an initial out-of-straightness of $L/1000$ has been found to be representative, and design as a beam-column using this value has been adopted.

3.6.3 Strength of Aluminum Alloy Columns

In design applications, aluminum alloy column strength has generally been based on the tangent-modulus theory because of the good agreement with column test results. Evaluation of the maximum strength of both straight and initially crooked columns is practicable with computers. A systematic study of the effects of important parameters that affect column strength has been made by Batterman and Johnston (1967) and Hariri (1967).

Initially Straight Columns Such members were studied by Duberg and Wilder (1950), and Johnston (1963, 1964). In studying the behavior above the critical load, Batterman and Johnston (1967) assumed the stress–strain curve of the material to be represented by the average of a large number of tests of aluminum alloy 6061-T6. By considering both major and minor axis buckling of an H-type section, the practical range of the shape effect was approximately covered. A section having a depth equal to the width was chosen, with flange thickness approximately one-tenth of the depth, and with a web having a thickness two-thirds that of the flange. The maximum increase in strength above the tangent-modulus load was found to be about 2% for minor axis bending. This small difference further justifies the use of the tangent-modulus load as a reasonable basis for estimating the strength of initially straight aluminum alloy columns.

Columns with Initial Out-of-Straightness The maximum strength of initially curved pin-ended aluminum alloy columns can be evaluated by use of a computer, as described previously (Batterman and Johnston, 1967). For a typical Hshape of alloy 6061-T6 with buckling about the strong axis, Fig. 3.29 shows typical plots of load versus midlength lateral deflection for an L/r value of 40 and for initial midlength out-of-straightness ranging from zero to $0.004L$. Figure 3.30 illustrates the strength reduction factor, referenced to the critical load and plotted as a function of L/r for both major and minor axis bending.

The effects of initial out-of-straightness are accentuated in unsymmetrical sections, such as the Tsection, as illustrated by the computer-generated load–deflection curves in Fig. 3.31. An initial crookedness of $0.001L$ (with the flange on the convex side) reduced the ultimate strength in comparison with the tangent-modulus load by about 18% at $L/r = 40$, which is about twice the reduction shown in Fig. 3.30 for the doubly symmetric section. Buckling of axially loaded straight members (as confirmed by tests) will occur so as to put the flange of the T-section on the convex side of the column. The shaded lines at the top of Fig. 3.31 indicate the upper bounds of theoretical strength of a straight column, namely the inelastic buckling gradients and the reduced-modulus strengths for buckling in either of the two possible directions (Johnston, 1964). Tests have also indicated that the effect of end eccentricity is somewhat more deleterious than the effect of the same magnitude of initial out-of-straightness (Hariri, 1967).

The effect of end restraint on aluminum columns with an initial out-of-straightness has been studied by Chapuis and Galambos (1982). They conclude: “It

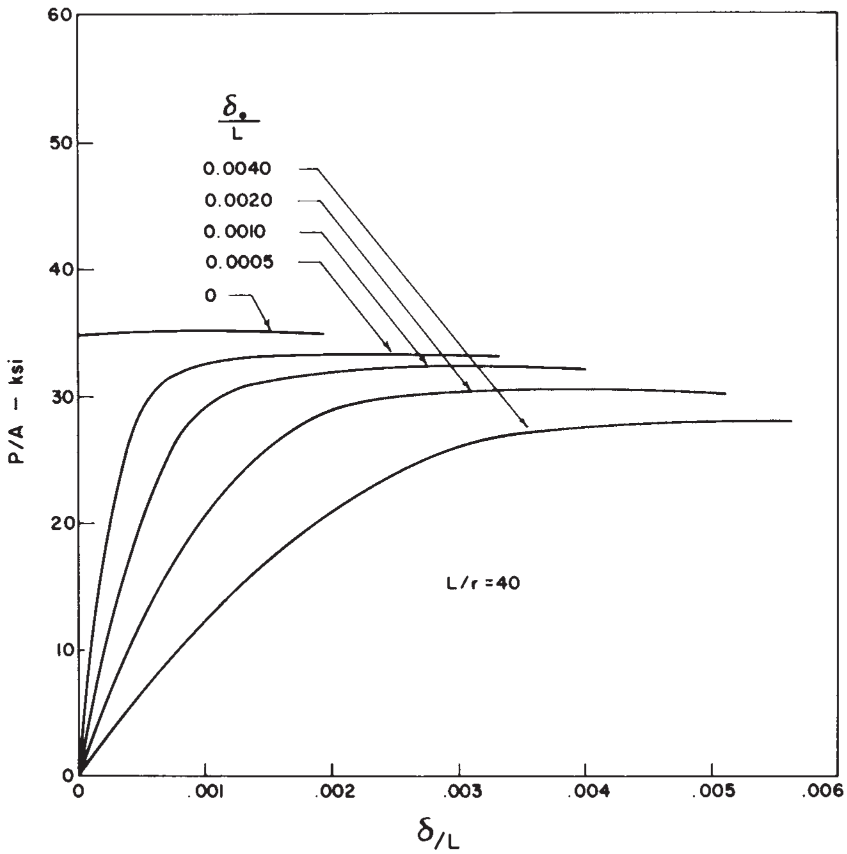

FIGURE 3.29 Effect of initial out-of-straightness on load–deflection relationships of an aluminum alloy column (Batterman and Johnston, 1967).

is conservative to base a design on K_{el} (the effective-length factor determined from elastic buckling analysis) and a column curve derived for pinned crooked columns."

3.6.4 Effects of Welding

For most alloys used in structural applications, the heat of welding reduces the strength of the metal in a narrow zone around the weld, thereby diminishing the capacity of columns of low and intermediate slenderness ratios. Welding can also introduce residual stresses and an initial out-of-straightness in the column. Rectangular section columns with longitudinal and transverse welds have been tested by Brungraber and Clark (1962). Wide-flange and tubular box section columns with longitudinal welds were tested by Mazzolani (1985), and experiments of tubular box section columns with transverse welds were performed by Hong (1991).

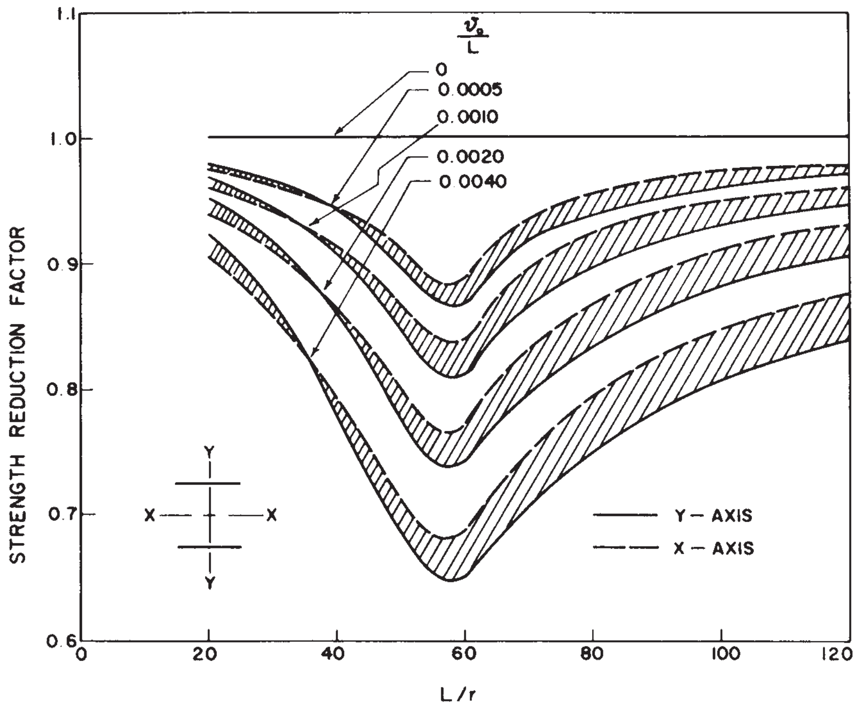

FIGURE 3.30 Ratio of maximum strength/tangent-modulus load of aluminum alloy columns for different amounts of initial out-of-straigthness (Batterman and Johnston, 1967).

Lai and Nethercot (1992) provided analytical results for aluminum wide-flange columns with transverse welds.

For columns with longitudinal welds or with transverse welds that affect only a portion of the cross section, the test values are reasonably predicted by

$$\sigma_{pw} = \sigma_n - \frac{A_w}{A}(\sigma_n - \sigma_w) \tag{3.17}$$

where

σ_{pw} = critical stress for columns with part of the cross section affected by welding

σ_n = critical stress for the same column if there were no welds

σ_w = critical stress for the same column if the entire cross section were affected by welding

A_w = area of affected zone

A = total area of cross section

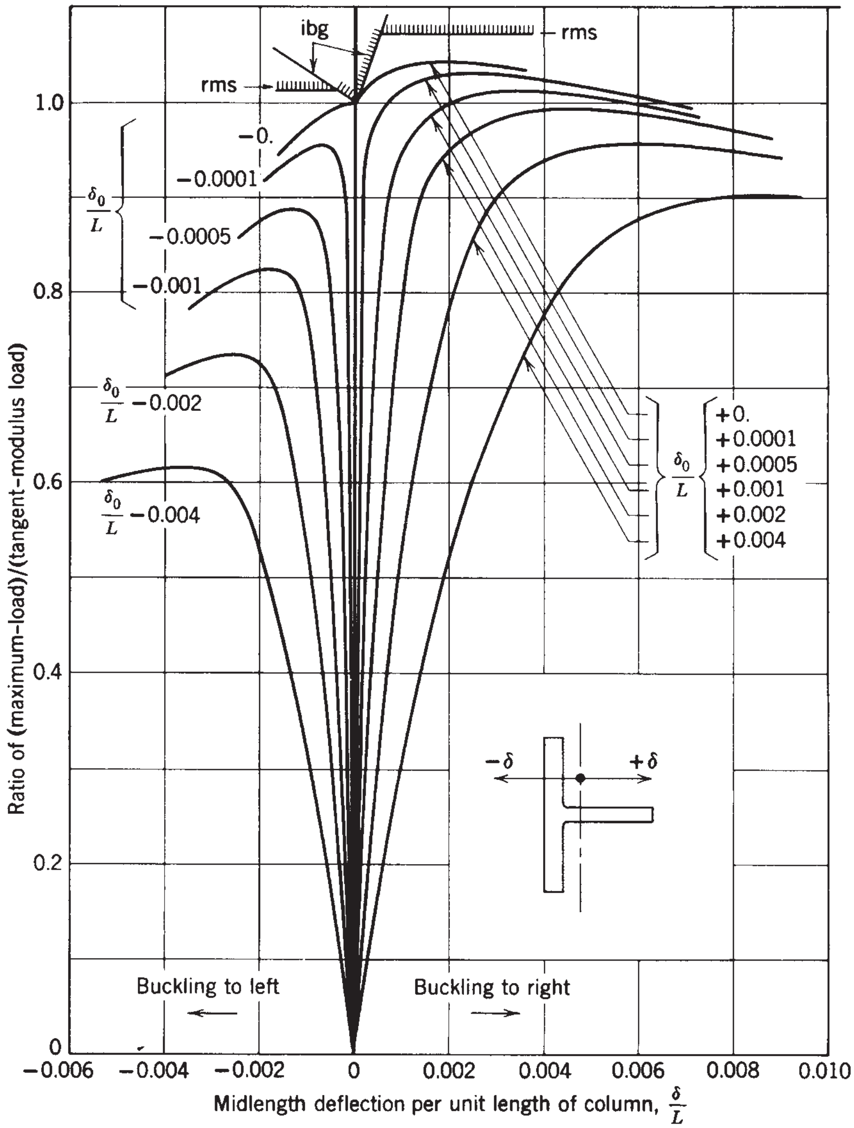

FIGURE 3.31 Theoretical behavior of straight and initially crooked T-section columns of aluminum alloy (Hariri, 1967).

Test data from Brungraber and Clark (1962) have been summarized by Sharp (1993) and are compared to straight-line approximations of predictions based on the tangent-modulus theory in Fig. 3.32 for columns with longitudinal welds and in Fig. 3.33 for columns with transverse welds. The measured values of the

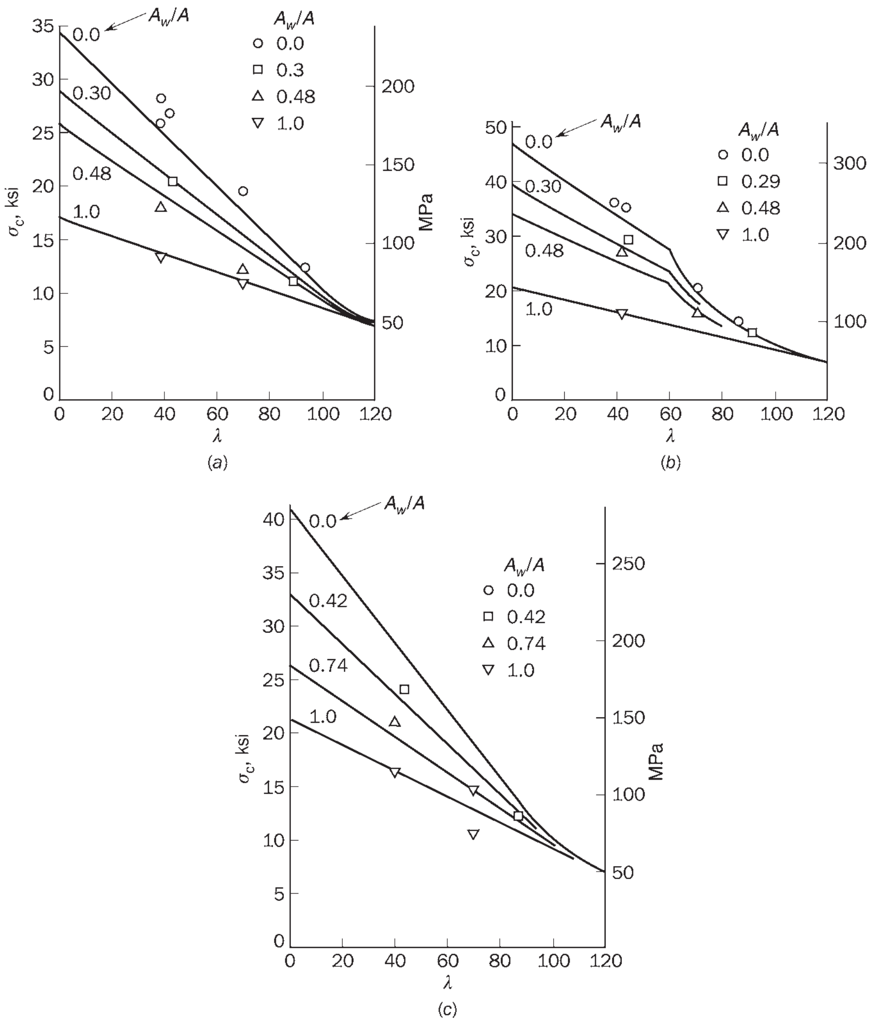

FIGURE 3.32 Columns with longitudinal welds: (*a*) 5154-H32 rectangular sections; (*b*) 6061-T6 rectangular sections; (*c*) 5456-H321 rectangular sections (Sharp, 1993).

heat-affected areas were used in the calculations for the data in these figures. In the absence of measured values, the heat-affected zone may be assumed to be a width of 1 in. (25 mm) on either side of the center of a groove weld or the root of a fillet weld. For columns with transverse welds that affect the entire cross section, the strength reduction is dependent on the location of the welds and the amount of material of reduced strength (Lai and Nethercot, 1992; Fig. 3.33). In general, heat-treatable alloys have a greater loss of strength due to welding than do non-heat-treatable alloys.

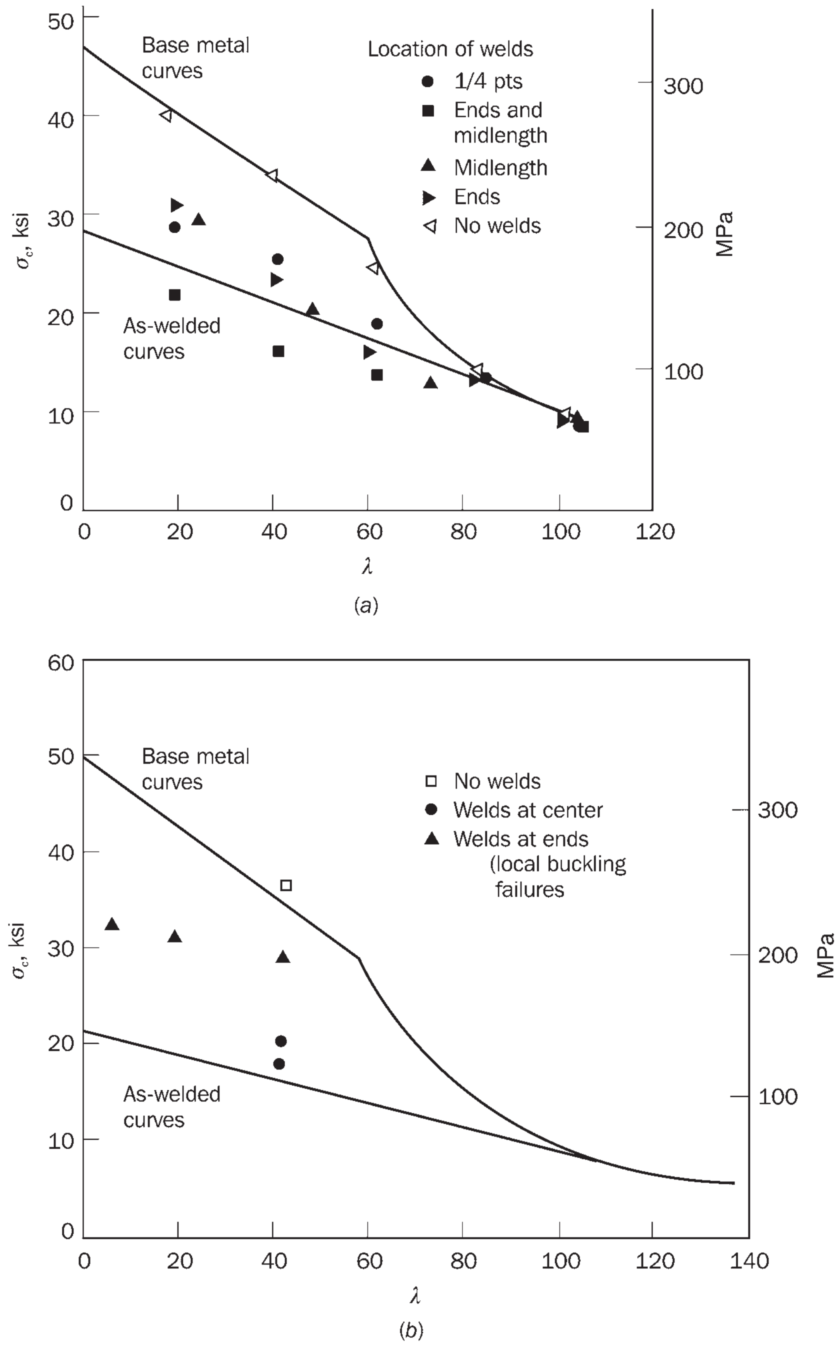

FIGURE 3.33 Columns with transverse welds: 6061-T6 rectangular sections [0.5 × 2.0 in. and 0.25 x 2.0 in. (12.7 x 50.8 mm and 6.3 x 50.8 mm]; (*b*) 6061-T6 tubes 3 in. (76 mm) outside diameter, 0.25 in. (6.4 mm) wall (Sharp, 1993).

3.6.5 Design of Aluminum Alloy Columns

U.S. and Australian Design Practice [Aluminum Association (AA), 2005; Standards Association of Australia (SAA), 1997]. The design formulas are based on the tangent-modulus formula, simplified to a straight line in the inelastic range, which can be expressed as

$$\sigma_c = B_c - D_c\ \lambda \quad \text{for } \lambda < C_c \tag{3.18}$$

in which $\lambda = KL/r$ and for artificially aged tempers,

$$B_c = \sigma_y[1 + (\sigma_y/2250)^{1/2}] \tag{3.19a}$$

$$D_c = (B_c/10)(B_c/E)^{1/2} \tag{3.19b}$$

$$C_c = 0.41B_c/D_c \tag{3.19c}$$

and for other tempers,

$$B_c = \sigma_y[1 + (\sigma_y/1000)^{1/2}] \tag{3.20a}$$

$$D_c = (B_c/20)(6B_c/E)^{1/2} \tag{3.20b}$$

$$C_c = 0.67B_c/D_c \tag{3.20c}$$

In no case can the stress exceed the yield strength. This classification is based on values of the ratios $\sigma_{0.2}/\sigma_{0.1}$ of 1.04 for artificially aged tempers and 1.06 for other tempers. For $\lambda > C_c$ the Euler elastic buckling formula is used.

Figures 3.34 and 3.35 compare the foregoing formulas with the results of tests on aluminum columns (Clark and Rolf, 1966). The test specimens were considered to have fixed ends (flat ends on rigid platens), and the deviations from straightness were less than $0.001L$. The effective-length factor K was assumed to be 0.5 in plotting the test results.

Allowable stresses for building design in the AA specification are obtained by applying a constant factor of safety of 1.95 to the straight-line and Euler formulas. Thus, the specifications do not directly consider the initial crookedness, which is specified by ASTM material specifications as $L/960$ for most extruded shapes. Batterman and Johnston (1967) showed that a small initial out-of-straightness can appreciably reduce the factor of safety, especially in the transition region between elastic and inelastic buckling. Figure 3.36 illustrates the results of calculations for columns of 6061-T6 alloy with $\delta_0 = 0.001L$. In a discussion of the specification, Hartmann and Clark (1963) noted that the effects of small amounts of initial out-of-straightness or eccentricity may be offset by the use of conservative values of the equivalent-length factor as a basis for the specification formulas. To illustrate this, Batterman and Johnston (1967) considered the hypothetical case of a column

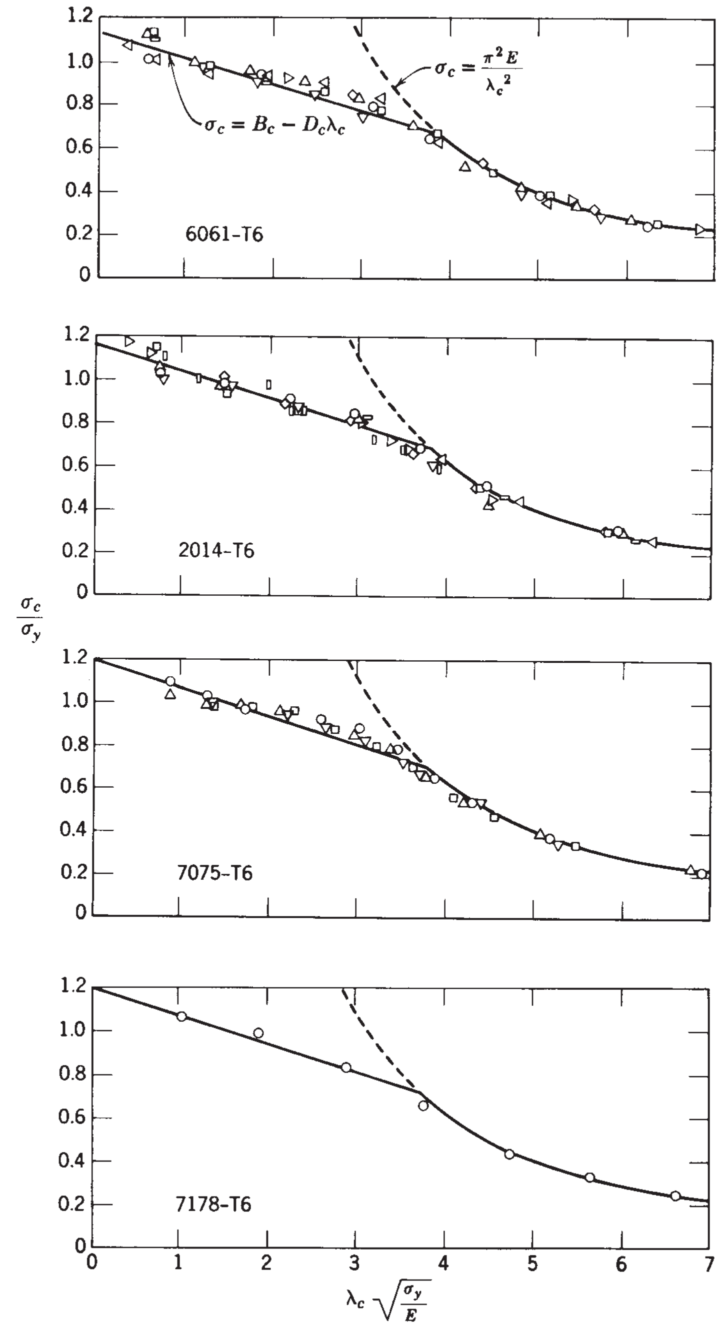

FIGURE 3.34 Column strength of aluminum alloys (artificially aged) (Clark and Rolf. 1966).

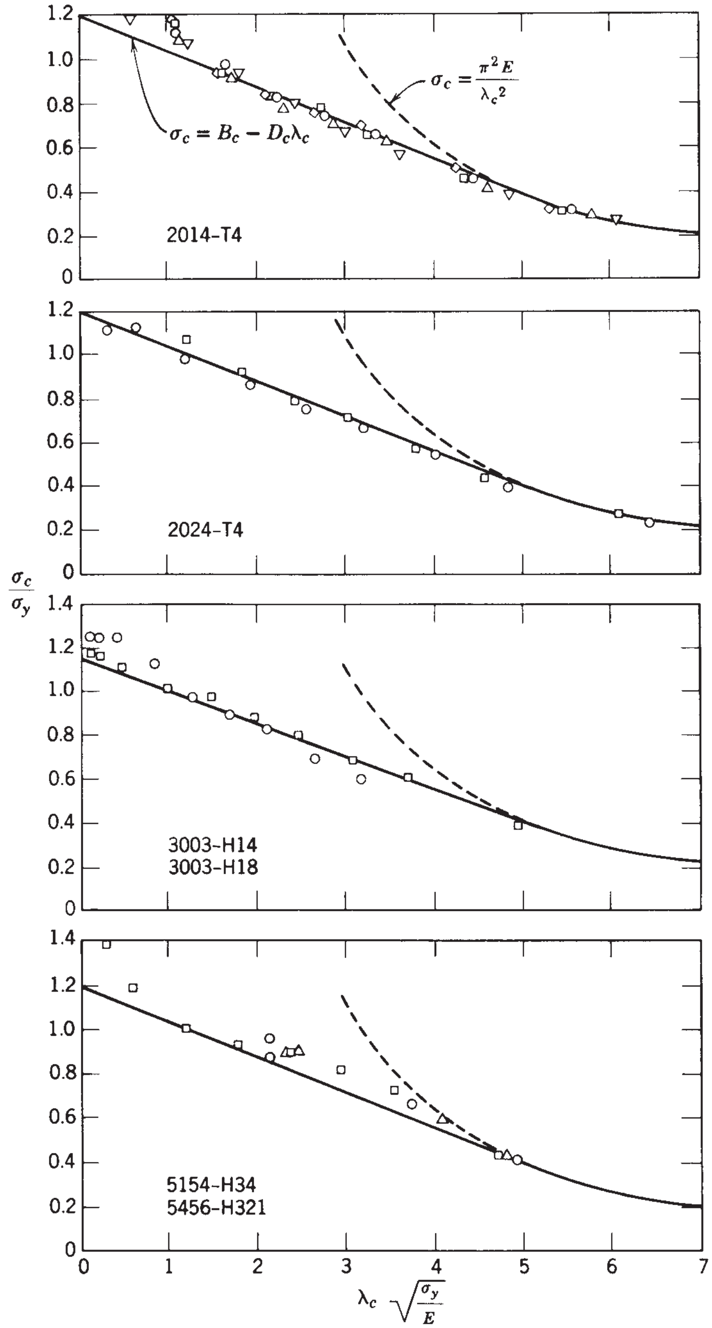

FIGURE 3.35 Column strength of aluminum alloys (not artificially aged) (Clark and Rolf. 1966).

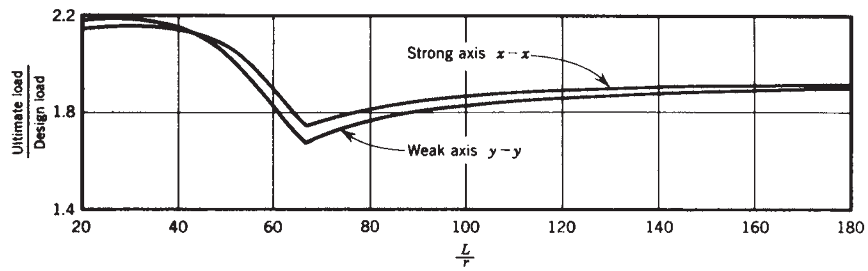

FIGURE 3.36 Design load factor for wide-flange shapes of aluminum alloy columns with $\delta_0 = 0.001L$ (Batterman and Johnston, 1967).

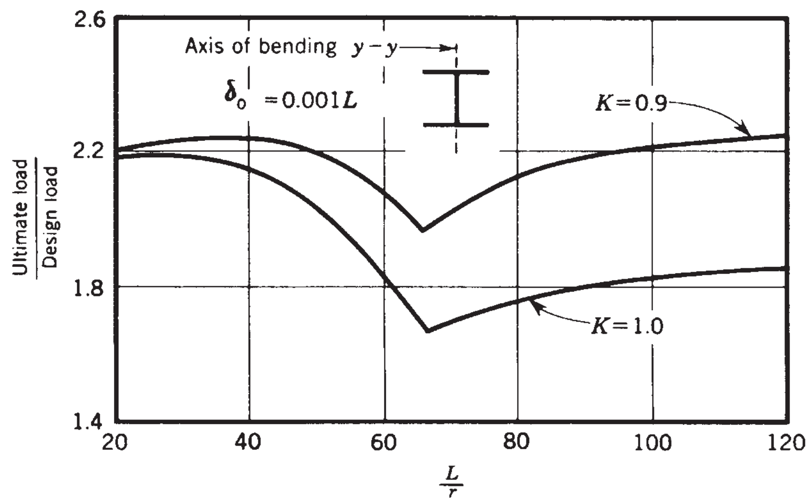

FIGURE 3.37 Comparison of safety factors for columns with and without end restraint (Batterman and Johnston, 1967).

with typical material properties and ends restrained such that throughout loading to maximum strength the column segment between inflection points is always 0.9*L*. For bending about the minor axis *(y–y)* and an initial out-of-straightness of 0.001*L*, the theoretical safety factor is plotted in Fig. 3.37, both for this case and for the case of pinned ends. Thus, for a relatively slight amount of end restraint, the safety factor varies from values slightly above 2.2 in the short-column range to a minimum of 1.97 at $L/r = 67$. It then increases to slightly above 2.2 at $L/r = 120$. The effect of the initial out-of-straightness in reducing the safety factor from 1.95 to 1.67 is thus offset if the column is restrained at the ends such that an actual *K* value of 0.9 is produced. In the load and resistance factor design version of the AA (2005) specification, a variable resistance factor is used to account for the effects of initial crookedness.

European Design Practice An earlier British code [Institution of Structural Engineers (ISE), 1962] adopted the Perry–Robertson formula, which can be expressed as

$$\frac{\sigma_c}{\sigma_y} = \frac{1}{2\lambda^2}\left\{(1+\eta+\lambda^2) - [(1+\eta+\lambda^2)^2 - 4\lambda^2]^{1/2}\right\} \tag{3.21}$$

The factor η is based on test results (Baker and Roderick, 1948) and thus incorporates all sources of imperfection and nonlinearity present in the tests. Two values are used, $0.0015L/r$ for heat-treated and $0.003L/r$ for non-heat-treated alloys. In a later code, straight-line formulas of the type used in North America were adopted. The British limit-states design specification, BS 8118 [British Standards Institute (BSI), 1991], provides curves relating the critical stress σ_{cr} to the slenderness ratio KL/r for three representative aluminum alloys for use by designers.

Research by Mazzolani and Frey (1980) and Bernard et al. (1973) provided the background information on imperfections, residual stresses, and the influence of welds, which led to the preparation of the ECCS (1978) recommendations and eventually the Eurocode rules. The Ramberg-Osgood formula was used to model the stress–strain relationship in the form

$$\epsilon = \frac{\sigma}{E} + 0.002\left(\frac{\sigma}{\sigma_{0.2}}\right)^n \tag{3.22}$$

Steinhardt's suggestion (1971) that n is equal to the value of the yield strength in kN/cm^2 gives close agreement with test results (n is a coefficient that reflects the shape in the knee location of the stress–strain curve).

Three curves have been adopted using values of n of 20, 15, and 10 to represent the various alloy types. Included in the computer evaluation were initial imperfections due to crookedness and eccentricity as well as unsymmetrical sections. The curves are shown in Fig. 3.38. The uppermost curve is for heat-treated, symmetrical, open or solid sections, with the lowest curve being for all hollow sections and all non-heat-treated sections other than symmetric open or solid sections. This lowest curve lies substantially below those in other standards, as it represents an extreme combination of adverse influences.

The ECCS column curves were presented in tabular form and were therefore not readily adaptable for design purposes. Rasmussen and Rondal (2000b) obtained analytic expressions that were in close agreement with the a-, b- and c-column curves shown in Fig. 3.39. The analytic column curves were based on the Perry–Robertson formula (Eq. 3.21) and a nonlinear expression for the imperfection parameter (η) as

$$\eta = \alpha\left[(\lambda - \lambda_1)^{\beta} - \lambda_0\right] \tag{3.23}$$

where the values of α, β, λ_0, and λ_1 defining the a-, b- and c-curves are shown in Table 3.1.

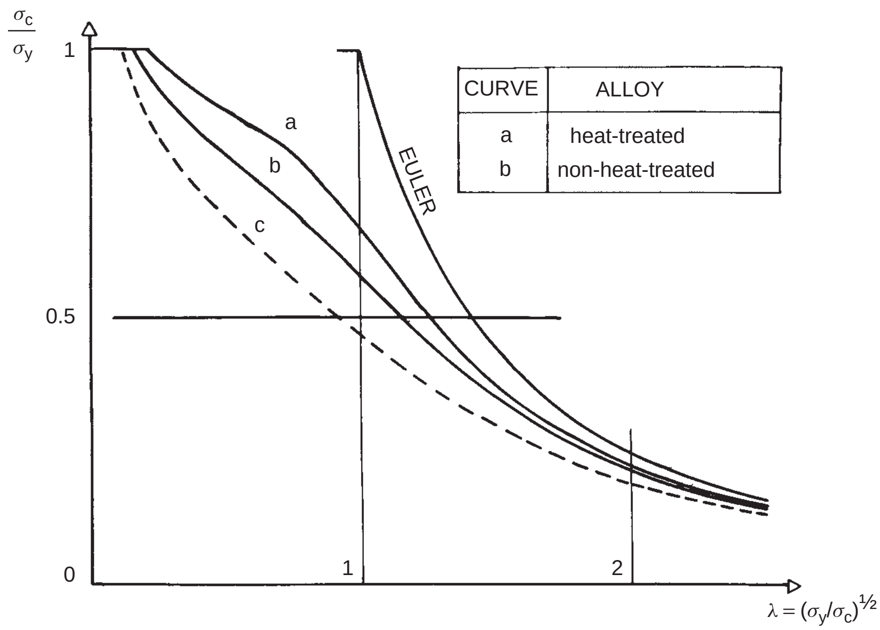

FIGURE 3.38 Basic column-buckling curves (ECCS aluminum structures.)

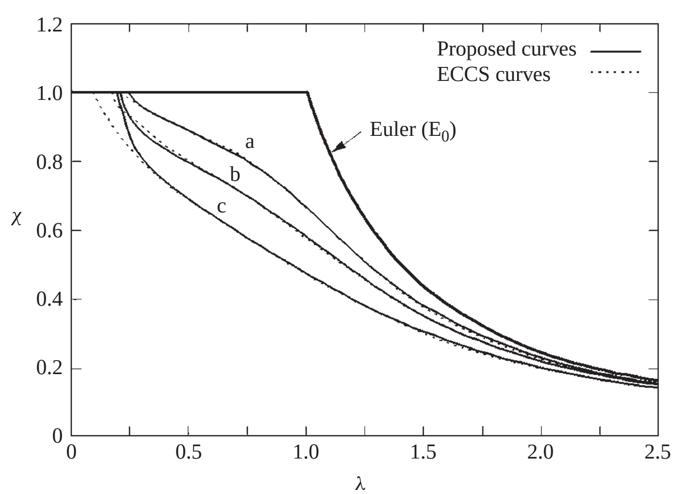

FIGURE 3.39 ECCS *a*, *b*, and *c* curves for aluminum columns and analytical fits (Rasmussen and Rondal, 2000b).

TABLE 3.1 Values of α, β, λ_0, and λ_1 for Analytic Approximations to ECCS Column Curves

Column Curve	α	β	λ_0	λ_1
a	0.4	0.2	0.55	0.2
b	0.7	0.15	0.55	0.2
c	0.95	0.25	0.35	0.2

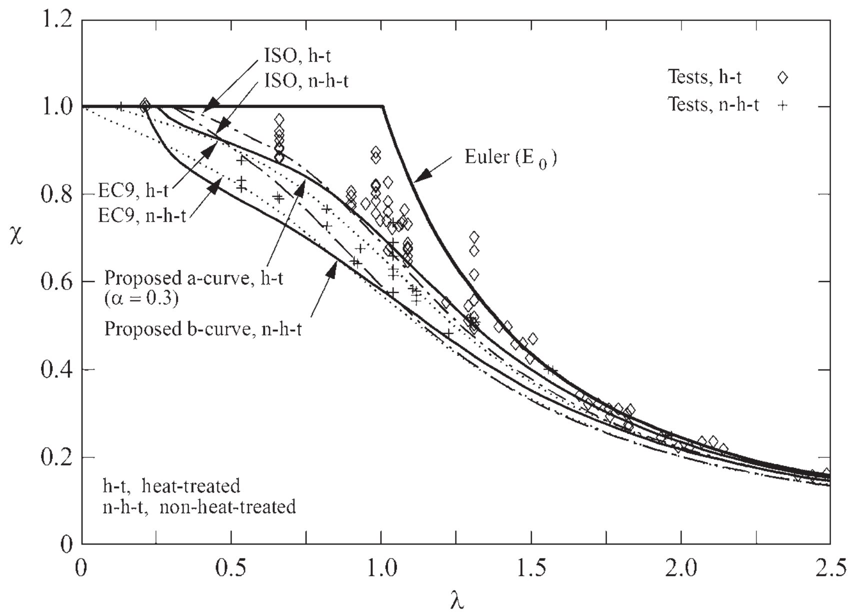

FIGURE 3.40 Comparison of ECCS column curves with tests (Rasmussen and Rondal, 2000b).

Figure 3.40 compares the ECCS *a* and *b* curves with tests on aluminum alloy columns. It can be seen that the *a* curve follows closely the trend of the test points for heat-treated alloys, while the *b* curve follows the trend of the test points for non-heat-treated alloys. The figure also includes the column curves of Eurocode 9 (CEN, 2007) and the International Organization for Standardization (ISO, 1992) specification for aluminum structures.

Canadian Design Practice The Canadian aluminum design standard S157 (CSA, 2005) uses two strength curves based on the Perry–Robertson relationship. The concept of a "limiting stress" F_o is used, which can be the yield stress or a lower stress that accounts for local buckling or welding effects. The slenderness, $\overline{\lambda}$, is a generalized term, as the expressions are used for all member instabilities.

The critical column stress, F_c, is defined as follows:

$$F_c = \overline{F} F_o \tag{3.24}$$

$$\overline{F} = \beta - \left(\beta^2 - \frac{1}{\overline{\lambda}^2}\right)^{1/2} \tag{3.25}$$

$$\beta = \frac{1 + \alpha(\overline{\lambda} - \overline{\lambda}_0) + \overline{\lambda}^2}{2\overline{\lambda}^2} \tag{3.26}$$

$$\overline{\lambda} = \left(\frac{F_o}{F_e}\right)^{1/2} = \frac{KL}{\pi r}\left(\frac{F_o}{E}\right)^{1/2} \tag{3.27}$$

For columns, $\overline{\lambda}_0$ is 0.3. The two curves are distinguished by the α parameter, which is 0.2 for heat-treated members and 0.4 for members that are not heat treated.

3.7 STAINLESS STEEL COLUMNS

The past two decades have seen unprecedented attention paid to the potential use of stainless steel for structural purposes. Several large-scale European research programs have been conducted under the auspices of the European Coal and Steel Community (ECSC) to investigate the strength of cold-formed and fabricated columns and beams at ambient and elevated temperatures, among many other aspects of the behavior and design of stainless steel structures [Burgan et al., 2000; Steel Construction Institute (SCI), 2000]. Research in South Africa (van den Berg, 2000) has included tests on cold-formed, hot-rolled, and fabricated stainless steel structural members with an emphasis on ferritic stainless steels and a chromium-weldable steel type 3Cr12 developed by Columbus Stainless Steel. In the past decade, research on tubular stainless steel structural members and connections has been undertaken in Australia (Rasmussen, 2000; Rasmussen and Hasham, 2001; Rasmussen and Young, 2001) and in Finland (Talja and Salmi, 1995). Recent attention has been paid to the use of high-strength stainless steel tubular columns (Young and Lui, 2006; Gardner et al., 2006).

The new findings reported over the last 20 years have triggered several revisions of the European standard for stainless steel structures, Part 1.4 of Eurocode 3. This standard complements the American Society of Civil Engineers ASCE-8 standard (ASCE, 2003) for cold-formed stainless steel structural members, which was first published by AISI in the late 1960s and has been revised several times since, including a conversion in 1991 to the LRFD format.

3.7.1 Stainless Steel Materials

Stainless steel is the common name applied to a range of iron-based alloys whose prime corrosion-resisting element is chromium. The minimum chromium content is approximately 11% and the maximum around 30%. The carbon content ranges from 0.02 to 0.12%, which is generally lower than that of ordinary structural carbon steels where the carbon content lies around 0.15 to 0.25%. Most stainless steels contain additional alloying elements, notably nickel, manganese, and titanium. The stainless steel alloys used for structural applications pertain to the following groups:

- Austenitic alloys
- Ferritic alloys
- Duplex alloys

The names of the austenitic and ferritic groups reflect the metallurgical (crystalline) structure of the alloys, being austenite and ferrite. The austenitic group is characterized by high contents of chromium and nickel, and includes the most commonly used alloys, AISI 304 and AISI 316. The ferritic steels contain medium to low contents of chromium and have no nickel. The duplex alloys contain a mixture of austenite and ferrite, which leads to high strength and good corrosion and fatigue properties.

A typical stress–strain curve for stainless steel is shown in Fig. 3.41. It is noted that there is no yield plateau and the proportionality stress, σ_p, is low compared to the equivalent yield stress, σ_y, which for structural applications is defined as the 0.2% proof stress. The gradual yielding taking place at stresses beyond the proportionality stress leads to a softening of the material and consequently a reduction in resistance to buckling. For this reason, the design strength curves for stainless steel

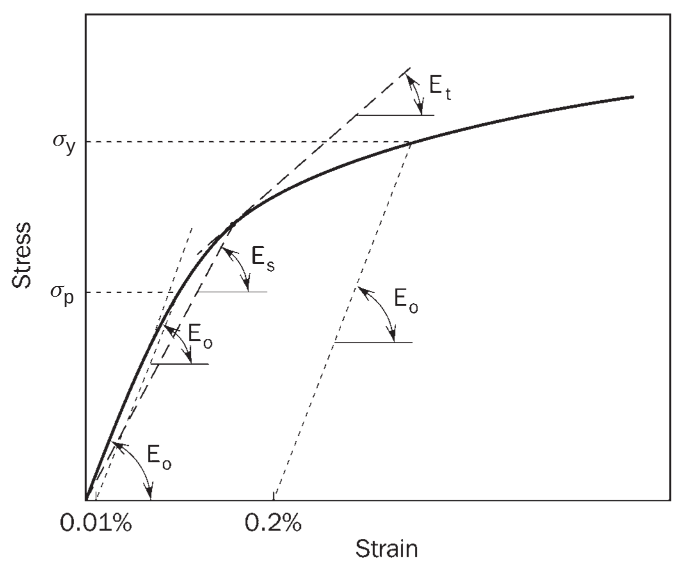

FIGURE 3.41 Typical stress–strain behavior of stainless steel (van den Merwe and van der Berg, 1992).

columns and unbraced beams differ from those for structural carbon steel columns and beams. Furthermore, unlike structural carbon steels, there are clear differences in the mechanical properties associated with the longitudinal direction of rolling and transverse direction, and the material responds differently in compression and tension.

The equivalent yield stress of austenitic stainless steel alloys can be enhanced greatly by cold working. This property is utilized in the production of cold-formed stainless steel tubes, which can be designed to and marketed at an enhanced equivalent yield stress. European tube manufacturers now exploit the strain-hardening capacity to raise the equivalent yield stress of cold-formed rectangular and circular hollow sections in AISI 304 and AISI 316 austenitic stainless steel from a nominal annealed value of 32 ksi (240 Mpa) to a nominal value of 50 ksi (350 Mpa).

While the equivalent yield stress and ultimate tensile strength vary significantly from alloy to alloy and depend on the degree of cold working, the initial elastic modulus lies in the narrow range from 28,000 ksi (195,000 Mpa) to 29,500 ksi (205,000 Mpa) and is only slightly lower than the elastic modulus for carbon structural steels. Representative values of the equivalent yield stress of austenitic alloys in their annealed states lie in the range from 32 ksi (220 Mpa) to 39 ksi (270 Mpa), while equivalent yield-stress values in excess of 50 ksi (350 Mpa) are achievable in the cold-worked condition. For ferritic alloys in the annealed state, the yield stress typically ranges from 38 ksi (260 Mpa) to 50 ksi (350 Mpa). Duplex alloys have equivalent yield-stress values in excess of 65 ksi (450 Mpa) in the annealed condition.

3.7.2 Residual Stresses

The coefficients of expansion of austenitic stainless steel alloys are generally larger than those of structural carbon steel, while the thermal conductivity is lower. The combination of a larger coefficient of expansion and a lower thermal conductivity has the potential of inducing higher welding residual stresses than those experienced in fabricating carbon structural steel sections.

Data on residual stresses in hot-rolled and fabricated (welded) stainless steel structural shapes are limited. Bredenkamp et al. (1992) found that the magnitudes and distribution of the residual stresses are comparable to those found in similar-sized carbon steel welded shapes, as shown in Fig. 3.42, while Lagerquist and Olsson (2001) observed considerably higher residual stresses in fabricated stainless steel sections compared to their carbon steel counterparts.

Rasmussen and Hancock (1993) reported residual stress measurements in cold-formed stainless steel square and circular hollow sections. The measurements showed that the membrane residual stresses were negligible, while the maximum bending residual stresses were on the order of the equivalent yield stress.

3.7.3 Column Strength

Research by Johnson and Winter (1967) and van den Berg and co-workers (van den Berg, 2000) supported using the tangent-modulus approach to account for gradual

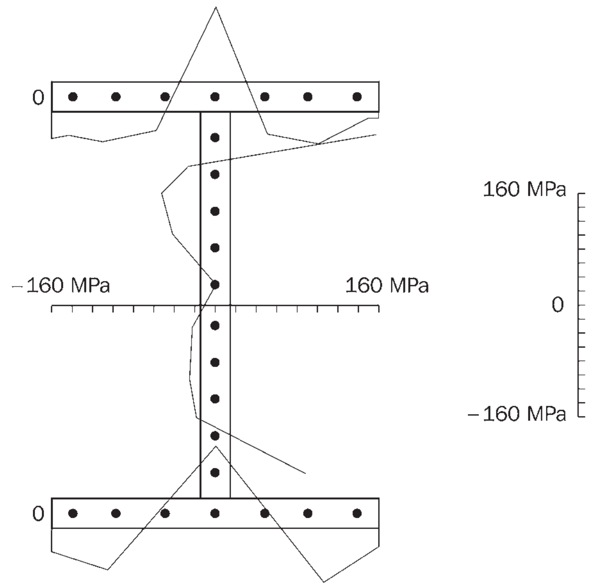

FIGURE 3.42 Residual-stress pattern for a welded stainless steel I-shape (Bredenkamp et al., 1992).

yielding in designing stainless steel columns. The ASCE standard for cold-formed stainless steel structural members (ASCE, 2003) is still based on this approach whereby the column strength is determined by replacing the elastic modulus by the tangent modulus, E_t, in the Euler formula, as described in Section 3.2.1. The tangent-modulus approach is iterative because the tangent modulus depends on the stress level (P_t/A) at the point of bifurcation, where the inelastic buckling load, P_t, is the object of the calculation.

Because the tangent modulus varies differently with stress level for various alloys, reflecting differences in their mechanical response, different column curves are derived for various alloys, as shown in Fig. 3.43. Unlike carbon structural steels, the nondimensional column strength curve for nonlinear materials, such as stainless steel, aluminum, and titanium, raises as the equivalent yield stress increases (Rasmussen and Rondal, 1997b). For this reason, a relatively high nondimensional column curve is derived for the duplex alloy S31803, popularly known as 2205, as shown in Fig. 3.43.

The Australian standard for cold-formed stainless steel structures (AS/NZS, 2001) is based on the ASCE standard. It features supplementary design rules based on research conducted at the University of Sydney, notably on tubular members. As an alternative to the tangent-modulus approach, the Australian standard also allows the column strength to be determined using the explicit method developed by Rasmussen and Rondal (1997a,b). According to this method, the column strength is

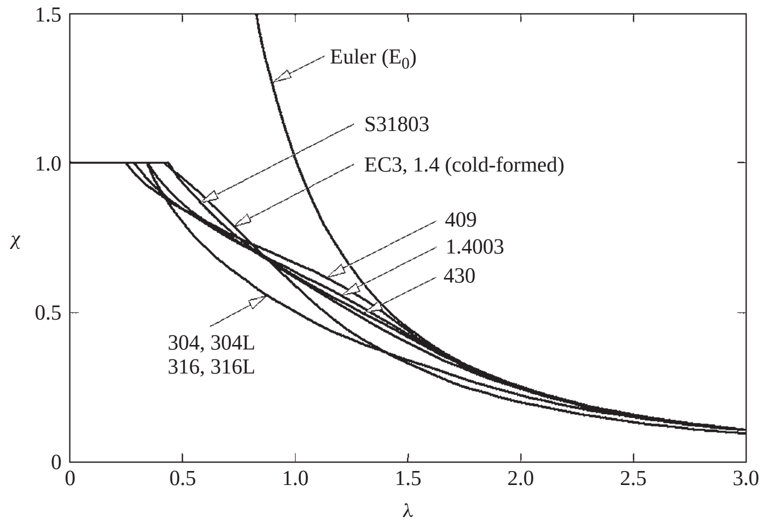

FIGURE 3.43 American (ASCE, 2003) and Australian (AS/NZS, 2001) column curves for cold-formed stainless steel sections based on the tangent-modulus approach.

given by

$$P_n = A_e \chi F_y \tag{3.28}$$

where the slenderness reduction factor, χ, is determined from the Perry–Robertson formulas,

$$\chi = \frac{1}{\phi + \sqrt{\phi^2 - \lambda^2}} \leq 1 \tag{3.29}$$

$$\phi = \tfrac{1}{2}(1 + \eta + \lambda^2) \tag{3.30}$$

$$\lambda = \frac{l_e}{r}\sqrt{\frac{F_y A_e}{\pi^2 A E_0}} \tag{3.31}$$

The imperfection parameter, η, appearing in Eq. 3.30 is tailored to produce strength curves for columns made from nonlinear materials (Rasmussen and Rondal, 1997b) and is given by Eq. 3.23. It involves the material-specific constants α, β, λ_0, and λ_1.

The Australian standard provides values of α, β, λ_0, and λ_1 for common structural stainless steel alloys. Figure 3.44 shows strength curves obtained using the explicit approach. They are generally slightly lower than those obtained using the tangent modulus (Fig. 3.43) because they incorporate geometric imperfections. Accordingly, a resistance factor of 0.9 is specified in the Australian standard

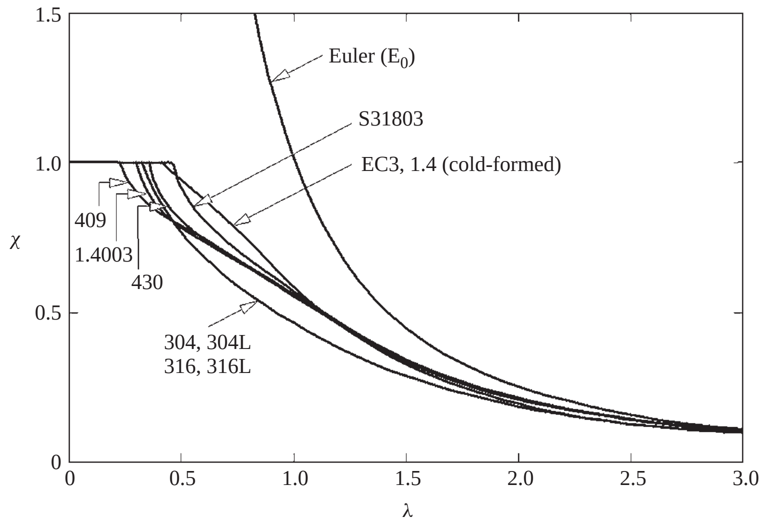

FIGURE 3.44 Australian column curves (AS/NZS, 2001) for cold-formed stainless steel sections based on explicit approach.

when using the explicit approach, whereas a resistance factor of 0.85 is specified when using the iterative tangent-modulus approach.

Part 1.4 of Eurocode 3 (CEN, 2006) provides supplementary rules for stainless steel structural members and connections. In contrast to the American and Australian standards, Eurocode 3, Part 1.4, is applicable to both cold-formed and fabricated sections. For column design, it uses the Perry–Robertson equations (Eqs. 3.28 to 3.31) in conjunction with the standard linear expression for the imperfection parameter also used for structural carbon steels:

$$\eta = \alpha\,(\lambda - \lambda_0) \tag{3.32}$$

Two column curves are specified in Eurocode 3, Part 1.4, one for cold-formed sections, $(\alpha, \lambda_0) = (0.49, 0.4)$, and one for fabricated (welded) sections, $(\alpha, \lambda_0) = (0.76, 0.2)$. The curve for cold-formed sections is compared with the Australian and American column curves in Figs. 3.43 and 3.44. The European curve for cold-formed sections is relatively high because it is calibrated (Burgan et al., 2000) against tests with high equivalent yield-stress values (Rasmussen and Rondal, 2000a). The column curve for welded sections is based on European tests on AISI 304, AISI 316, and S31803 alloys (Burgan et al., 2000). Further tests on welded and hot-rolled sections have been conducted in South Africa (Bredenkamp et al., 1994; Bredenkamp and van den Berg, 1995).

3.8 TAPERED COLUMNS

Tapered structural members are beams, columns, or beam-columns that have a continuously varying cross section along their length. Such structural components are used in many applications, such as gable frames, towers, and architecturally exposed steel columns in stores, halls, or airports. These types of members provide several advantages over prismatic members. Tapered members can be made more efficient structurally by the use of larger cross sections at locations where the demands are higher and smaller cross sections elsewhere. Furthermore, fabricators equipped to produce web-tapered members can create a wide range of optimized profiles from a minimal stock of different plates and coil. This can result in time and cost savings compared to the alternative ordering or stocking of an array of rolled shapes. It is important to note that tapered members are often used in applications where the members are dominated by bending. Metal building manufacturers commonly taper the webs of their primary members to match the section modulus or capacity to the moment envelope determined from the various design loadings. There are no structural advantages of tapering concentrically loaded columns subjected to a constant axial force.

Due to the variation of the cross section along the member length, and the corresponding variation in the flexural, axial, and torsional stiffness, the stability analysis of tapered members is more complicated than that of prismatic members. Therefore, exact analytical solutions for the buckling of tapered columns are available only for relatively simple cases involving elastic flexural buckling. For more general cases, numerical methods and energy methods may be used for calculating the buckling loads of tapered and of general nonprismatic columns. Also, a number of useful procedures have been recommended for simplified approximate calculation of elastic buckling strengths for I-section members with linear web taper and assumed simply supported end conditions.

Although there are a large number of recommended procedures for calculating elastic flexural buckling loads, a relatively small number of studies have been conducted to evaluate the inelastic buckling capacity and the design strength of tapered columns. Timoshenko and Gere (1961) provided one of the earliest discussions of the calculation of inelastic buckling loads of non-prismatic bars. They suggested an approximate calculation of the inelastic strength of variable cross-section bars using column curves based on the tangent modulus E_t at the cross section with the largest axial stress. In more recent years, a number of researchers have studied the effect of residual stress, initial out-of-straightness, and end restraints from adjacent unbraced lengths on the inelastic flexural buckling of tapered members (Kim et al, 1995; Jimenez-Lopez, 1998; and Jimenez and Galambos, 2001).

In 1966, the CRC and the Welding Research Council (WRC) initiated the first concerted effort to address the complete strength behavior of metal building frames using tapered I-section members. This work was a continuation of earlier work at Columbia University under the direction of Butler (Butler and Anderson, 1963; Butler, 1966). From this effort, Lee and his associates at the University of New York at Buffalo developed an overall design approach for tapered steel members documented in Lee et al. (1972, 1981). Two of the main characteristics of this approach are the concept of equivalent prismatic members and the mapping of the elastic buckling strength of tapered members to the elastic or inelastic design strength of equivalent prismatic members. Recently, these concepts have been refined further by White and Kim (2006) and published by the Metal Buildings Manufacturers Association in an MBMA/AISC design guide (Kaehler et al., 2008). The MBMA/AISC design guide extends the analysis and design procedures provided in the 2005 AISC specification to the design of frames using web-tapered and general non-prismatic members.

In this section, various procedures are reviewed for calculating the elastic buckling strength of tapered columns and methods for calculating the column axial strength of tapered members are summarized. The concept of an equivalent prismatic member, originally suggested by Timoshenko and Gere (1961) and subsequently applied and developed by Lee et al. (1972), is addressed in detail. Furthermore, recent updates by White and Kim (2006) and Kaehler et al. (2008) are discussed. These updates simplify and generalize the application of this concept.

3.8.1 Elastic Buckling Strength of Tapered Columns

The elastic buckling of tapered columns can be determined by solving the governing differential equation of equilibrium for the case of linear buckling. For tapered columns, the second moment of area is a function of the longitudinal coordinate of the member. This analytically exact solution is possible only for special cases of the variation of the second moment of area and involves substantial mathematical manipulation. Timoshenko (1936) solved the elastic flexural buckling of a simply supported column with a step in the cross section and a cantilever column with a second moment of area that varies according to the power of the distance along the member length. Bleich (1952) provided analytical solutions for simply supported I-section columns with linear or parabolic tapers. For these solutions, Bleich assumed an approximate variation of the second moment of area as a power function along the unbraced length.

Various numerical and energy method solutions can be used for calculating the elastic flexural buckling load of general tapered columns. Timoshenko (1936) discussed energy method solutions for the elastic flexural buckling of nonprismatic columns. He also discussed a procedure called the method of successive approximations, which allows the estimation of elastic flexural buckling loads for any variation of the geometry and/or axial loading along the member length. Other discussions of the method of successive approximations are provided by Salvadori (1951), Bleich (1952), Chen and Lui (1987), and Bažant and Cedolin (1991). Newmark (1943) showed that the method of successive approximations could be used with finite difference expressions to provide effective practical solutions for the elastic flexural buckling strengths of columns. This numerical method, which is also known as the *numerical integration method*, or *Newmark's method*, can be applied to members with any variation in cross section and applied loads. This method is particularly powerful in that it provides both upper and lower bounds on the exact solution and can be iterated to obtain any desired degree of accuracy. Furthermore, the use of the deflected shape associated with a uniform transverse load often results in accurate solutions without iteration. Timoshenko and Gere (1961) provided an example elastic buckling solution for a stepped column subject to an end compression force using Newmark's method. Kaehler et al. (2008) summarize the general procedures and the implementation details of the method.

The finite element method has been employed extensively for more general cases involving general boundary conditions and modes other than just flexural buckling. Recent solutions of this type include Ronagh et al. (2000a,b) and Boissonnade and Maquoi (2005). It should be noted that these and other authors have documented the fact that the use of prismatic beam finite elements for the analysis of tapered members (by subdividing the members into small segments) can lead to significant errors when the behavior is influenced by torsion. Kaehler et al. (2008) provide an extensive annotated bibliography outlining various numerical procedures that have been employed historically for the calculation of column elastic buckling loads as well as other theoretical and design calculations for frames using web-tapered members.

For tapered I-section columns with a linearly tapered web and prismatic flanges, Kaehler et al. (2008) also provide simple procedures for calculating the elastic buckling strengths with assumed simply supported end conditions. The limit states of in-plane and out-of-plane flexural buckling, torsional buckling, flexural–torsional buckling, and constrained-axis torsional buckling are considered. These approaches involve the use of an average or weighted average cross section along the length, along with the analytical linear buckling equations for prismatic members.

3.8.2 Design Strength of Tapered Columns

As noted above, a joint task committee of the CRC and the WRC was formed in 1966 to address the strength behavior of tapered members. Prawel et al. (1974) provided the first set of experimental tests conducted under the guidance of this joint task committee. In this research, the inelastic stability of tapered I-section beam-columns was studied. In addition, residual stresses were measured in representative welded tapered I-sections. These tests and other analytical studies served as the basis of the overall design procedures developed by Lee et al. (1972, 1981).

One of the key characteristics of the design approaches by Lee et al. (1972, 1981) is the concept of an equivalent prismatic member. These researchers developed member length modification factors, which mapped a given linearly tapered member to a hypothetical prismatic member composed of the cross section at the shallow end of the tapered member. The modified length of the equivalent prismatic member was determined such that this hypothetical member would buckle elastically at the same total load or maximum stress as the given linearly tapered member. Figure 3.45 shows an equivalent prismatic column having the smaller end cross section and the same elastic in-plane flexural buckling load as the given tapered column.

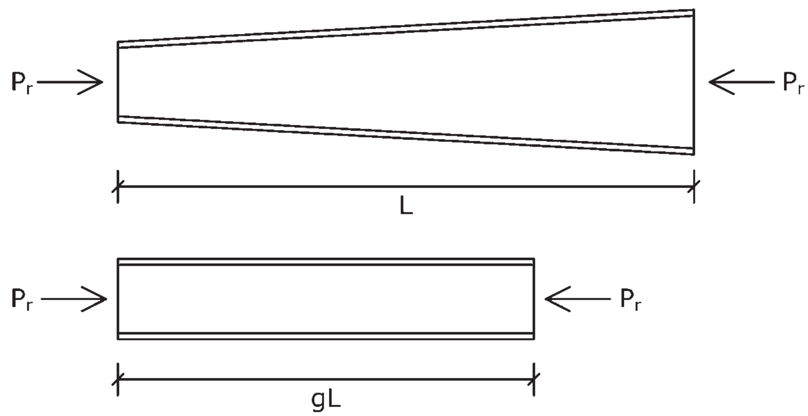

FIGURE 3.45 Equivalent prismatic column with modified length *gL* (Lee et al., 1972, 1981).

An equation for a length modification factor, g, was determined based on curve fitting to representative results from members with five different cross sections. This length modification factor only addressed the in-plane flexural buckling strength of columns with simply supported end conditions. For the rotational restraint effects from the adjacent members, design charts for an effective-length factor K_γ were derived. Once the equivalent prismatic column was determined with the smallest cross section of the given tapered column and the modified length $K_\gamma gL$ (L being the length of the physical tapered column), the AISC Allowable Stress Design (ASD) equations were used to determine the column elastic or inelastic design strengths. It is important to note that this mapping of the elastic buckling strength to the elastic or inelastic design strength is the same mapping of the theoretical elastic buckling strength to the design resistance employed for prismatic members. This approach is conservative because it assumes the same extent of yielding in all the nominal cross sections along the length, even though the actual cross sections are of larger area than the smallest reference section. The above design procedures were adopted in the AISC (1978) specification provisions. A detailed summary of the design procedures by Lee et al. (1972, 1981) is provided in Chapter 9 of the fourth edition of this guide (Galambos, 1988) and in Section 3.3 of the fifth edition of this guide (Galambos, 1998).

The provisions within the AISC specifications from AISC (1978) through AISC (1999) were limited only to I-section members with equal-size flanges and linearly varying web depths. This, combined with the unpopularity of design charts without underlying equations for calculation of the corresponding parameters, has led to limited acceptance of the AISC provisions. Metal building manufacturers have tended to develop their own specific mappings of the AISC prismatic member equations for design of the wide range of general nonprismatic member geometries encountered in practice. A number of the metal building manufacturers have made substantial investments of their own resources into research to validate their design approaches. To complicate matters, the AISC provisions for design of prismatic I-section members have been greatly improved over the past 40 years relative to the 1963 specification procedures upon which the tapered-web member provisions of AISC (1978) were based. This has led to awkward differences in the design equations for prismatic and linearly tapered I-section members in the AISC (1986, 1993, 1999) provisions. As a result, the AISC Specification Committee decided to drop the explicit consideration of non-prismatic I-section members entirely from the unified 2005 AISC provisions (AISC, 2005a) in favor of subsequent development of separate updated guidelines for these member types. It was anticipated that the subsequent developments could take significant advantage of the many advances that have been implemented for member and frame stability design in the time since the seminal work by Lee et al. (1981).

White and Kim (2006) conducted a pilot study for the application of the AISC (2005a) stability analysis and design provisions to metal building frames with web-tapered members. General procedures developed in this research were later adopted in the MBMA/AISC design guide for frame design using web-tapered members (Kaehler et al., 2008). The following basic concepts employed by White and Kim (2006) and in the MBMA/AISC design guide are essentially the same as those used by Lee et al. (1972, 1981): (1) the concept of an equivalent prismatic member and (2) the mapping of the elastic buckling strength of tapered members to the elastic or inelastic design strength of equivalent prismatic members. Instead of focusing on length modification factors, however, the updated procedures require two different quantities to determine an equivalent prismatic member: (1) the ratio of the elastic buckling load level to the required load level $\gamma_e (= P_e/P_r = F_e/f_r)$ and (2) the maximum value of the ratio of the required flange stress to the yield stress $(f_r/F_y)_{\max}$ within the unbraced length. The equivalent prismatic column is a hypothetical member that has the same γ_e and the same $(f_r/F_y)_{\max}$ as the physical tapered column under consideration. Figure 3.46 shows the equivalent prismatic column concept used in the MBMA/AISC design guide. The product of these two parameters, $\gamma_e (f_r/F_y)_{\max}$, is the ratio of the elastic buckling load level to the yield load level. By using this ratio and the design equations for prismatic members, one can calculate the inelastic buckling strength of tapered members. In the MBMA/AISC design guide, the AISC (2005a) design equations are used for mapping the elastic buckling strength of tapered members to the inelastic buckling strength of equivalent prismatic members.

The explicit use of γ_e has several advantages compared to the use of the length modification factors. One advantage is that if designers obtain the appropriate value of γ_e, the mapping of elastic buckling strength to inelastic buckling strength is possible as a design approximation for any type of nonprismatic member and buckling limit state. Furthermore, if an eigenvalue buckling analysis is performed, the eigenvalue obtained from the analysis is the value of γ_e. Therefore, complex considerations involving general nonprismatic geometries, different end-restraint effects, and nonuniform axial forces can be directly accounted for by determining the appropriate γ_e. Furthermore, by focusing on the elastic buckling load level γ_e

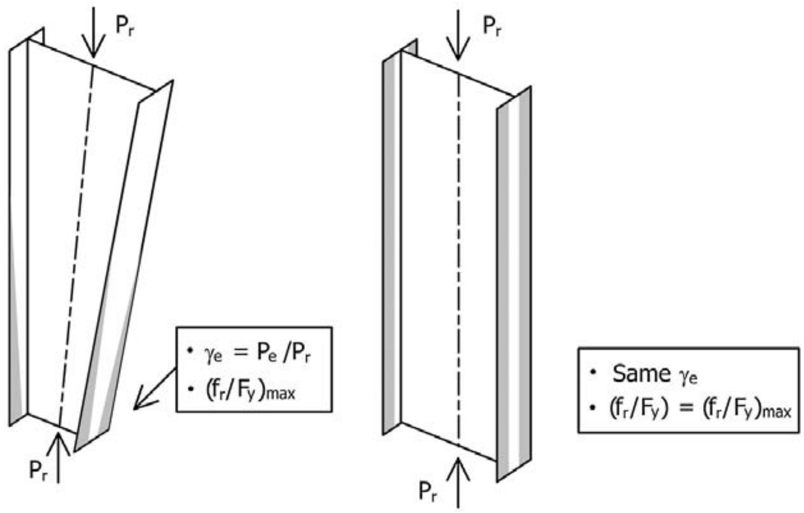

FIGURE 3.46 Equivalent prismatic column concept in MBMA/AISC design guide (Kaehler et al., 2008; White and Kim, 2006).

along with the flange stress ratio f_r/F_y, designers can use any applicable design standard for calculating the design strength of tapered members based on the above concept in the MBMA/AISC design guide.

3.9 BUILT-UP COLUMNS

The effect of shear in built-up columns sets apart the design of these members from that of other columns. The importance of designing the elements connecting the main longitudinal components for shear was tragically demonstrated by the failure of the first Quebec Bridge during construction over the St. Lawrence River, Canada, in 1907. Bridge design practice in North America today reflects the lessons learned from the extensive research that followed that failure. Wyly (1940) concluded that about three-fourths of the failures of laced columns resulted from local, rather than general, column failure. Moreover, the critical load of a built-up column is less than that of a comparable solid column because the effect of longitudinal shear on flexural deflections is much greater for the former. Thus, the longitudinal shear in built-up columns needs to be evaluated in order to (1) determine the possible reduction in the buckling load and (2) design the lacing bars, battens, and their connections.

Three common types of built-up columns are illustrated in Fig. 3.47. They are used when the loads to be carried are large or when a least-weight member or a member with similar radii of gyration in orthogonal directions is desired. Laced or latticed columns (Fig. 3.47*a*) are frequently used in guyed antenna towers, in derrick booms, and in space exploration vehicles. In modern bridge construction,

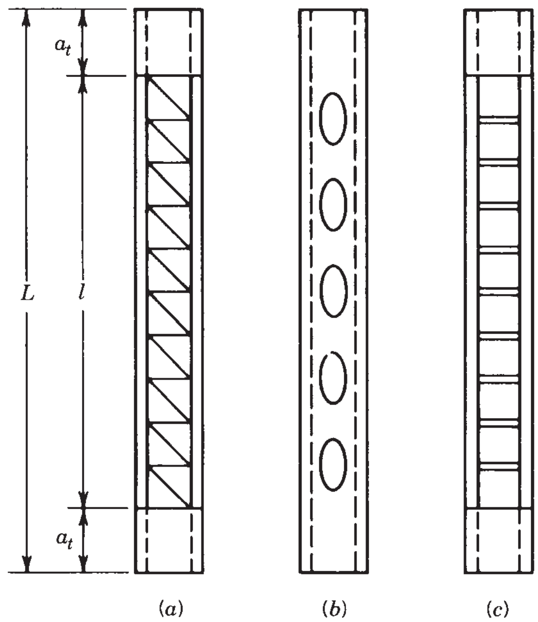

FIGURE 3.47 Common types of built-up columns: (a) laced; (b) perforated cover plated; (c) battened.

perforated cover-plated columns (Fig. 3.47b) are likely to be used rather than laced columns. Of the three, battened columns (Fig. 3.47c) are the least resistant to shear and they are not generally used for bridge or building construction. Box columns with perforated cover plates designed to specification rules require no special considerations for shear effects.

Engesser (1891) considered the effect of shear on the Euler load of an axially loaded column. His buckling formulas have been reevaluated by Ziegler (1982). Bleich (1952) and Timoshenko and Gere (1961) discuss the shear effects in axially loaded columns and laced columns. Additional references are given in the third edition of this guide (Johnston, 1976) and the SSRC Centrally Loaded Column Research Inventory (Driver et al., 2003).

The shear in a column may be caused by:

1. Lateral loads from wind, earthquake, gravity, or other sources
2. The slope of the column with respect to the line of thrust due both to unintentional initial curvature and the increased curvature during buckling
3. The eccentricity of the load due to either end connections or fabrication imperfections

The slope effect is most important for slender columns and the eccentricity effect for stocky columns.

Worldwide, the design requirements for shear in built-up columns vary widely (Beedle, 1991). Eurocode 3 (CEN, 2005) recommends evaluating shear on the basis of the end slope due to a specified initial out-of-straightness, magnified by the effect of axial load and added to the transverse shear due to the applied loads. The American Association of State and Highway Transportation Officials (AASHTO, 2007) and the American Railway Engineering and Maintenance-of-Way (AREMA, 2008) provide an empirical formula for shear to be added to that due to the weight of the member or the external forces

$$V = \frac{P}{100}\left[\frac{100}{(l/r)+10} + \frac{(l/r)\,F_y}{c_u}\right] \tag{3.33}$$

where

V = normal shearing force, lb (N)
P = allowable compressive axial load on members, lb (N)
l = length of member, in. (m)
r = radius of gyration of section about the axis perpendicular to plane of lacing or perforated plate, in. (m)
F_y = specified minimum yield point of type of steel being used, psi (MPa)
C_u = 3,300,000 when the unit of psi is used and 22,750 when Mpa is used.

The AISC specification for buildings (2005a) calls for the calculation of an increased slenderness ratio for use in the column formula to account for the shear effect. The design formula is based on the research by Zandonini (1985) and Aslani and Goel (1991).

3.9.1 Effect of Shear Distortion on Critical Load

Shear distortion reduces the compression capacity of built-up columns. The shear flexibility of battened or laced structural members can be characterized by a shear flexibility parameter, μ (Lin et al., 1970). The parameter μ takes account of the added distortion due to axial force or bending in the web elements. It is assumed that end stay plates do not undergo shear deformations. The effect of shear on the elastic critical load is depicted in Fig. 3.48 for three basic end conditions:

1. Both ends hinged (subscript *h)*
2. One end fixed, one hinged (subscript *f-h)*
3. Both ends fixed (subscript *f)*

One enters Fig. 3.48 with a chosen value of a_t/L and a calculated shear flexibility factor of μ. The load ratio P_{cr}/P_e can then be read for the appropriate end conditions, after which the effective-length factor may be calculated:

$$K = \sqrt{\frac{P_e}{P_{cr}}} \tag{3.34}$$

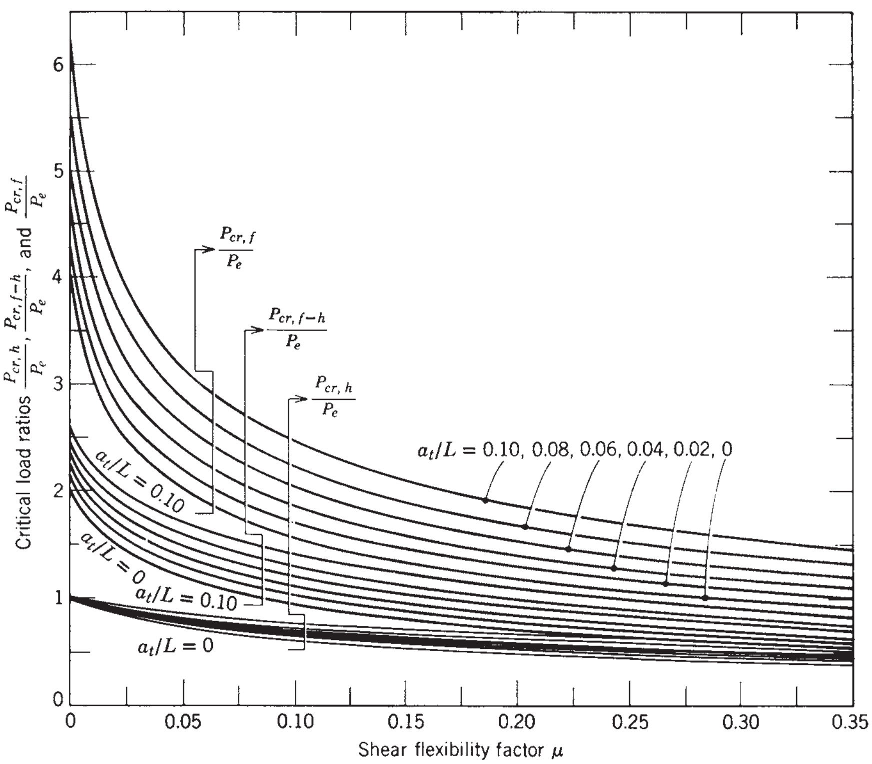

FIGURE 3.48 Critical loads of columns with various end conditions, shear flexibility factor μ, and rigid stay plates.

In Eq. 3.34 and Fig. 3.48, P_{cr} is the elastic critical load of the given open-web or open-flange column, and $P_e = \pi^2 EI/L^2$, the Euler load for a solid column with both ends hinged. Compressive resistance is then obtained for a given specification as a function of *KL/r*.

For a laced column, the elastic critical load, $P_{cr,}$ may be determined using a method proposed by Razdolsky (2005).

3.9.2 Laced Columns

For a typical laced member (Fig. 3.47*a*), consisting of two main longitudinal elements and two planes of diagonal lacing and transverse struts, Lin et al. (1970) provide the following formula for the shear flexibility factor, μ:

$$\mu = \frac{\xi_b}{1+\xi_a}\left(\frac{b}{l}\right)^2 \frac{A_c}{A_d}\left\{\frac{b}{\xi_a a}\left[1+\left(\frac{\xi_a a}{b}\right)^2\right]^{3/2} + \frac{b}{\xi_a a}\frac{A_d}{A_c}\right\} \tag{3.35}$$

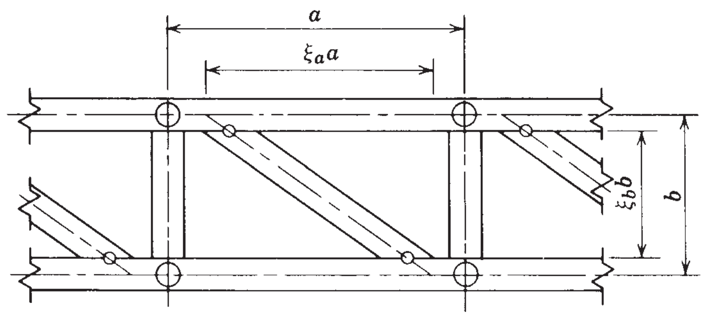

FIGURE 3.49 Typical panel of a laced structural member. Circles indicate where hinges were assumed in the analysis.

The notation used in Eq. 3.35 is defined in Figs. 3.47*a* and 3.49. The third edition of this guide (Johnston, 1976) provides an illustrative example of the application of Eq. 3.35 to a typical design.

In view of the usual small effect of shear in laced columns, Bleich (1952, p. 174) has suggested that a conservative estimate of the influence of 60° or 45° lacing, as generally specified in bridge design practice, can be made by modifying the effective-length factor, K (determined by end-restraint conditions), to a new factor, K', as follows:

$$K' = \begin{cases} K\sqrt{1 + \dfrac{300}{(KL/r)^2}} & \text{for } KL/r > 40 \\ 1.1K & \text{for } KL/r \leq 40 \end{cases} \tag{3.36}$$

The change in K is significant only for small KL/r values, in which case there is little change in the compressive design strength.

Bridge design practice in the United States (AASHTO, 2007; AREMA, 2008) requires that the slenderness ratio of the portion of the flange between lacing bar connections have a slenderness ratio of no more than 40, or two-thirds that of the entire member. Canadian bridge specifications (CSA, 2006) change the foregoing limits to 60 and three-fourths, respectively.

The lacing bars and their connections must be designed to act either in tension or in compression, and the rules for general column design apply to them as well. In exceptional cases, such as very large members, double diagonals can be designed as tension members and the truss system completed by compression struts. The importance of adequate and tight-lacing bar connections has been demonstrated experimentally (Hartmann et al., 1938).

Crane booms frequently consist of latticed columns. Vroonland (1971) analyzed nonuniform booms under combined lateral and axial loads and included the effects of deflections and intermediate lateral supports. Brolin et al. (1972) tested four booms, varying from 60 ft (18.2 m) to 200 ft (61.0 m) in length, to destruction. The failure loads were in good agreement with the analyses of Vroonland. Failures

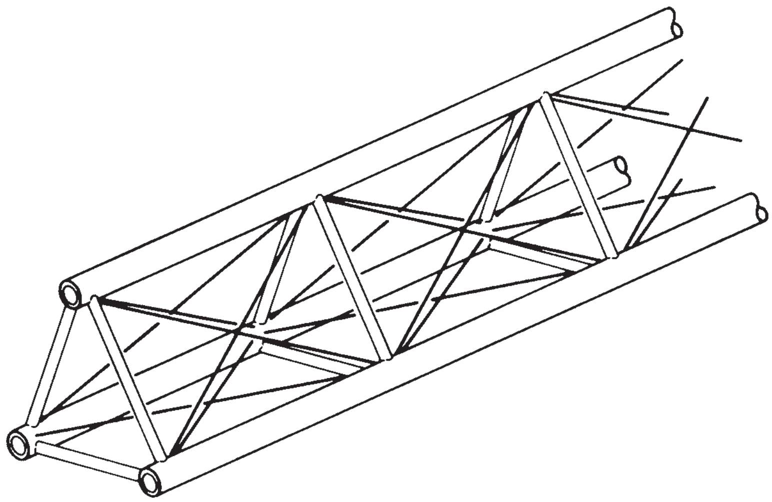

FIGURE 3.50 Triangular latticed column.

occurred when the compressive force in an individual chord member reached the failure load predicted for the unsupported length between brace points.

Interest in laced members has recently been renewed by the needs of the space industry for minimum-weight members to carry very small loads. Figure 3.50 illustrates a member with three longitudinal tubular chords (longerons) with tension diagonals and transverse compression struts. The overall slenderness and chord slenderness are approximately equal and are very large.

Miller and Hedgepeth (1979) studied the harmful effects of initial out-of-straightness of the column as a whole combined with that of the chords between struts. They provide charts that predict the maximum buckling load as a fraction of the Euler bifurcation load of a perfectly straight member. For slenderness ratios of both the member and chord of about 279, the maximum load is less than 50% of the Euler load. Crawford and Benton (1980) studied similar members and obtained comparable results. These studies indicate that for latticed members with very large slenderness ratios the interaction of local and overall out-of-straightness is the dominating factor, not the effect of shear.

3.9.3 Battened Columns

Figure 3.51 shows the basic elements of a battened column consisting of two main longitudinal chords rigidly connected by battens in one, two, or more planes. The battens act as the web and transmit shear from one chord to the other by flexural action in combination with local bending of the chords.

Because a battened column acts as a Vierendeel truss, it is more flexible in shear than either a laced column or even a column with perforated cover plates. The effect of shear distortions can be significant and should be considered in calculating the

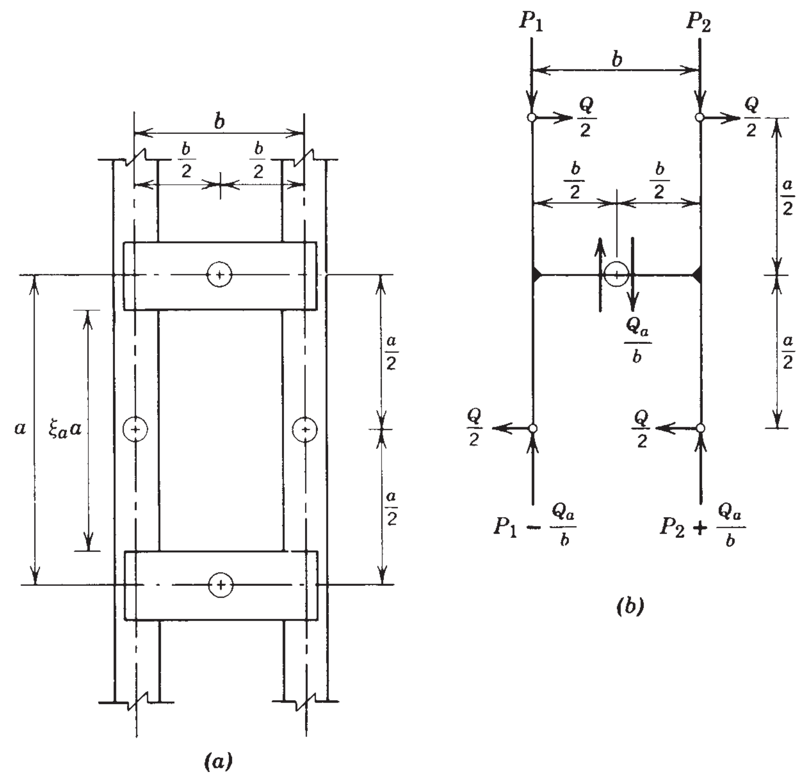

FIGURE 3.51 Typical panel of battened structural member: (a) geometrical configuration; (b) force equilibrium. Circles indicate assumed points of inflection.

compressive strength of the column. Battened columns are generally not allowed in current U.S. design specifications but are in some circumstances used in Canada. Battened columns are used for antenna towers and on occasion for secondary members. It should be noted that, while the lower portion of columns in mill buildings that support crane runway girders may look like battened columns, they really are spaced columns because the battens are not rigidly connected to the chords, as discussed in Section 3.9.4.

The typical unit of a battened column has a length a equal to the center-to-center distance between two battens, and a width b between centroids of the chords. The properties of the battened column are characterized by shear shape factors and the second moments of area of the battens and chords.

In developing the shear flexibility effect for the highly redundant battened member, Lin et al. (1970) assumed points of inflection for symmetric members at the midpoints of the battens and midway between the battens for the chords. The analysis is conservative because the overall continuity of the longitudinal members is neglected. The shear flexibility parameter is then given by

$$\mu = \left[\frac{1}{(l/r_c)^2} + \left(\frac{b}{2l}\right)^2\right]\left[\frac{A_c}{A_b}\left(\frac{ab}{6r_b^2} + 5.2\frac{a}{b}\eta_b\right) + 2.6\xi_a\eta_c + \frac{\xi_a^3}{12}\left(\frac{a}{r_c}\right)^2\right] \tag{3.37}$$

The nomenclature for Eq. 3.37 is shown in Fig. 3.51 and (additionally) as follows:

A_c, A_b = areas of a single longitudinal and of all batten elements within a unit, respectively

r_c, r_b = radii of gyration of the longitudinal and of the batten elements, respectively

η_c, η_b = shear shape factors of the longitudinal and of the batten elements, respectively, where the shear shape factor is the ratio of the total cross-section area to the shear area (Timoshenko and Gere, 1961)

l = length of column between end tie plates

Equation 3.37 accounts for the amplification of deflection in the column segments between battens. These may be neglected if the slenderness ratio of the chord segment between battens, $\xi_a\ a/r_c$, does not exceed $80\sqrt{\sigma_a}$, where σ_a is the average stress in ksi at the specified load level. This limit is considerably more stringent than the batten spacing requirements in some specifications. Because it is likely to be impractical to determine the partial rigidity of semirigid batten connections experimentally, it is recommended that whenever semirigid connections exist, the column be considered as a system of spaced columns.

Example 3.1: Battened Column As shown in Fig. 3.52, batten flange stiffeners have been included to eliminate local web distortion and to ensure that the

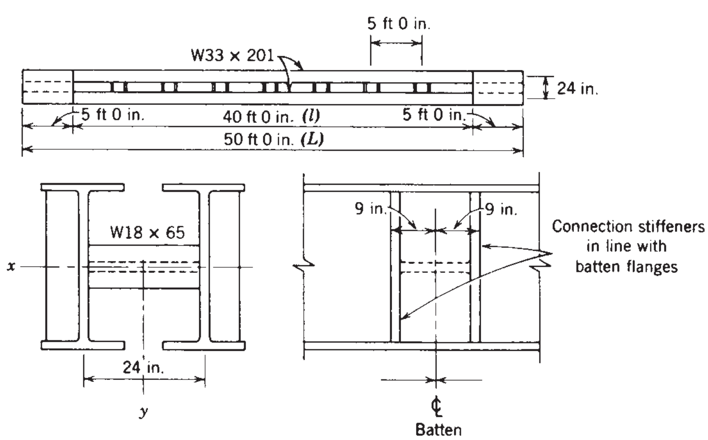

FIGURE 3.52 Example details.

(continued)

battens are fully effective. If such stiffeners were not provided, the column could be treated as a spaced column. From the AISC manual,

$$
\begin{aligned}
&W33 \times 201 \text{ (longitudinal)}\\
A_c &= 59.1 \text{ in.}^2\\
r_c &= r_y = 3.56 \text{ in.}\\
r_x &= 14.0 \text{ in.}\\
I_y &= 749 \text{ in.}^4\\
&W18 \times 65 \text{ (batten)}\\
A_b &= 19.1 \text{ in.}^2\\
r_b &= r_x = 7.49 \text{ in.}\\
a &= 60 \text{ in.}\\
b &= 24 \text{ in.}\\
\xi_a &= \frac{60 - 18}{60} = \frac{42}{60} = 0.70\\
l &= 480 \text{ in.}\\
L &= 600 \text{ in.}\\
\eta_c &= 1.6\\
a/L &= 0.10\\
\eta_b &= 2.6
\end{aligned}
$$

For the combined cross section,

$$
\begin{aligned}
I_y &= \frac{59.1 \times 24^2}{2} + 2 \times 749 = 18{,}519 \text{ in.}^4\\
r &= \sqrt{\frac{18{,}519}{2 \times 59.1}} = 12.5 \text{ in.} < r_x
\end{aligned}
$$

Substituting Eq. 3.37 yields

$$
\begin{aligned}
\mu = {} & \left[\frac{1}{(480/3.56)^2} + \left(\frac{24}{2 \times 480}\right)^2\right]\left[\frac{59.1}{19.1}\left(\frac{60 \times 24}{6 \times 7.49^2} + 5.2 \times \frac{60}{24} \times 2.6\right)\right.\\
& \left. + 2.6 \times 0.7 \times 1.6 + \frac{0.70^3}{12}\left(\frac{60}{3.56}\right)^2\right] = 0.088
\end{aligned}
$$

The critical load ratio for three sets of end conditions is obtained from Fig. 3.48 and the effective-length factor is evaluated from Eq. 3.34. The results are given in Table 3.2. If no reduction were made, the value of KL/r for the pinned–pinned case would be $600/12.5 = 48$.

TABLE 3.2 Results for Example 3.1

				$\phi_c F_{cr}$ (AISC) (ksi)	
End Conditions	P_{cr}/P_c (Fig. 3.48)	K	KL/r	$F_y = 36$ ksi	$F_y = 50$ ksi
Hinged-hinged	0.80	1.12	53.8	26.3	34.4
Hinged-fixed	1.45	0.83	39.9	28.1	37.8
Fixed-fixed	2.52	0.63	30.3	29.2	39.9

Bleich (1952) gives the following approximate formula for the effective length of a battened column with both ends pinned

$$\frac{KL}{r} = \sqrt{\left(\frac{L}{r}\right)^2 + \frac{\pi^2}{12}\left(\frac{a}{r_c}\right)^2} \tag{3.38}$$

where L/r is the slenderness ratio of the column as a whole and a/r_c is the slenderness ratio of one chord center-to-center of battens. Bleich (1952) estimates that the buckling strength of a steel column having an L/r ratio of 110 is reduced by about 10% when $a/r_c = 40$, and by greater amounts for larger values of a/r_c.

For Example 3.1, $a/r_c = 60/3.56 = 16.9$ and Eq. 3.38 gives

$$\frac{KL}{r} = \sqrt{\left(\frac{600}{12.5}\right)^2 + \frac{\pi^2}{12}(16.9)^2} = 50.4$$

which is lower than the 53.8 determined by Eqs. 3.34 and 3.37.

An unconservative assumption has been made that the addition of two stay plates gives the end regions full rigidity with respect to shear. It has also been assumed, however, that the effective length of a battened column is not decreased by the bending resistance due to the stay plates in the end regions. The two assumptions offset each other and their net effects may be neglected. Alternatively, more refined methodologies that consider the effects of stay plates have been proposed by Gjelsvik (1990) and Paul (1995).

The design of the chords and the batten plates and their connections should take into account the local bending resulting from specified shear forces. The batten plates and their connections to the chords are designed for the combination of shear, Qa/nb, and moment at the connection of

$$M_b = \frac{Qa}{2n} \tag{3.39}$$

(continued)

where Q is the shear required by specification plus shear due to any transverse loading, a is the center-to-center distance between battens, and n is the number of parallel planes of battens.

The section capacity of the chords should be checked for the combination of axial load and the bending moment:

$$M_c = \frac{Q\xi_a a}{4} \tag{3.40}$$

3.9.4 Stay Plates and Spaced Columns

End stay plates in battened columns may contribute significantly to the buckling strength. Their importance is revealed by the study of a spaced column, defined herein as the limiting case of a battened column in which the battens are attached to the longitudinal column elements by pinned connections. The battens then act simply as spacers, with no shear transmitted between the longitudinal elements. Without end stay plates, the buckling strength of such a spaced column is no greater than the sum of the critical loads of the individa1 longitudinal components of the built-up member. The strengthening effect of the end stay plates arises from two sources: (1) a shortening of the length within which the column components can bend about their own axes and (2) enforcing of the longitudinal components to buckle in a modified second-mode shape and thus have an elastic buckling coefficient that may approximate four times that of the first mode. The buckling load of a spaced column with end tie plates is a lower bound to the buckling load of the battened column (also with tie plates) but with low or uncertain moment resistance in the connections between battens and the longitudinal components. Such columns are sometimes used in mill building construction. In addition to their contribution to column strength, end tie plates perform their usual role of distributing the applied forces or moment to the component elements of either laced or battened columns. They also provide a means of transmitting load to another member or to a footing. With regard to the distance along the column between spacer elements, the same rule as for battens should provide a conservative basis for design.

Example 3.1 involved a battened column. If the stiffener plates to provide rigidity of the batten connections were omitted, the behavior would approach the conditions assumed for the spaced column because the attachment of the battens to the column webs would not transmit moment effectively.

Using the notation adopted for battened columns, the second moment of area of two longitudinals about the y–y axis would be, as in Example 3.1,

$$I = \frac{A_c b^2}{2} + 2I_c \tag{3.41}$$

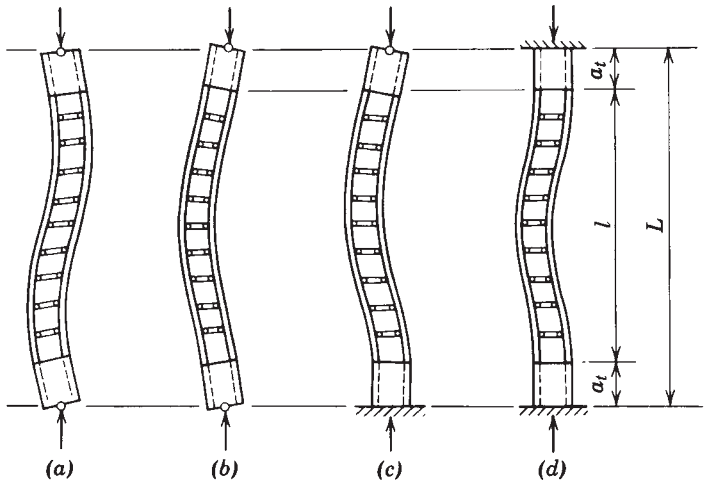

FIGURE 3.53 Spaced column buckling modes: (a) mode A, hinged–hinged; (b) mode E, hinged–hinged; (c) mode C, hinged–fixed; (d) mode D, fixed-fixed.

where I_c is the second moment of area of one of the individual longitudinal elements.

The ratio I/I_c in mill building columns is usually at least 40 and could be greater than 100. This ratio is used as a parameter for the determination of the buckling load of a spaced column with end tie plates.

Four modes of buckling for spaced columns without sidesway are treated in Johnston (1971), as illustrated in Fig. 3.53. Spaced columns with sidesway permitted also are considered briefly.

For the pinned-end condition, the spaced column with end stay plates buckles either in S-curvature (mode A in Fig. 3.53a) or in mode B curvature (Fig. 3.53b), depending on the values of I/I_c and a_t/L. It is noted that in S-curvature there is no differential change of length of the two longitudinal column components between the end tie plates; thus, they buckle under identical loads $P/2$, and the critical load is independent of the ratio I/I_c. When the column buckles in mode B curvature (Fig. 3.53b), the component on the concave side (at the center) shortens more than on the convex; thus, there arises overall moment resistance due to the difference in the axial forces. This resistance is in addition to the moments induced in the components as a result of their own curvature. The critical loads for S-curvature buckling could be less than those for mode B curvature when the ratio I/I_c is relatively small and a_t/L is large.

In practice, the base of a column will often be fixed to a footing, and S-curvature buckling cannot take place. Buckling will be in mode C, as illustrated in Fig. 3.53c, but as I/I_c gets large it will tend toward the shape with both ends fixed, as illustrated in Fig. 3.53d. In fixed-end buckling (Fig. 3.53d), as in mode A, the moment resistance is simply the sum of the moments in the component parts, with no contribution due to differential axial forces as in Figs. 3.53*b* or *c*.

The fixed-end case is the simplest to evaluate, because the critical load is simply twice the critical load of a longitudinal component with both ends fixed, that is, the Euler load with an effective length of $0.5L$ multiplied by 2.

Added moment resistance in a spaced column due to differential changes in component length occurs only when the end rotations are different in magnitude and/or sense, as in Figs. 3.53*b* and *c*. Within length l between the tie plates there is no shear transfer between the longitudinals; hence, the differential axial forces and the resisting moment that they contribute must remain constant within l.

Although Johnston (1971) gives critical-load information for a variety of end conditions, including the four shown in Fig. 3.53, the fixed-base and pinned-top case (Fig. 3.53*c*) is possibly of greatest practical application. In terms of the overall length $L = l + 2a_t$, the equation for elastic critical load is written

$$P_{cr} = \frac{CEI_c}{L^2} \tag{3.42}$$

in which C is termed the elastic buckling coefficient. For the determination of approximate critical loads in the inelastic range or for evaluation of compressive strengths by column design formulas, it is convenient to determine the effective-length factor, K, for use in the equation

$$P_{cr} = \frac{2\pi^2 EI_c}{(KL)^2} \tag{3.43}$$

where

$$K = \pi\sqrt{\frac{2}{C}} \tag{3.44}$$

Elastic-buckling coefficients, C, for the pinned–fixed case are plotted in Fig. 3.54, the use of which is illustrated in the following example.

Example 3.2: Spaced Column The column is identical to the one in Example 3.1, but omitting the batten-flange stiffeners and considering the design as a spaced column,

$$\frac{a_t}{L} = \frac{5}{50} = 0.10 \qquad \frac{I}{I_c} = \frac{18{,}519}{749} = 24.7$$

From Fig. 3.54, $C = 100$. By Eq. 3.44,

$$K = \pi\sqrt{\frac{2}{100}} = 0.445$$

$$\frac{KL}{r_c} = \frac{0.445 \times 600}{3.56} = 75.0$$

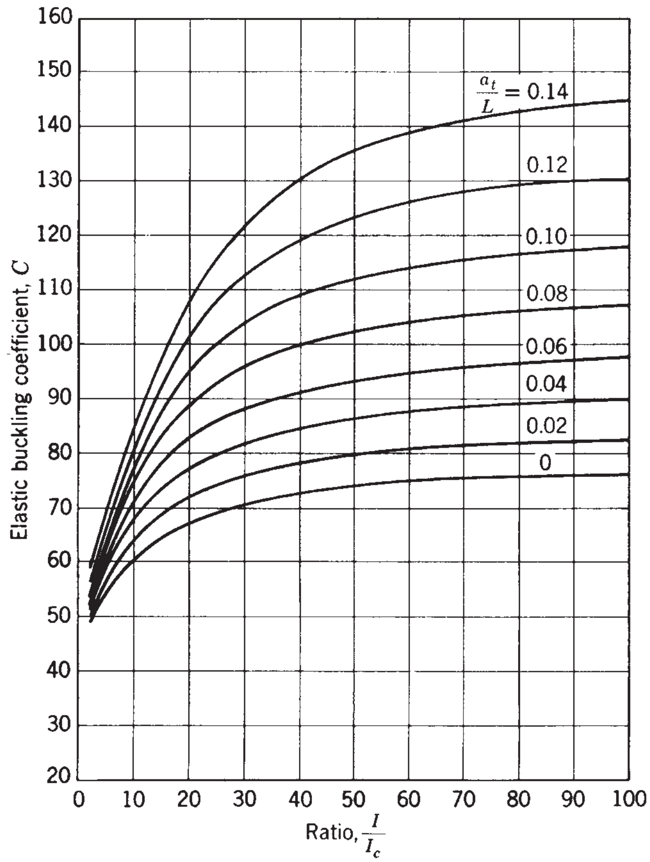

FIGURE 3.54 Elastic buckling coefficients, one end hinged, one end fixed (mode C of Fig. 3.53).

(Note that K is now referenced to L/r_c, not L/r.) Results using the AISC specification (2005a) are presented in Table 3.3.

TABLE 3.3 Results for Example 3.2

	$\phi_c F_{cr}$ ksi	
F_y	Spaced Column	Battened (Example 3.1)
36	22.8	28.1
50	28.2	37.8

In a limited number of tests on spaced columns (Freeman, 1973), the maximum failure loads fell short of the predicted, due in part to open holes in the bolted specimens and to deformation of the end stay plates. Pending further tests,

(continued)

it is recommended that only half of the length of the end stay plates be considered effective and that 90% of the theoretical failure loads be used as a basis for design.

3.9.5 Columns with Perforated Plates

White and Thűrlimann (1956) provide (in addition to the results of their own research) a digest of investigations at the National Bureau of Standards (Stang and Greenspan, 1948) and give recommendations for the design of columns with perforated cover plates. The following design suggestions for such columns are derived from the White–Thűrlimann study and from AASHTO specifications (2007).

When perforated cover plates are used, the following provisions govern their design:

1. The ratio of length, in the direction of stress, to width of perforation should not exceed 2.
2. The clear distance between perforations in the direction of stress should not be less than the distance between points of support [i.e., $(c - a) \geq d$ in Fig. 3.55*a*].
3. The clear distance between the end perforation and the end of the cover plate should not be less than 1.25 times the distance between points of support.
4. The point of support should be taken as the inner line of fasteners or fillet welds connecting the perforated plate to the flanges. For plates butt welded to the flange edge of rolled segments, the point of support may be taken as the weld whenever the ratio of the outstanding flange width to the flange thickness of the rolled segment is less than 7. Otherwise, the point of support should be taken as the root of the flange of the rolled segment.
5. The periphery of the perforation at all points should have a minimum radius of $1\frac{1}{2}$ in. (38 mm).
6. The transverse distance from the edge of a perforation to the nearest line of longitudinal fasteners, divided by the plate thickness, that is, the *b/t* ratio of the plate adjacent to a perforation (see Fig. 3.55), should conform to minimum specification requirements for plates in main compression members.

3.10 STEPPED COLUMNS

Stepped columns are often used in mill buildings to support roof or upper wall loads and runway girders on which cranes travel, as illustrated in Fig. 3.56.

A notional load approach to the design of mill building columns has been presented by Schmidt (2001). In general, however, the effective length of a uniform or prismatic column having the same buckling characteristics as that of the stepped

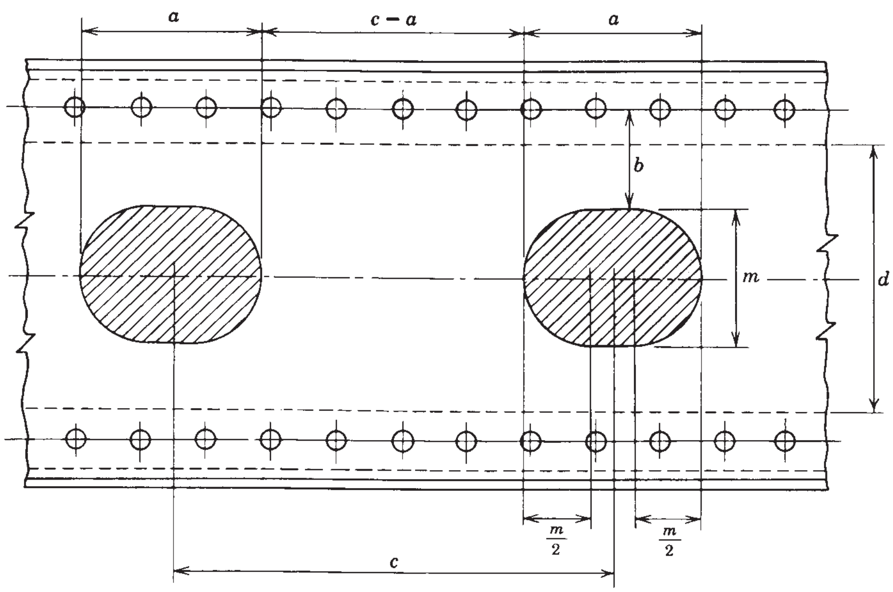

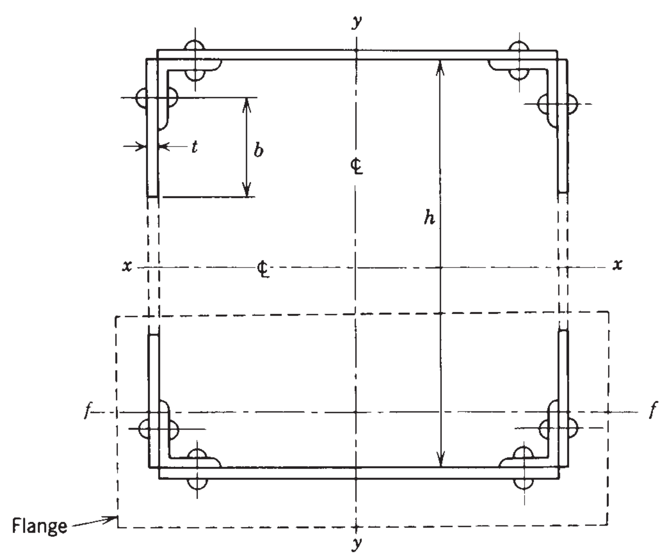

FIGURE 3.55 Column with perforated web plates.

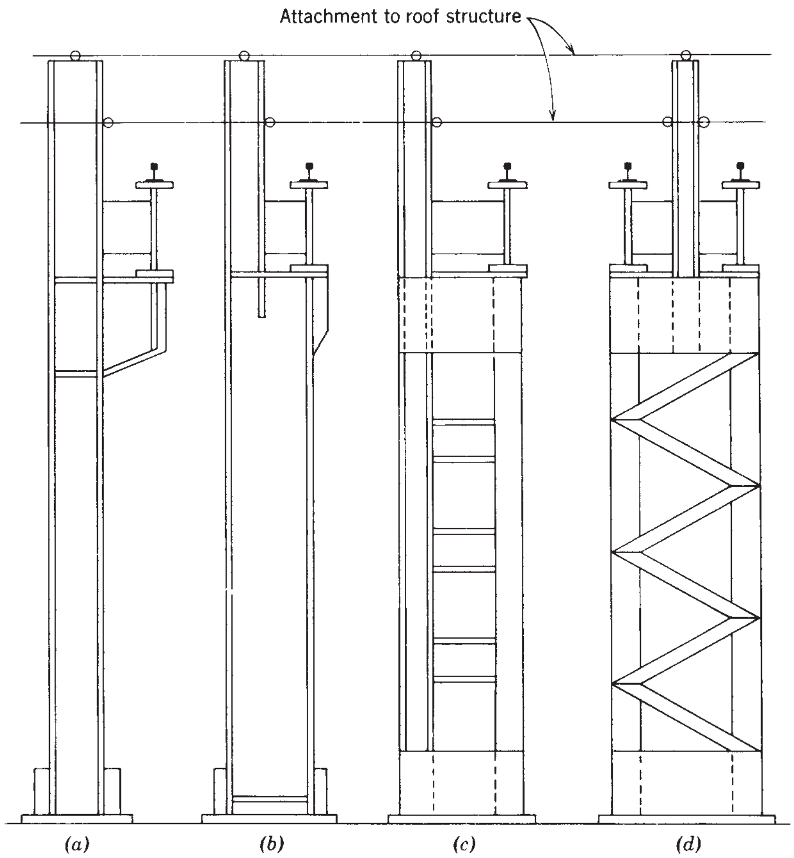

FIGURE 3.56 Type of columns in mill buildings.

column is needed to determine the axial compressive resistance and the Euler buckling load for potential modes of failure by buckling or bending about the x–x axis (see Fig. 3.57). Tables to determine effective-length factors are provided in the Association of Iron and Steel Engineers guide (AISE, 1979) for a range of the three parameters defined in Fig. 3.57 and for the cases when the column base is either fixed or pinned and the column top is pinned. The parameter a is the ratio of the length of the upper (reduced) segment to the total length. The parameter B is the ratio of the second moment of area (about the centroidal x–x axes) of the combined (lower) column cross section to that of the upper section. The parameter P_1/P_2 is the ratio of the axial force acting in the upper segment (roof and upper wall loads) to that applied to the lower segment (crane girder reactions with an allowance for lower wall loads and the column weight). Other notations are also given in Fig. 3.57. The AISE tables give ranges for a from 0.10 to 0.50, for B from 1.0 to 100, and for P_1/P_2 from 0.0 to 0.25. Huang (1968) provides values of the

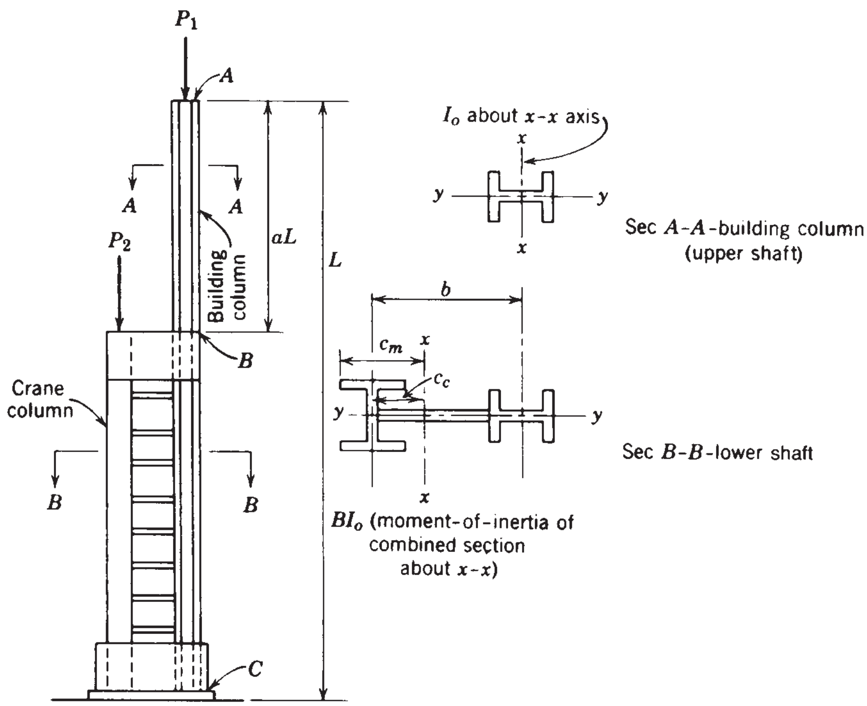

FIGURE 3.57 Notation for stepped columns (AISE, 1979).

effective-length factors in graphs over a somewhat different range of parameters for stepped columns with fixed bases and pinned tops and for values of P_1/P_2 up to 1.0. Further values tabulated for the effective-length factors for stepped columns are given in Timoshenko and Gere (1961), the Column Research Committee of Japan handbook (CRCJ, 1971, English edition), and Young (1989). A method for determining the effective-length factor of a stepped column without using charts was proposed by Lui and Sun (1995). A hand calculation method for determining the buckling load of a stepped column was also proposed by Fraser and Bridge (1990).

The interaction equations used for the design of stepped columns depend on the potential modes of failure and therefore on how the columns are braced. Stepped columns are usually laterally unsupported over the entire length for buckling or bending about the x–x axis. For buckling about the y–y axis, lateral support is usually provided at the level of the crane runway girder seat, location B in Fig. 3.57. Therefore, the following potential failure modes exist:

1. Bending of the overall column in-plane about the x–x axis. It is for this case that the equivalent length for the stepped column is needed in order that the compressive resistance and the Euler buckling load may be determined.

2. Buckling about the y–y axis of the lower segment.
3. Yielding of the cross section of the lower segment.
4. Buckling about the y–y axis of the upper (reduced) segment of the column.
5. Yielding of the cross section of the upper segment.

The interaction equations for axial compression and biaxial bending are

$$\frac{P_u}{\phi P_n} + \frac{8}{9}\left(\frac{M_{ux}}{\phi_b M_{nx}} + \frac{M_{uy}}{\phi_b M_{ny}}\right) \le 1.0 \quad \text{for} \quad P/\phi P_n \ge 0.2 \tag{3.45a}$$

$$\frac{P_u}{2\phi P_n} + \left(\frac{M_{ux}}{\phi_b M_{nx}} + \frac{M_{uy}}{\phi_b M_{ny}}\right) \le 1.0 \quad \text{for} \quad P/\phi P_n < 0.2 \tag{3.45b}$$

where M_{ux} would include second-order effects, which could be modeled by

$$B_{1x} = \frac{C_{mx}}{1 - P_u/P_{ex}} \ge 1.0 \tag{3.45c}$$

with a similar term for B_{1y} related to bending about the y–y axis, M_{uy}.

It is conservatively assumed that the moments M_{uy} due to eccentric crane girder reactions are all taken by the lower segment and therefore the moments about the y–y axis in the upper segment are zero.

Following the AISC LRFD procedures, failure modes 1, 2, and 3 are considered together, as are modes 4 and 5. When using the AISC LRFD equations for failure modes 1, 2, and 3 combined, the following values are suggested. The factored axial load, P_u, is $P_1 + P_2$, and M_{ux} and M_{uy} are the maximum modified factored moments within the length. Based on AISE (1979), C_{mx} is taken as 0.85 when all bents are under simultaneous wind load with sidesway. For crane load combinations, with only one bent under consideration, take C_{mx} equal to 0.95. Because it has been assumed that the lower segment takes all the moments about the y–y axis, C_{my} equals 0.6 when the base is pinned and 0.4 when the base is fixed about the y–y axis. The compressive resistance is the least of ϕP_{nx} of the equivalent column and ϕP_{ny} of the bottom segment, taking, in this case, $K = 0.8$ if the base is considered to be fully fixed, and $K = 1.0$ if the base is considered to be pinned. The factored moment resistance $\phi_b M_{nx}$ is based on the possibility of lateral–torsional buckling and $\phi_b M_{ny}$ is the full cross-section strength. This being the case, both factors B_{1x} and B_{1y} as given previously are limited to a value of' 1.0 or greater. The value of P_{ex} is as determined for the equivalent column and P_{ey} is based on 0.8 of the lower segment for a fixed base and 1.0 of the lower segment if the base is pinned. When using the AISC LRFD equations for failure modes 4 and 5 combined for the upper segment, the values suggested parallel those for the lower segment with the exceptions that there are moments only about the x–x axis and C_{mx} depends directly on the shape of the moment diagram.

The five failure modes could also be checked independently when the values for checking are as follows: For bending failure about the x–x axis, failure mode 1 (the predominant moments are about the x–x axis), the factored axial load is $P_1 + P_2$, and M_{ux} and M_{uy} are the maximum modified factored moments within the length. C_{mx} is taken as 0.85 when all bents are under simultaneous wind load with sidesway. For crane load combinations, with only one bent under consideration, take C_{mx} equal to 0.95. Because it has been assumed that the lower segment resists all the moments about the y–y axis, $C_{my} = 0.6$ when the base is pinned and 0.4 when the base is fixed about the y–y axis. The value of B_1 is not restricted. The compressive resistance is the least of ϕP_{nx} of the equivalent column and ϕP_{ny} of the bottom segment with $K = 0.8$ if the base is taken to be fully fixed and with $K = 1.0$ if the base is taken as pinned. The factored moment resistances, $\phi_b M_{nx}$ and $\phi_b M_{ny}$, are the full cross-section strengths. The value of P_{ex} is as determined for the equivalent column and P_{ey} is based on 0.8 of the lower segment for a fixed base and 1.0 of the lower segment if the base is pinned.

The values for checking the last four potential failure modes, modes 2 to 5, independently (for y–y axis buckling and for cross-section strength) are as follows. The factored force effects P_u, M_{ux}, and M_{uy} are those for the appropriate segment. When checking for cross-section strength, the resistances ϕP_n, $\phi_b M_{nx}$, and $\phi_b M_{ny}$ are the full factored cross-section strengths for the appropriate segment. When checking for y–y axis buckling, ϕP_{ny} is based on y–y axis end conditions for the segment being considered. The effective length is the full length AB for the upper segment and the length BC for the lower segment if full base fixity does not exist and 0.80 of the length BC if fully fixed at the base. In Eq. 3.45, M_{nx} is the appropriate lateral–torsional buckling strength taking into account the shape of the moment diagram, and M_{ny} is the full cross-section strength. C_{mx} and C_{my} have minimum values of 1.0 because the variation of moment has been accounted for in finding the moment resistance. The value of P_{ex} is that determined for the equivalent column and P_{ey} is taken as that for the appropriate segment.

A demonstration of the LRFD approach to the design of stepped crane columns has been presented by MacCrimmon and Kennedy (1997). The design of a column with constant cross section subject to lateral loads and moments applied at a bracket has been considered by Adams (1970). The upper and lower segments are treated as separate beam-columns. Horne and Ajmani (1971) and Albert et al. 1995 take into account the lateral support provided by the girts attached to one flange of the column.

3.11 GUYED TOWERS

Guyed towers are used for communication structures, for electrical transmission structures (ASCE, 1972), and, more recently, for compliant offshore platforms and wind energy conversion systems. They consist of a mast supported at one or more levels by guy cables that are anchored at the base. The masts are generally three-dimensional steel trusses of either triangular or square cross section, but occasionally may be of circular cross section. The loading on a guyed tower may include:

1. Self-weight
2. Initial guy tensions (also called guy pretensions)

3. Wind, ice, and earthquake loads
4. Loads due to falling ice, sudden rupture of guy cables, conductors, ground wire
5. For communication towers, loads on antennas
6. For electrical transmission towers, loads on conductors and ground wire
7. For compliant offshore platforms, operational loads and wave loading
8. Transportation and erection loads

The annual failure rate of existing towers was estimated by Magued et al. (1989) to be 55/100,000. This is considered to be high when compared to other structures. Contrary to most other structures for which the dead load is the major load, wind loads and combined wind and ice loads are the major loads on towers (Wahba et al., 1993).

The complete design of a guyed tower includes consideration of vibration and fatigue phenomena in which ice-covered cables tend to vibrate with large amplitudes perpendicular to the direction of wind. Galloping, which generally results from some form of icing on the cables when there is sufficient energy to produce large oscillations, may often lead to failure of the tower. Saxena et al. (1989) reported that there were many incidents where some form of ice storm accompanied by moderate wind speed led to the collapse of transmission and communication towers. Considerable work has been done on the prediction of dynamic behavior and the effect of wind and ice loads on such towers (McCaffrey and Hartman, 1972; Novak et al., 1978; Nakamoto and Chiu, 1985; Saxena et al., 1989). Simplified methods for estimating the dynamic response using a series of static patch loads have been developed (Gerstoft and Davenport, 1986; Davenport and Sparling, 1992). McClure et al. (1993) identified sudden ice shedding and earthquakes as some of the other causes of concern for the safety of these towers.

The following deals only with buckling aspects of guyed tower design. Although instability may not be the failure mode of all guyed towers, the possibility of general instability of a guyed tower should be investigated by the designer (Hull, 1962; Goldberg and Gaunt, 1973; Williamson, 1973; Chajes and Chen, 1979; Chajes and Ling, 1981; Costello and Phillips, 1983).

Because the governing equilibrium equations are not linear homogeneous equations, instability is not a bifurcation problem, but rather occurs as a large deformation for a small increase in applied load. The stability of a guyed tower is influenced principally by (1) the cross-section area of guy cables, (2) the second moment of area of the cross section of the mast, and (3) the initial tension in the guy cables. For the case of buckling of a guyed tower, the axial stiffness of the guy cables is, perhaps, more important than the bending stiffness of the mast. The buckling load can be increased effectively by increasing the cross-section area of guy cables up to the point where the mast would buckle in a number of half-waves equal to the number of guy levels. To increase the buckling load further, the second moment of area (i.e., the bending stiffness) of the mast must be increased. An increase in guy pretensions has both beneficial and detrimental effects on the stability of guyed towers. An increase in guy pretension is beneficial as it results in reduced deflections of the mast. On the other hand, an increase in guy pretension is detrimental as it increases the compressive force in the mast, thus reducing its resistance to buckling. Initially, the increase in guy pretension results in an increase in buckling load because of reduced tower deflections. After a certain stage, however, the increase in the buckling load produced by increasing guy pretension will be more than offset by the decrease in the buckling load due to increasing compressive force on the mast.

The analysis of a guyed tower is complicated because of its geometrically nonlinear behavior even at low-load levels. This nonlinearity is due to the increase in axial stiffness of guy cables with increasing tension and the decrease in the bending stiffness of the mast due to the increase in compressive forces. A guyed tower is usually analyzed by approximating it as an equivalent continuous beam-column on nonlinear elastic supports (Cohen and Perrin, 1957; Rowe, 1958; Dean 1961; Livesley and Poskitt, 1963; Goldberg and Meyers, 1965; Odley, 1966; Williamson and Margolin, 1966; Rosenthal and Skop, 1980; Ekhande and Madugula, 1988). Issa and Avent (1991) presented a method to obtain the forces in all individual members of the mast directly by the use of discrete field mechanics techniques. Sometimes the analytical model for the guyed tower analysis may be a finite element representation using beam-column elements for the mast and cable elements for the guys [International Association for Shell and Spatial Structures (IASS), 1981].

Two basic approaches are used for the second-order elastic analysis (geometric nonlinear analysis): the stability function approach and the geometric stiffness approach. This type of analysis includes both $P - \Delta$ (chord rotation) and $P - \delta$ (member curvature) effects, thus eliminating the need for moment amplification factors. The use of member effective-length factors (K-factors) is also not required when the design is carried out in accordance with CSA S16-09 (CSA, 2009). As all the force resultants acting on the ends of the members are established from the second-order analysis, the member design is based on its actual length, that is, the member is designed assuming that $K = 1$. The tower legs can be designed as beam-columns in the usual manner.

3.11.1 Strengthening of Existing Towers

Solid round and pipe steel members are widely used as leg and bracing members in lattice guyed communication towers because they are subjected to less wind load than angle members and have the same compressive strength about all axes leading to economy in design. The increase in instant voice and data communication and the advent of new technology such as digital television make it necessary for owners to re-evaluate the capacity of existing antenna towers. If there are additional loads (e.g., antennas) added to an antenna tower and/or if there is an increase in the strength requirements, the existing antenna tower has to be reinforced to bring it into compliance with the latest antenna tower standards. The method generally used to increase the compressive strength of the members consists of attaching an angle/rod/split pipe section to the members. The reinforcing members are connected to the main members at intervals by means of clamps (e.g., U-bolts) which are sometimes welded at the ends.

Work was initiated at the University of Windsor in 2004 to determine the strength of reinforced members (Bhuiyan, 2005; Kumalasari et al., 2004, 2005a, 2006b; Siddiqui, 2005; Tickle, 2004; Zeineddine, 2004). Tests and preliminary analyses have been carried on steel members that include:

(i) Solid round sections strengthened with rods
(ii) Solid round sections strengthened with angles
(iii) Solid round sections strengthened with split pipe
(iv) Pipe sections strengthened with split pipe

Because there are very few facilities available in North America for testing large-size rods up to 300 mm diameter which are used in practice, the only realistic method of design has to be based on numerical modeling of the strengthened member, validated by experimental data on small-size specimens.

3.11.2 Strength of Bolted Ring-Type and Flange-Type Connections

Guyed lattice communication tower sections are fabricated using welded splices, and these welded sections are bolted together in the field. There are two types of bolted splices, namely, bolted ring-type splices for leg diameters up to 65 mm (2.5 in.) and bolted flange-type splices for leg diameters greater than 65 mm (2.5 in.). The leg members of a steel tower are subjected to compressive loads due to dead load and guy tension and tensile–compressive loads due to bending moments caused by wind/seismic loads. The strength of splices between the leg sections is vital because it affects the overall performance of the tower.

Bolted Ring-Type Splices The Canadian Institute of Steel Construction *Handbook of Steel Construction* (CISC, 2006) and the AISC *Steel Construction Manual* (AISC, 2005b) do not provide any guidance for analyzing bolted ring-type splices subject to tension. Ignoring the eccentricity of the splice and using the axial tensile capacity of the bolt to design the splice is unsafe, as shown by Kumalasari et al. (2005b) and Shen (2002). The splice should be designed for combined stresses due to axial tension and bending, with a moment equal to the axial load times half the distance between the center of the leg and the center of the bolt (to take into account the fixity of the splice).

Bolted Flange-Type Splices One common type of splice for solid round leg members of guyed lattice communication towers consists of circular flange plates welded to the members and bolted together. These are subjected to tension due to the applied lateral loads (wind or earthquake). Both the *Handbook of Steel Construction* (CISC, 2006) and the *Steel Construction Manual* (AISC, 2005b) discuss prying action only in tee-type and angle-type connections subjected to tensile force and no guidance is provided to determine the prying force in bolted steel circular flange connections. In order to use the formulas given in those publications, Kumalasari et al. (2006a) and Hussaini (2004) suggest that the value of "p", that is, the length of flange tributary to each bolt (bolt pitch), be taken as the distance between the centers of bolts measured along the bolt circle (which is equal to the circumference of the bolt circle divided by the number of bolts).

3.11.3 Dynamic Impact Factor Due to Sudden Guy Ruptures and Guy Slippage

There are several instances of collapse of guyed towers due to the failure of the guy. The most significant failure was the collapse of a 646 m mast (the tallest guy mast in the world) in Gabin, Poland. Guys could be ruptured either intentionally due to sabotage or accidentally (e.g., an airplane or farming equipment hitting one of the guy wires). Also, during tower erection, a guy wire can slip at the anchor location before it is set firmly in place. Several different factors, such as guy damping and mast damping, affect the behavior of the mast after guy rupture or slippage. The dynamic impact factor can be very high for guy wires located immediately below the ruptured guy wire.

The effects of sudden guy rupture at the mast attachment point were investigated numerically by Kahla (1997, 2000). Eurocode 3.1 (CEN, 2006) suggests the dynamic effects caused by guy rupture can be conservatively estimated by (1) the static method and (2) a simplified energy approach. Nielsen (1999) compared the Eurocode procedures with full dynamic analysis for a 244-m mast in Finland and found that both the static method and the simplified energy approach are conservative.

3.11.4 Aeolian Vibration and Galloping of Guy Wires

The mast guys can be subjected to high-frequency, low-amplitude vortex-excited vibrations (Aeolian vibrations) and to low-frequency, large-amplitude vibrations (guy galloping). Guys may be subject to low-amplitude resonant-type vibrations at low wind speeds caused by vortex excitation at high frequency. Guys may be subject to galloping excitation when coated with ice or thick grease. The accretion of ice or grease can form aerodynamic shapes, which provide lift and drag instabilities. These result in low-frequency, high-amplitude vibration. Similar vibrations can also occur under conditions of rain.

Guyed structures are characterized by a certain vibration frequency spectrum (Ciesielski and Koziol, 1995). To suppress guy vibrations that occur under wind, Eurocode prescribes that dampers should be mounted on guys in all cases where initial tension is greater than 10% of the rated breaking strength of the guy.

The dynamic response of guyed towers differs considerably from self-supporting towers, primarily due to the nonlinear behavior of the guys attached to them. To avoid failures, such as fatigue in connections, insulators, anchorage system, and the individual wires of the guys, high and low frequency guyed dampers have been developed to control vibrations of tall guyed towers. Various dampers used for vibration control of guyed towers are discussed in the ASCE Task Committee Report on Dynamic Response of Lattice Towers (Madugula, 2002) and these are briefly described below.

Dampers Used for Control of Aeolian Vibrations Appropriate dampers should be installed in all cases where Aeolian vibrations are predicted or have been observed. Various types of dampers are available, such as:

1. Tuned inertial-type (Stockbridge) dampers consisting of two masses on the ends of short cantilever lengths of spiral strand tuned to the same frequency as the guy
2. Rope loops clamped to the guys
3. Hydraulic dashpots

The tuned inertial type dampers have a long and successful history. There is evidence that partial control of galloping may be obtained by the attachment of a hemp rope from guy to guy, connecting the points of maximum amplitude of two or more guys. The dashpot damper is one of the most common types of guy dampers that have proven effective.

Dampers Used for Control of Guy Galloping Dampers in use to suppress or reduce galloping excitations are the sandamper, the snubber damper, and the hanging chain damper. The sandamper consists of a closed cylinder partially filled with dry sand such that when the cylinder rotates, energy is dissipated. The size, diameter, and mass of the cylinder and the amount of sand must be determined by the modes to be damped and the amount of damping required for controlling the guy vibrations. The snubber damper consists of a tie-down attached to the lower portion of a guy by a pulley. The tie-down has a standard automotive shock absorber installed. The hanging chain damper consists of a heavy chain suspended from a guy rope. Hanging chains, however, constitute a major obstacle to guy inspection and regreasing—both operations involve running a man-riding chair up the full length of each guy. Also, there is a long-term possibility of mechanical damage to the guy wire where the chain is suspended from the guy wire. In addition, the dampers themselves represent a long-term maintenance liability and would require extensive fencing to protect them from grazing farm animals. Guy galloping can probably be controlled with Stockbridge-type dampers if they can be obtained in the appropriate sizes. These are not readily available in the large sizes encountered on guys for tall masts (Wiskin 1995).

REFERENCES

AA (2005), *Specifications for Aluminum Structures*, Aluminum Association, Arlington, VA.

AASHTO (1996), *Standard Specification for Highway Bridges*, 16th ed., American Association of State Highway and Transportation Officials, Washington, DC.

AASHTO (2007), *Standard Specification for Highway Bridges*, 4th ed., American Association of State Highway and Transportation Officials, Washington, DC.

Ackroyd, M. H. (1979), "Nonlinear Inelastic Stability of Flexibly Connected Plane Steel Frames," PhD. dissertation, University of Colorado, Boulder, CO.

Ackroyd, M. H., and Bjorhovde, R. (1981), "Effect of Semi-rigid Connections on Steel Column Strength" (discussion), *J. Const. Steel Res. (London)*, Vol. 1, No. 3, pp. 48–51.

Adams, P. F. (1970), "Segmental Design of Steel Beam-Columns," *Proc. Can. Struct. Eng. Conf.*, Toronto, Ontario, Canada.

AISC (1978), *Specification for the Design, Fabrication and Erection of Structural Steel Buildings*, American Institute of Steel Construction, Chicago, IL.

AISC (1986), *Load and Resistance Factor Design Specification for Structural Steel Buildings*, American Institute of Steel Construction, Chicago, Il.

AISC (1993), *Load and Resistance Factor Design Specification for Structural Steel Buildings*, American Institute of Steel Construction, Chicago, IL.

AISC (1999), *Load and Resistance Factor Design Specification for Structural Steel Buildings*, American Institute of Steel Construction, Chicago, IL.

AISC (2005), "Specification for Structural Steel Buildings", ANSI/AISC Standard 360-05, American Institute of Steel Construction, Chicago, IL.

AISC (2005), Steel Construction Manual. American Institute of Steel Construction, Chicago, IL.

AISE (1979), "Guide for the Design and Construction of Mill Buildings," AISE Tech. Rep. No. 13, Association of Iron and Steel Engineers, Pittsburgh, PA.

Albert, C, Srna, P., Kennedy, S. J., and Kennedy, D. J. L. (1995), "Inelastic Distortional Strength of Steel Beam-Columns," *Int. Conf. Struct. Stab. Design*, Oct. 30–Nov. 1, Australian Institute of Steel Construction, Sydney, Australia.

Alpsten, G. A. (1970), "Residual Stresses and Strength of Cold-Straightened Wide Flange Shapes," *Jernkontorets Ann.*, Vol. 154 (in Swedish), pp. 1–9.

Alpsten, G. A. (1972a), "Prediction of Thermal Residual Stresses in Hot Rolled Plates and Shapes," 9th Congr. IABSE, Final Rep., Amsterdam, May, pp. 1–13.

Alpsten, G. A. (1972b), "Residual Stresses, Yield Stress and Column Strength of Hotrolled and Roller-Straightened Steel Shapes," Colloq. Column Strength, Paris.

Alpsten, G. A., and Tall, L. (1970) "Residual Stresses in Heavy Welded Shapes," *Weld. J.*, Vol. 49, No. 3, pp. 93–105.

AREMA (2008), *Manual for Railway Engineering*, American Railway Engineering and Maintenance-of-Way Association, Chicago, IL.

ASCE (1972), "Guide for the Design of Aluminum Transmission Towers," Task Committee on Lightweight Alloys of the Committee on Metals of the Structural Division, American Society of Civil Engineers, *Proc. ASCE*., Vol. 98, No. ST12.

ASCE (2003). *Specification for the Design of Cold-formed Stainless Steel Structural Members*, SEI/ASCE-8, American Society of Civil Engineers, New York.

Aslani, F. and Goel, S. C. (1991), "An Analytical Criterion for Buckling Strength of Built-up Compression Members," *AISC Eng. J.*, Vol. 28, No. 4, pp. 159–168.

AS/NZS (2001). *Cold-formed Stainless Steel Structures*, AS/NZS 4673, Standards Australia, Sydney.

Baker, J. F., and Roderick, J. W. (1948), "The Strength of Light Alloy Struts," Res. Rep. No. 3, Aluminum Development Association, London.

Barakat, M. A., and Chen, W. F. (1990), "Practical Analysis of Semi-rigid Frames," *AISC Eng. J.*, Vol. 27, No. 2, pp. 54–68.

Batterman, R. H., and Johnston, B. G. (1967), "Behavior and Maximum Strength of Metal Columns," *ASCE J. Struct. Div.*, Vol. 93, No. ST2, pp. 205–230.

Bažant, Z. P., and Cedolin, L. (1991), *Stability of Structure—Elastic, Inelastic, Fracture and Damage Theories*, Oxford University Press, New York.

Beaulieu, D. and Adams, P. F. (1980), "Significance of Structural Out-of-Plumb Forces and Recommendations for Design," *Can. J. Civil Eng.*, Vol. 7, No. 1, pp. 105–113.

Beedle, L. S. (ed.) (1991), *Stability of Metal Structures: A World View*, Structural Stability Research Council, Bethlehem, PA.

Beedle, L. S. (ed.) (1993), *Semi-rigid Connections in Steel Frames*, Council on Tall Buildings and Urban Habitat, McGraw-Hill, New York.

Beedle, L. S., and Tall, L. (1960), "Basic Column Strength," *ASCE J. Struct. Div.*, Vol. 86, No. ST5, pp. 139–173.

Beer, H., and Schultz, G. (1970), "Theoretical Basis for the European Column Curves," *Constr. Met.*, No. 3, p. 58.

Beer, G., and Tall, L. (1970), "The Strength of Heavy Welded Box Columns," Fritz Eng. Lab. Rep. No. 337.27, Lehigh University, Bethlehem, PA, Dec.

Bernard, A., Frey, F., Janss, J., and Massonnet, C. (1973), "Research on the Buckling Behavior of Aluminum Columns," *IABSE Mem.* (in French), Vol. 33, No. 1, pp. 1–33.

Bhuiyan, P. A. (2005), "Effect of Spacers on the Compressive Strength of Solid Round Steel Members Reinforced with Split Pipe,' M.A.Sc. Major Paper, University of Windsor, Windsor, Ontario, Canada.

Bijlaard, F. S. K., Gresnigt, A. M., and van der Vegte, G. J. (2005), *Connections in Steel Structures V—Behaviour, Strength and Design*, Bouwen met Staal, The Netherlands.

Birkemoe, P. C. (1977a), "Column Behavior of Heat-Treated Cold-Formed Hollow Structural Shapes," *Stability of Structures Under Static and Dynamic Loads, Proc. 2nd Int. Colloq.*, Washington, DC.

Birkemoe, P. C. (1977b), "Development of Column Curves for H.S.S.," *Int. Symp. Hollow Struct. Sec.*, CIDECT, Toronto, Ontario, Canada.

Bjorhovde, R. (1972), "Deterministic and Probabilistic Approaches to the Strength of Steel Columns," Ph.D. dissertation, Lehigh University, Bethlehem, PA.

Bjorhovde, R. (1977), "Strength and Behavior of Cold-Formed H.S.S. Columns," Struct. Eng. Rep. No. 65, University of Alberta, Edmonton, Alberta, Canada, Dec.

Bjorhovde, R. (1978), "The Safety of Steel Columns," *ASCE J. Struct. Div.*, Vol. 104, No. ST3, pp. 463–477.

Bjorhovde, R. (1980), "Research Needs in Stability of Metal Structures," *ASCE J. Struct. Div.*, Vol. 106, No. ST12, pp. 2425–2442.

Bjorhovde, R. (1981), "End Restraint and Column Stability" (discussion), *ASCE J. Struct. Div.*, Vol. 107, No. ST8, pp. 1696–1700

Bjorhovde, R. (1984), "Effect of End Restraint on Column Strength: Practical Applications," *AISC Eng. J.*, Vol. 21, No. 1, pp. 1–13.

Bjorhovde, R. (1988), "Columns: From Theory to Practice," *AISC Eng. J.*, Vol. 25, No. 1, pp. 21–34.

Bjorhovde, R. (1991), "The Strength of Heavy Columns," *J. Constr. Steel Res.*, Vol. 19, No. 4, pp. 313–320.

Bjorhovde, R. (1992), "Compression Members," in *Constructional Steel Design: An International Guide* (P. J. Dowling, J. E. Harding, and R. Bjorhovde, eds.), Elsevier Applied Science, London, Chap. 2.3.

Bjorhovde, R. (2006), "Cold Bending of Wide-Flange Shapes for Construction," *Eng. J. AISC*, Vol. 43, Fourth Quarter, pp. 271–286.

Bjorhovde, R., and Birkemoe, P. O. (1979), "Limit States Design of H.S.S. Columns," *Can. J. Civ. Eng.*, Vol. 8, No. 2, pp. 276–291.

Bjorhovde, R., and Tall, L. (1971), "Maximum Column Strength and the Multiple Column Curve Concept," Fritz Eng. Lab. Rep. No. 338.29, Lehigh University, Bethlehem, PA, Oct.

Bjorhovde, R., Brozzetti, J., Alpsten, G. A., and Tall, L. (1972), "Residual Stresses in Thick Welded Plates," *Weld J.*, Vol. 51, No. 8, pp. 392–405.

Bjorhovde, R., Brozzetti, J., and Colson, A. (1988), *Connections in Steel Structures—Behaviour, Strength and Design*, Elsevier Applied Science, London, England.

Bjorhovde, R., Colson, A. and Brozzetti, J. (1990), "Classification System for Beam-to-Column Connections," *J. Struct. Eng.*, ASCE, Vol. 116, No. 11, pp. 3063–3080.

Bjorhovde, R., Colson, A., Haaijer, G., and Stark, J. W. B. (1992), *Connections in Steel Structures II—Behavior, Strength and Design*, AISC, Chicago, IL.

Bjorhovde, R., Colson, A., and Zandonini, R. (1996), *Connections in Steel Structures III—Behaviour, Strength and Design*, Pergamon/Elsevier Science, London.

Bleich, F. (1952), *Buckling Strength of Metal Structures*, McGraw-Hill, New York.

Boissonnade, N., and Maquoi, R. (2005), "A Geometrically and Materially Non-linear 3-D Beam Finite Element for the Analysis of Tapered Steel Members," *Steel Struct.*, Vol. 5, pp. 413–419.

Bredenkamp, P. J. and van den Berg, G. J. (1995), "The Strength of Stainless Steel Built-up I-Section Columns," *J. Constr. Steel Res.*, Vol. 34, No. 2–3, pp. 131–144.

Bredenkamp, P. J., van den Berg, G. J., and van der Merwe, P. (1992), "Residual Stresses and the Strength of Stainless Steel I-Section Columns," *Proc. SSRC 1992 Annu. Tech. Session*, Pittsburgh, PA, Apr.

Bredenkamp, P. J., Human, J. J., and van den Berg, G. J. (1994), "The Strength of Hot-Rolled Stainless Steel Columns," *Proc. SSRC 1994 Annu. Tech. Session*, Apr., Milwaukee, WI.

Brockenbrough, R. L. (1992), "Material Behavior," in *Constructional Steel Design: An International Guide* (P. J. Dowling, J. E. Harding, and R. Bjorhovde, eds.), Elsevier Applied Science, London, Chaps. 1.1 and 1.2.

Brolin, C. A., Durscher, H. E., and Serentha, G. (1972), "Destructive Testing of Crane Booms," *SAE Trans.*, Vol. 81, Pap. 720784.

Brozzetti, J., Alpsten, G. A., and Tall, L. (1970a) "Residual Stresses in a Heavy Rolled Shape 14WF730," Fritz Eng. Lab. Rep. No. 337.1, Lehigh University, Bethlehem, PA, Jan.

Brozzetti, J., Alpsten, G. A., and Tall, L. (1970b), "Welding Parameters, Thick Plates and Column Strength," Fritz Eng. Lab. Rep. No. 337.21, Lehigh University, Bethlehem, PA, Feb.

Brungraber, R. J., and Clark, J. W. (1962), "Strength of Welded Aluminum Columns," *Trans. Am. Soc. Civ. Eng.*, Vol. 127, Part 11, pp. 202–226.

BSI (1991), *Structural Use of Aluminium: Code of Practice for Design*, BS 81181, British Standards Institution, London

Burgan B. A., Baddoo, N. R., and Gilsenan, K. A. (2000), "Structural Design of Stainless Steel Members—Comparison between Eurocode 3, Part 1.4 and Test Results," *J. Constr. Steel Res.*, Vol. 54, No. 1, pp. 51–73.

Butler, D. J. (1966), "Elastic Buckling Tests on Laterally and Torsionally Braced Tapered I-Beams," *Weld. J. Res. Suppl.*, Vol. 44, No. 1, pp. 41–48.

Butler, D. J., and Anderson, G. C. (1963), "The Elastic Buckling of Tapered Beam Columns," *Weld J. Res. Suppl.*, Vol. 42, No. 1, pp. 29–36.

CEN (2003a), Eurocode 3: *Design of Steel Structures*, EN 1993, Comité Européen de Normalisation (CEN), European Committee for Standardization Brussels, Belgium.

CEN (2003b), *Design of Steel Structures*, Part 3-2: Supplementary Rules for Towers, Masts and Chimneys, EN 1993-3-2, Comité Européen de Normalisation (CEN), European Committee for Standardization, Brussels, Belgium.

CEN (2006), Eurocode 3: *Design of Steel Structures*, Part 1.4: Supplementary Rules for Stainless Steel, EN-1993-1-4, Comité Européen de Normalisation (CEN), European Committee for Standardization, Brussels, Belgium.

CEN (2007), Eurocode 9: *Design of Aluminium Alloy Structures: General Rules*, EN 1999-9, Comité Européen de Normalisation (CEN), European Committee for Standardization, Brussels, Belgium.

Chajes, A., and Chen, W. S. (1979), "Stability of Guyed Towers," *ASCE J. Struct. Div.*, Vol. 105, No. ST1, pp. 163–174.

Chajes, A., and Ling, D. (1981), "Post-buckling Analysis of Guyed Towers," *ASCE, J. Struct. Eng.*, Vol. 107, No. 12, pp. 2313–2323.

Chapuis, J., and Galambos, T. V. (1982), "Restrained Crooked Aluminum Columns," *ASCE J. Struct. Div.*, Vol. 108, No. ST3, pp. 511–524.

Chen, W. F. (1980), "End Restraint and Column Stability," *ASCE J. Struct. Div.*, Vol. 105, No. ST11, pp. 2279–2295.

Chen, W. F. (ed.) (1987), "Joint Flexibility in Steel Frames," Special Issue, *J. Constr. Steel Res.*, Vol. 8.

Chen, W. F. (ed.) (1988), *Steel Beam-to-Column Building Connections*, Elsevier Applied Science, London.

Chen, W. F., and Atsuta, T. (1976), *Theory of Beam-Columns*, Vol. 1, McGraw-Hill, New York.

Chen, W. F., and Han, D. C. (1985), *Tubular Members in Offshore Structures*, Pitman, London.

Chen, W. F., and Kishi, N. (1989), "Semi-rigid Steel Beam-to-Column Connections: Data Base and Modeling," *ASCE J. Struct. Eng.*, Vol. 115, No. 1, pp. 105–119.

Chen, W. F., and Lui, E. M. (1985), "Stability Design Criteria for Steel Members and Frames in the United States," *J. Constr. Steel Res.*, Vol. 5, No. 1, pp. 51–94.

Chen, W. F., and Lui, E. M. (1987), *Structural Stability, Theory and Implementation*, Elsevier, New York.

Chen, W. F., and Lui, E. M. (1991), *Stability Design of Steel Frames*, CRC Press, Boca Raton, FL.

Chen, W. F., and Sohal, I. S. (1995), *Plastic Design and Second-Order Analysis of Steel Frame*, Springer-Verlag, New York.

Chen, W. F., Goto, Y., and Liew, J. Y. R. (1996), *Stability Design of Semi-rigid Frames*, Wiley, New York.

Chernenko, D. E., and Kennedy, D. J. L. (1991), "An Analysis of the Performance of Welded Wide Flange Columns," *Can. J. Civil Eng.*, Vol. 18, pp. 537–555.

Christopher, J. E. and Bjorhovde, R. (1999), "Semi-Rigid Frame Design Methods for Practicing Engineers," *Eng. J. AISC*, Vol. 36, First Quarter, pp. 12–28.

Ciesielski, R., and Koziol, K. (1995), "Dynamic Investigations of a Guyed Mast Model," *Proceedings of IASS Working Group no. 4 for Masts and Towers*, Winchester, England, International Association for Shell and Spatial Structures, Madrid, Spain.

CISC (2006), *Handbook of Steel Construction*, 8th ed., Canadian Institute of Steel Construction, Willowdale, Ontario, Canada.

Clark, J. W., and Rolf, R. L. (1966), "Buckling of Aluminum Columns, Plates and Beams," *ASCE J. Struct. Div.*, Vol. 92, No. ST3, pp. 17–38.

Cohen, E., and Perrin, H. (1957), "Design of Multi-level Guyed Towers: Structural Analysis," *ASCE J. Struct. Div.*, Vol. 83, No. ST5, pp. 1356–1 to 1356–29.

Column Research Committee of Japan (CRCJ) (1971), *Handbook of Structural Stability*, English ed., Corona Publishing Company, Tokyo.

Costello, G. A., and Phillips, J. W. (1983), "Post-buckling Behavior of Guyed Towers," *ASCE J. Struct. Eng.*, Vol. 109, No. 6, pp. 1450–1459.

Crawford, R. F., and Benton, M. D. (1980), "Strength of Initially Wavy Lattice Columns," *AIAA J.*, Vol. 18, No. 5, p. 581.

CSA (2001), *Antennas, Towers, and Antenna-supporting Structures*. CSA S37-01, Canadian Standards Association (CSA), Toronto, Ontario, Canada.

CSA (2005), *Strength Design in Aluminum*. CSA S157-05, Canadian Standards Association (CSA), Toronto, Ontario, Canada.

CSA (2006), *Canadian Highway Bridge Design Code*, CSA-S6-06, Canadian Standards Association (CSA), Toronto, Ontario, Canada.

CSA (2009), *Design of Steel Structures*, CSA-S16-01, Canadian Standards Association (CSA), Toronto, Ontario, Canada.

Davenport, A. G., and Sparling, B. F. (1992), "Dynamic Gust Response Factors for Guyed Towers," *J. Wind Eng. Ind. Aerodyn*, Vol. 41–44, pp. 2237–2248.

Dean, D. L. (1961), "Static and Dynamic Analysis of Guy Cables," *ASCE J. Struct. Div.*, Vol. 87, No. ST1, pp. 1–21.

DeFalco, F., and Marino, F. J. (1966), "Column Stability in Type 2 Construction," *AISC Eng. J.*, Vol. 3, No. 2, pp. 67–71.

Disque, R. O. (1973), "Inelastic K-Factor in Column Design," *AISC Eng. J.*, Vol. 10, No. 2, pp. 33–35.

Disque, R. O. (1975), "Directional Moment Connections: A Proposed Design Method for Unbraced Steel Frames," *AISC Eng. J.*, Vol. 12, No. 1, pp. 14–18.

Driver, R. G., Grondin, G. Y., and Teh, L. (2003), *Centrally Loaded Column Research Inventory*, Structural Stability Research Council, Task Group 1, University of Missouri-Rolla.

Duberg, J. E., and Wilder, T. W. (1950), "Column Behavior in the Plastic Strength Range," *J. Aeronaut. Sci.*, Vol. 17, No. 6, p. 323.

Dux, P. F., and Kitipornchai, S. (1981), "Inelastic Beam-Buckling Experiments," Res. Rep. No. CE24, Department of Civil Engineering, University of Queensland, St. Lucia, Australia.

ECCS (1978), *European Recommendation for Aluminium Structures*, Committee T2, European Convention for Constructional Steelwork, Brussels, Belgium.

Ekhande, S. G., and Madugula, M. K. S. (1988), “Geometric Nonlinear Analysis of Three-Dimensional Guyed Towers,” *Comput. Struct.*, Vol. 29, No. 5, pp. 801–806.

Engesser, F. (1891), “Die Knickfestigkeit gerader Stabe,” *Zentralbl. Bauverwaltung*, Vol. 11, pp. 483–486.

Essa, H. S., and Kennedy, D. L. J. (1993), “Distortional Buckling of Steel Beams,” Struct. Eng. Rep. No. 185, Department of Civil Engineering, University of Alberta, Edmonton, Alberta, Canada.

Fraser, D. J., and Bridge, R. Q. (1990), “Buckling of Stepped Crane Columns,” *J. Constr. Steel Res.*, Vol. 16, No. 1, pp. 23–38.

Freeman, B. G. (1973), “Tie Plate Effects in Weakly Battened Columns,” Ph.D. dissertation, Department of Civil Engineering, University of Arizona, Tucson, AZ.

Frey, F. (1969), “Effect of the Cold-Bending of H-Shaped Rolled Steel Sections on Column Strength,” *IABSE Mem.* (in French), Vol. 291, pp. 101–124.

Frye, M. J., and Morris, G. A. (1975), “Analysis of Flexibly Connected Steel Frames,” *Can. J. Civ. Eng.*, Vol. 2, No. 3, pp. 280–291.

Fukumoto, Y., Nethercot, D. A., and Galambos, T. V. (1983), “Experimental Data for the Buckling of Steel Structures–NDSS Stability of Metal Structures,” *Proc. 3rd Int. Colloq. SSRC*, Toronto, Ontario, Canada, May, pp. 609–630.

Galambos, T. V. (ed.) (1988), *Guide to Stability Design Criteria for Metal Structures*, 4th ed., Structural Stability Research Council, Wiley Interscience, New York, 786 pp.

Galambos, T. V. (ed.) (1998), *Guide to Stability Design Criteria for Metal* Structures, 5th ed., Structural Stability Research Council, Wiley Interscience, New York, 911 pp.

Gardner, L., Talja, A., and Baddoo, N. R. (2006), ”Structural Design of High-strength Austenitic Stainless Steel.” *Thin-walled Struct.* Vol. 44, pp. 517–528.

Gere, J. M., and Carter, W. O. (1962), “Critical Buckling Loads for Tapered Columns,” *ASCE J. Struct. Div.*, Vol. 88, No. ST1, Proc. Pap. 3045, pp. 1–11.

Gerstoft, P., and Davenport, A. G. (1986), “A Simplified Method for Dynamic Analysis of a Guyed Mast,” *J. Wind Eng. Ind. Aerodyn.*, Vol. 23, pp. 487–499.

Gjelsvik, A. (1990), “Buckling of built-up columns, with or without Stay Plate,” *ASCE J. Eng. Mech.*, Vol. 116, No. 5, pp. 1142–1159.

Goldberg, J. E. (1954), “Stiffness Charts for Gusseted Members Under Axial Load,” *Trans. ASCE*, Vol. 119, p. 43.

Goldberg, J. E., and Gaunt, J. T. (1973), “Stability of Guyed Towers,” *ASCE J. Struct. Div*, Vol. 99, No. ST4, pp. 741–756.

Goldberg, J. E., and Meyers, V. J. (1965), “A Study of Guyed Towers,” *ASCE J. Struct. Div.*, Vol. 91, No. ST4, pp. 57–76.

Goto, Y., Suzuki, S., and Chen, W. F. (1993), “Stability Behavior of Semi-rigid Sway Frames,” *Eng. Struct.*, Vol. 15, No. 3, pp. 209–219.

Hall, D. H. (1981), “Proposed Steel Column Strength Criteria,” *ASCE J. Struct. Div.*, Vol. 107, No. ST4, pp. 649–670.

Hariri, R. (1967), “Post-buckling Behavior of Tee-Shaped Aluminum Columns,” Ph.D. dissertation, University of Michigan, Ann Arbor, MI, June.

Hartmann, E. C., and Clark, J. W. (1963), “The U.S. Code,” *Proc. Symp. Alum. Struct. Eng.*, London, June 11–12, The Aluminum Federation.

Hartmann, E. C., Moore, R. L., and Holt, M. (1938), “Model Tests of Latticed Structural Frames,” Alcoa Res. Lab. Tech. Pap. No. 2, Pittsburgh, PA.

Hellesland, J. and Bjorhovde, R. (1996), "Restraint Demand Factors and Effective Length of Braced Columns," *J. Struct. Eng., ASCE*, Vol. 122, No. 10, pp. 1216–1224.

Hellesland, J., and Bjorhovde, R. (1996a), "Improved Frame Stability Analysis with Effective Lengths," *J. Struct. Eng., ASCE*, Vol. 122, No. 11, pp. 1275–1283.

Hong, G. M. (1991), "Effects of Non-central Transverse Welds on Aluminum Columns," in *Aluminum Structures: Recent Research and Development* (S. I. Lee, ed.), Elsevier Applied Science, London.

Horne, M. R., and Ajmani, J. L. (1971), "Design of Columns Restrained by Side-Rails and the Post-bucking Behavior of Laterally Restrained Columns," *Struct. Eng.*, Vol. 49, No. 8, pp. 339–352.

Howard, J. E. (1908), "Some Results of the Tests of Steel Columns in Progress at the Watertown Arsenal," *Proc. A.S.T.M.*, Vol. 8, p. 336.

Huang, H. C. (1968), "Determination of Slenderness Ratios for Design of Heavy Mill Building Stepped Columns," *Iron Steel Eng.*, Vol. 45, No. 11, p. 123.

Huber, A. W. (1956), "The Influence of Residual Stress on the Instability of Columns," Ph.D. dissertation, Lehigh University, Bethlehem, PA.

Hull, F. H. (1962), "Stability Analysis of Multi-level Guyed Towers," *ASCE J. Struct. Div.*, Vol. 88, No. ST2, pp. 61–80.

Hussaini, A. (2004), "Tensile Strength of Bolted Flange Connections." M.A.Sc. Major Paper, University of Windsor, Windsor, Ontario, Canada.

IASS (1981), *Recommendations for Guyed Masts*, Working Group 4, International Association for Shell and Spatial Structures, Madrid, Spain.

ISO (1992), "Aluminium Structures: Material and Design, Part 1: Ultimate Limit State - Static Loading," Technical Report, Doc. No 188, International Standards Organisation Committee TC 167/SC3, International Standards Organisation, Geneva.

ISE (1962), *Report on the Structural Use of Aluminum*, Institution of Structural Engineers, London.

Issa, R. R. A., and Avent, R. R. (1991), "Microcomputer Analysis of Guyed Towers as Lattices," *ASCE J. Struct. Div.*, Vol. 117, No. 4, pp. 1238–1256.

Jacquet, J. (1970), "Column Tests and Analysis of Their Results," *Constr. Met.*, No. 3, pp. 13–36.

Jimenez-Lopez, G. A. (1998), "Inelastic Stability of Tapered Structural Members," Ph. D. dissertation, University of Minnesota, Minneapolis-St. Paul, MN.

Jimenez, G., and Galambos, T. V. (2001), "Inelastic Stability of Pinned Tapered Columns," Proceedings of SSRC Annual Technical Session, Ft. Lauderdale, FL, pp. 143–158

Johnson A. L. and Winter, G. (1966), "The Structural Performance of Austenitic Stainless Steel Members," Report No. 327, Department of Structural Engineering, Cornell University, Ithaca, NY.

Johnston, B. G. (1963), "Buckling Behavior Above the Tangent Modulus Load," *Trans. ASCE*, Vol. 128, Part 1, pp. 819–848.

Johnston, B. G. (1964), "Inelastic Buckling Gradient," *ASCE J. Eng. Mech. Div.*, Vol. 90, No. EM5, pp. 31–48.

Johnston, B. G. (1971), "Spaced Steel Columns," *ASCE J. Struct. Div.*, Vol. 97, No. ST5, p. 1465.

Johnston, B. G. (ed.) (1976), *Guide to Stability Design Criteria for Metal Structures*, 3rd ed., Wiley, New York.

Jones, S. W., Kirby, P. A., and Nethercot, D. A. (1980), “Effect of Semi-rigid Connections on Steel Column Strength,” *J. Constr. Steel Res.*, Vol. 1, No. 1, pp. 35–46.

Jones, S. W., Kirby, P. A., and Nethercot, D. A. (1982), “Columns with Semi-rigid Joints,” *ASCE J. Struct. Div.*, Vol. 108, No. ST2, pp. 361–372.

Kaehler, R. C., White, D. W., and Kim, Y. D. (2008), *Frame Design Using Web-Tapered Members*, Metal Building Manufacturers Association, Cleveland, OH, and American Institute of Steel Construction, Chicago, IL.

Kahla, N. B. (1997), “Nonlinear Dynamic Response of a Guyed Tower to a Sudden Guy Rupture,” *Eng. Struct.*, Vol. 19, pp. 879–890.

Kahla, N. B. (2000), “Response of a Guyed Tower to a Guy Rupture under No Wind Pressure,” *Eng. Struct.*, Vol. 22, pp. 699–706.

Kato, B. (1977), “Column Curves for Cold-Formed and Welded Tubular Members,” *2nd Int. Colloq. Stab. Steel Struct.*, Liege, Belgium, pp. 53–60.

Kennedy, D. J. L. and Gad Aly, M. (1980), “Limit States Design of Steel Structures Performance Factors,” *Can. J. Civil Eng.*, Vol. 7, No. 1, pp. 45–77.

Kim, M. C., Lee, G. C., and Chang, K. C. (1995), “Inelastic Buckling of Tapered Members with Accumulated Strain,” *Int. J. Struct. Eng. Mech.*, Vol. 3, No. 6, pp. 611–622.

King, W. S., and Chen, W. F. (1993), “LRFD Analysis for Semi-rigid Frame Design,” *AISC Eng. J.*, Vol. 30, No. 4, pp. 130–140.

King, W. S., and Chen, W. F. (1994), “Practical Second-Order Inelastic Analysis of Semi-rigid Frames,” *ASCE J. Struct. Eng.*, Vol. 120, No. 7, pp. 2156–2175.

Kishi, N., and Chen, W. F. (1986), “Data Base of Steel Beam-to-Column Connections,” Struct. Eng. Rep. No. CE-STR-86-26, School of Civil Engineering, Purdue University, West Lafayette, Ind., 2 vols.

Kishi, N., and Chen, W. F. (1990), “Moment-Rotation Relations of Semi-rigid Connections with Angles,” *ASCE J. Struct. Eng.*, Vol. 116, No. 7, pp. 1813–1834.

Kishi, N., Chen, W. F., Goto, Y., and Matsuoka, K. G. (1993a), “Design Aid of Semi-rigid Connections for Frame Analysis,” *AISC Eng. J.*, Vol. 30, No. 3, pp. 90–103.

Kishi, N., Goto, Y., Chen, W. F., and Matsuoka, K. (1993b), “Analysis Program for the Design of Flexibly Jointed Frames,” *Comput. Struct.*, Vol. 49, No. 4, pp. 705–713.

Kishima, V., Alpsten, G. A., and Tall, L. (1969), “Residual Stresses in Welded Shapes of Flame-Cut Plates in ASTM A572(50) Steel,” Fritz Eng. Lab. Rep. No. 321.2, Lehigh University, Bethlehem, PA, June.

Korol, R. M., Rutenberg, A., and Bagnariol, D. (1986), “On Primary and Secondary Stresses in Triangulated Trusses,” *J. Constr. Steel Res.*, Vol. 6, pp. 123–142.

Kumalasari, C. (2004), “Compressive Strength of Solid Round Steel Leg and Bracing members of Lattice Communication Towers Reinforced with Rods or Angles,” M.A.Sc. Thesis, University of Windsor, Windsor, Ontario, Canada.

Kumalasari, C., Ding, Y., and Madugula, M. K. S. (2006a), “Prying Action in Bolted Steel Circular Flange Connections,” *Can. J. Civil Eng.*, April 2006.

Kumalasari, C., Ding, Y., Madugula, M. K. S., and Ghrib, F. (2006b), “Compressive strength of Solid Round Steel Members Strengthened with Rods or Angles,” *Can. J. Civil Eng.*, April 2006.

Kumalasari, C., Madugula, M. K. S., and Ghrib, F. (2005a), “Reinforcement of Lattice Communication towers with Rods and Angles,” Proc., Annual General Conference of the Canadian Society for Civil Engineering, June 2-4, Toronto, Ontario, Canada, p. GC–255.

Kumalasari, C., Shen, L., Madugula, M. K. S., and Ghrib, F. (2005b), "Tensile Strength of Bolted Ring-type Splices of Solid Round Leg Members of Guyed Communication Towers," *Can. J. Civil Eng.*, Vol. 32, No. 3, pp. 595–600.

Lai, Y. F. W., and Nethercot, D. A. (1992), "Strength of Aluminium Members Containing Local Transverse Welds," *Eng. Struct.*, Vol. 14, No. 4, pp. 241–254.

Lagerquist, O., and Olsson, A. (2001), "Residual Stresses in Welded I-girders Made from Stainless Steel and Structural Steel," in *Proceedings of the 9th Nordic Steel Construction Conference* (P. Makelainen et al., eds.), Helsinki, Finland, pp. 737–744.

Lee, G. C., Morrell, M. L., and Ketter, R. L. (1972), "Design of Tapered Members," *Weld. Res. Counc. Bull. No. 173*, June, pp. 1–32.

Lee, G. C., Ketter, R. L., and Hsu, T. L. (1981), *The Design of Single Story Rigid Frames*, Metal Building Manufacturer's Association, Cleveland, OH.

Leon, R. T. and Easterling, W. S. (2002), *Connections in Steel Structures IV—Behavior, Strength and Design*, AISC, Chicago, IL.

Lin, F. J., Glauser, E. C., and Johnston, B. G. (1970), "Behavior of Laced and Battened Structural Members," *ASCE J. Struct. Div.*, Vol. 96, No. ST7, p. 1377.

Lindner, J., and Gietzelt, R. (1984), "Imperfectionsannahmen für Stützenschiefstellungen," *Stahlbau*, Vol. 53, No. 4, pp. 97–101.

Livesley, R. K., and Poskitt, T. J. (1963), "Structural Analysis of Guyed Masts," *Proc. Inst. Civil Eng. (London)*, Vol. 24, pp. 373–386.

Loov, R. (1996), "A Simple Equation for Axially Loaded Steel Column Design Curves," *Can. J. Civil Eng.*, Vol. 23, No. 11, pp. 272–276.

Lui, E. M., and Chen, W. F. (1983a), "Strength of H-Columns with Small End-Restraints," *Struct. Eng.*, Vol. 61B, No. 1, Part B, pp. 17–26.

Lui, E. M., and Chen, W. F. (1983b), "End Restraint and Column Design Using LRFD," *Eng. J. Am. Inst. Steel Constr.*, Vol. 20, No. 1, pp. 29–39.

Lui, E. M., and Chen, W. F. (1984), "Simplified Approach to the Analysis and Design of Columns with Imperfections," *AISC Eng. J.*, Vol. 21, No. 2, pp. 99–117.

Lui, E. M., and Chen, W. F. (1988), "Behavior of Braced and Unbraced Semi-rigid Frames," *Solids Struct.*, Vol. 24, No. 9, pp. 893–913.

Lui, E. M., and Sun, M. (1995), "Effective Lengths of Uniform and Stepped Crane Columns," *AISC Eng. J.*, Vol. 32, No. 3, pp. 98–106.

MacCrimmon, R. A., and Kennedy D. J. L. (1997), "Load and Resistance Factor Design and Analysis of Stepped Crane Columns in Industrial Buildings," *AISC Eng. J.*, Vol. 34, No. 1, pp. 26–36.

Madsen, I. (1941), "Report of Crane Girder Tests." *Iron Steel Eng.*, Vol. 18, No. 11, p. 47.

Madugula, M. K. S. (ed.) (2002), "Dynamic Response of Lattice Towers and Guyed Masts," Task Committee Report, Structural Engineering Institute of the American Society of Civil Engineers, Reston, VA.

Magued, M. H., Bruneau, M., and Dryburgh, R. B. (1989), "Evolution of Design Standards and Recorded Failures of Guyed Towers in Canada," *Can. J. Civil Eng.*, Vol. 16, No. 5, pp. 725–732.

Masur, E. F. (1954), "Lower and Upper Bounds to the Ultimate Loads of Buckled Trusses," *Q. Appl. Math.*, Vol. 11, No. 4, p. 385.

Maugh, L. C. (1963), *Statically Indeterminate Structures*, 2nd ed., Wiley, New York.

Mazzolani, F. M. (1985), *Aluminium Alloy Structures*, Pitman, Marshfield, MA.

Mazzolani, F. M., and Frey, F. (1977), "Buckling Behavior of Aluminium Alloy Extruded Members," *2nd Int. Colloq. Stabil. Steel Struct.*, Liege, Belgium, pp. 85–94.

Mazzolani, F. M., and Frey, F. (1980), "The Bases of the European Recommendations for the Design of Aluminum Alloy Structures," *Alluminio*, No. 2, pp. 77–94.

McCaffrey, R. J., and Hartman, A. J. (1972), "Dynamics of Guyed Towers," *ASCE J. Struct. Div.*, Vol. 98, No. ST6, pp. 1309–1323.

McClure, G., Guevara, E., and Lin, N. (1993), "Dynamic Analysis of Antenna-Supporting Towers," *Proc. Annu. Conf. Can. Soc. Civ. Eng.*, June 8–11, Fredericton, New Brunswick, Canada, pp. 335–344.

McFalls, R. K., and Tall, L. (1970), "A Study of Welded Columns Manufactured from Flame-Cut Plates," *AWS Weld. J.*, Vol. 49, No. 4, pp. 141s–153s.

Michalos, J., and Louw, J. M. (1957), "Properties for Numerical Analysis of Gusseted Frameworks," *Proc. Am. Railw. Eng. Assoc.*, Vol. 58, p. 1.

Miller, R. K., and Hedgepeth, J. M. (1979), "The Buckling of Latticed Columns with Stochastic Imperfections," *Int. J. Solids Struct.*, Vol. 15, pp. 71–84.

Nakamoto, R. T., and Chiu, A. N. L. (1985), "Investigation of Wind Effects on Guyed Towers," *ASCE J. Struct. Div.*, Vol. 111, No. 11, pp. 2320–2332.

Nethercot, D. A., and Chen, W. F. (1988), "Effects of Connections on Columns," *J. Constr. Steel Res.*, Vol. 10, pp. 201–239.

Newmark, N. M. (1943), "A Numerical Procedure for Computing Deflections, Moments and Buckling Loads," *Trans. ASCE*, Vol. 108, pp. 1161–1188.

Nielsen, M. G. (1999), "Analysis of Guy Failure," *Proceedings of IASS Working Group No. 4 for Masts and Towers, Krakow, Poland*, International Association for Shell and Spatial Structures, Madrid, Spain.

Novak, M., Davenport, A. G., and Tanaka, H. (1978), "Vibration of Towers Due to Galloping of Iced Cables," *ASCE J. Eng. Mech. Div.*, Vol. 104, No. EM2, pp. 457–473.

Odley, E. G. (1966), "Analysis of High Guyed Towers," *ASCE J. Struct. Div.*, Vol. 92, No. ST1, pp. 169–197.

Osgood, W. R. (1951), "The Effect of Residual Stress in Column Strength," *Proc. First U.S. Natl. Congn. Appl. Mech.*, June, p. 415.

Paul, M. (1995), "Buckling Loads for Built-up Columns with Stay Plates," *ASCE J. Eng. Mech.*, Vol. 121, No. 11, pp. 1200–1208.

Prawel, S. P., Morrell, M. L., and Lee, G. C. (1974), "Bending and Buckling Strength of Tapered Structural Members," *Weld. Res. Suppl.*, Vol. 53, February, pp. 75–84.

Rasmussen K. J. R. (2000), "Recent Research on Stainless Steel Tubular Structures," *J. Constr. Steel Res.*, Vol. 54, No. 1, pp. 75–88.

Rasmussen K. J. R. and Hancock, G. J. (1993), "Stainless Steel Tubular Members. I: Columns," *J. Struct. Eng. ASCE*, Vol. 119, No. 8, pp. 2349–2367.

Rasmussen K. J. R. and Hasham, A. S. (2001), "Tests of X- and K-joints in CHS Stainless Steel Tubes," *J. Struct. Eng. ASCE*, Vol. 127, No. 10, pp. 1183–1189.

Rasmussen K. J. R. and Rondal, J. (1997a), "Explicit Approach to Design of Stainless Steel Columns," *J. Struct. Eng. ASCE*, Vol. 123, No. 7, pp. 857–863.

Rasmussen K. J. R. and Rondal, J. (1997b), "Strength Curves for Metal Columns," *J. Struct. Eng. ASCE*, Vol. 123, No. 6, pp. 721–728.

Rasmussen K. J. R. and Rondal, J. (2000a), "Column Curves for Stainless Steel Alloys," *J. Struct. Eng. ASCE*, Vol. 54, No. 1, pp. 89–107.

Rasmussen K. J. R. and Rondal, J. (2000b), "Strength Curves for Aluminium Alloy Columns," *Eng. Struct.*, Vol. 22, No. 11, pp. 1505–1517.

Rasmussen K. J. R. and Young, B. (2001), "Tests of X- and K-joints in SHS Stainless Steel Tubes," *J. Struct. Eng. ASCE*, Vol. 127, No. 10, pp. 1173–1182.

Razdolsky, A. G. (2005), "Euler Critical Force Calculation for Laced columns," *ASCE J. Engrg. Mech.*, Vol. 131, No. 10, pp. 997–1003.

Razzaq, Z., and Chang, J. G. (1981), "Partially Restrained Imperfect Columns," *Proc. Conf. Joints Struct. Steelwork*, Teesside, England. Apr., Pentech Press, Chichester, West Sussex, England.

Robertson, A. 1925. "The Strength of Struts." *Selected Engineering Papers*, No. 28, The Institution of Civil Engineers, London.

Romstad, K. M., and Subramanian, C. V. (1970), "Analysis of Frames with Partial Connection Rigidity," *ASCE J. Struct. Div.*, Vol. 96, No. ST11, pp. 2283–2300.

Ronagh, H. R., Bradford, M. A., and Attard, M. M. (2000a), "Nonlinear Analysis of Thin-walled Members of Variable Cross-section. Part I: Theory," *Comput. Struct.*, Vol. 77, pp. 285–299.

Ronagh, H. R., Bradford, M. A., and Attard, M. M. (2000b), "Nonlinear Analysis of Thin-walled Members of Variable Cross-section. Part II: Application," *Comput. Struct.*, Vol. 77, pp. 301–313.

Rondal, J., and Maquoi, R. (1979), "Single Equation for SSRC Column Strength Curves," *ASCE J. Struct. Div.*, Vol. 105, No. ST1, pp. 247–250.

Rosenthal, F., and Skop, R. A. (1980), "Guyed Towers Under Arbitrary Loads," *ASCE J. Struct. Div.*, Vol. 106, No. ST3, pp. 679–692.

Rotter, J. M. (1982), "Multiple Column Curves by Modifying Factors," *ASCE J. Struct. Div.*, Vol. 108, No. ST7, pp. 1665–1669.

Rowe, R. S. (1958), "Amplification of Stress and Displacement in Guyed Towers," *ASCE J. Struct. Div.*, Vol. 84, No. ST6, pp. 1821.1–1821.20.

SAA (1997), *Aluminum Structures—Limit State: Design*, AS 1664.1, Standards Association of Australia, North Sydney, New South Wales, Australia.

Salmon, E. H. (1921), *Columns*, Oxford Technical Publishers, London.

Salvadori, M. G. (1951), "Numerical Computation of Buckling Loads by Finite Differences," *Trans. ASCE*, Vol. 116, pp. 590–625.

Saxena, R., Popplewell, N., Trainor, P. G. S., and Shah, A. H. (1989), "Vibration of Complex Guyed Towers," *Proc. ASME 12th Bienn. Conf. Mech. Vib. Noise*, Montreal, Quebec, Canada, Sept. 17–21, pp. 1–7.

Schmidt, J. A. (2001), "Design of Mill Building Columns Using Notional Loads," *AISC Eng. J.*, Vol. 38, No. 2, pp. 90–99.

SCI (2000), "Development of the Use of Stainless Steel in Construction," Main Work Package Reports–Vols. 1 and 2, Document RT810, Ver. 01, Steel Construction Institute, London.

Sfintesco, D. (1970), "Experimental Basis for the European Column Curves," *Constr. Met.*, No. 3, p. 5.

Sfintesco, D. (ed.) (1976), *ECCS Manual on the Stability of Steel Structures*, 2nd ed., European Convention for Constructional Steelwork, Brussels, Belgium.

Shanley, F. R. (1947), "Inelastic Column Theory," *J. Aeronaut. Sci.*, Vol. 14, No. 5, p. 261.

Sharp, M. L. (1993), *Behavior and Design of Aluminum Structures*, McGraw-Hill, New York.

Shen, L. (2002), "Strength of Bolted Ring-type Connections of Solid Round Leg Members of Guyed Communication Towers," M.A.Sc. Thesis, University of Windsor, Windsor, Ontario, Canada.

Shen, Z.-Y., and Lu, L.-W. (1983), "Analysis of Initially Crooked, End Restrained Columns," *J. Constr. Steel Res.*, Vol. 3, No. 1, pp. 10–18.

Sherman, D. R. (1976), *Tentative Criteria for Structural Applications of Steel Tubes*, American Iron and Steel Institute, Washington, DC.

Siddiqui, M. M. R. (2005), "Additional Tests on Compressive Strength of Solid Round Steel Members Reinforced with Split Pipe," M.A.Sc. Major Paper, University of Windsor, Windsor, Ontario, Canada.

Stang, A. H., and Greenspar, M. (1948), "Perforated Cover Plates for Steel Columns: Summary of Compression Properties," *U.S. Nat. Bur. Stand. J. Res.*, Vol. 40, No. 5 RP.

Steinhardt, G. (1971), "Aluminum in Engineered Construction," *Aluminum*, No. 47 (in German).

Sugimoto, H., and Chen, W. F. (1982), "Small End Restraint Effects in Strength of H-Columns," *ASCE J. Struct. Div.*, Vol. 108, No. ST3, pp. 661–681.

Surovek, A. E., White, D. W., and Leon, R. T. (2005), "Direct Analysis for Design Evaluation of Partially Restrained Steel Framing Systems," *J. Struct. Eng. ASCE*, Vol. 131, No. 9, pp. 1376–1389.

Talja, A. and Salmi, P. (1995), "Design of Stainless Steel RHS Beams, Columns and Beam-columns." Research Notes 1619, Technical Research Centre of Finland, VTT, Espoo.

Tall, L. (1964), "Recent Developments in the Study of Column Behavior," *J. Inst. Eng. Aust.*, Vol. 36, No. 12, pp. 319–333.

Tall, L. (1966), "Welded Built-up Columns," Fritz Eng. Lab. Rep. No. 249.29, Lehigh University, Bethlehem, PA, Apr.

Tickle, V. (2004), "Compressive Strength of Solid Round Steel Leg Members of Lattice Communication Towers Strengthened with Split Pipe," M.A.Sc. Major Paper, University of Windsor, Windsor, Ontario, Canada.

Timoshenko, S. P. (1936), *Theory of Elastic Stability*, McGraw-Hill, New York.

Timoshenko, S. P., and Gere, J. M. (1961), *Theory of Elastic Stability*, 2nd ed., McGraw-Hill, New York.

Tomonaga, K. (1971), "Actually Measured Errors in Fabrication of Kasumigaseki Building," *Proc. 3rd Reg. Conf. Plan. Des. Tall Build.*, Tokyo, Sept.

Trahair, N. S. (1988), *The Behavior and Design of Steel Structures*, Chapman and Hall, London.

van den Berg, G. J. (2000), "The Effect of the Non-linear Stress-strain Behaviour of Stainless Steels on Member Capacity," *J. Constr. Steel Res.*, Vol. 54, No. 1, pp. 135–160.

Vinnakota, S. (1982), "Planar Strength of Restrained Beam-Columns," *ASCE J. Struct. Div.*, Vol. 108, No. ST11, pp. 2496–2516.

Vinnakota, S. (1983), "Planar Strength of Directionally and Rotationally Restrained Steel Columns," *Proc. 3rd Int. Colloq. Stab. Met. Struct.*, Toronto, May, pp. 315–325.

Vinnakota, S. (1984), "Closure," *ASCE J. Struct. Div.*, Vol. 110, No. ST2, pp. 43–435.

Vroonland, E. J. (1971), “Analysis of Pendant-Supported Latticed Crane Booms,” *SAE Trans.*, Vol. 80, Pap. 710697.

Wahba, Y. M. F., Madugula, M. K. S., and Monforton, G. R. (1993), “Combined Wind and Ice Loading on Antenna Towers,” *Can. J. Civil Eng.*, Vol. 20, No. 6, pp. 1047–1056.

Wang, C.-K. (1967), “Stability of Rigid Frames with Non-uniform Members,” *ASCE J. Struct. Div.*, Vol. 93, No. ST1, pp. 275–294.

White, D., W., and Kim, Y. D. (2006), “A Prototype Application of the AISC (2005) Stability Analysis and Design Provisions to Metal Building Structural Systems,” Report prepared for Metal Building Manufacturers Association, School of Civil and Environmental Engineering, Georgia Institute of Technology, Jan.

White, M. W., and Thürlimann, B. (1956), “Study of Columns with Perforated Cover Plates,” *AREA Bull. No. 531*.

Williamson, R. A. (1973), “Stability Study of Guyed Towers Under Ice Loads,” *ASCE J. Struct. Div.*, Vol. 99, No. ST12, pp. 2391–2408.

Williamson, R. A., and Margolin, M. N. (1966), “Shear Effects in Design of Guyed Towers,” *ASCE J. Struct. Div.*, Vol. 92, No. ST5, pp. 213–233.

Wiskin, G. (1995), “Recent Guyed Mast Vibrations,” *Proceedings of IASS Working Group No. 4 for Masts and Towers, Winchester, England*, International Association for Shell and Spatial Structures, Madrid, Spain.

Wyly, L. T. (1940), “Brief Review of Steel Column Tests,” *J. West. Soc. Eng.*, Vol. 45, No. 3, p. 99.

Yang, H., Beedle, L. S., and Johnston, B. G. (1952), “Residual Stress and the Yield Strength of Steel Beams,” *Weld. J. Res. Suppl.*, Vol. 31, pp. 224–225.

Young, W. C. (1989), *Roark’s Formulas for Stress and Strain*, McGraw-Hill, New York.

Young, B., and Lui, W.-M. (2006), “Tests of Cold-formed High Strength Stainless Steel Compression Members,” *Thin-walled Struct.*, Vol. 44, pp. 224–234.

Yu, W. W. (1992), *Cold-Formed Steel Design*, 2nd ed., Wiley, New York.

Yura, J. A. (1971), “The Effective Length of Columns in Unbraced Frames,” *AISC Eng. J.*, Vol. 8, No. 2, pp. 37–42.

Zandonini, R. (1985), “Stability of Compact Built-up Struts: Experimental Investigation and Numerical Simulation,” *Costruzioni Metalliche*, No. 4.

Zeineddine, M. (2004), “Compressive Strength of Steel Pipe Leg Members Reinforced with Split Pipe(s),” M.A.Sc. Major Paper, University of Windsor, Windsor, Ontario, Canada.

Ziegler, H. (1982), “Arguments for and Against Engesser’s Buckling Formulas,” *Ing. Arch.*, Vol. 52, pp. 105–113.

Queries in Chapter 3

Q1. In this figure, the caption is incomplete. Please confrim.